

Computation of a separatrix map and a normally hyperbolic invariant lamination for the RP3BP

M. Guardia,^{*} V. Kaloshin,[†] P. Martin,[‡] P. Roldan,[§]

March 23, 2026

Abstract

In this paper we discuss the existence of a normally hyperbolic invariant lamination (NHIL) at the Kirkwood gap 3 : 1 for the Restricted Planar Elliptic 3 Body Problem.

This problem models the Sun–Jupiter–Asteroid dynamics. We also show that the induced dynamics on the NHIL is a partially hyperbolic skew-shift which is of the form

$$f : (\omega, I, \theta) \rightarrow (\sigma\omega, I + e_0 A_\omega(I) \cos(\theta + \psi_\omega) + \mathcal{O}(e_0^2), \theta + \Omega_\omega(I) + \mathcal{O}(e_0)),$$

where $I \in [a, b]$, $\theta \in \mathbb{T}$, $\omega \in \Sigma = \{0, 1\}^{\mathbb{Z}}$, the space of sequences of 0, 1's, $\sigma : \Sigma \rightarrow \Sigma$ is the shift in this space, Ω_ω is the shear, A_ω is an amplitude, and e_0 is the eccentricity of Jupiter, which is taken as a small parameter.

In the companion paper [GKMR23], relying on these skew-shift, we show the existence of stochastic diffusing behavior for Asteroids belonging to the Kirkwood gap provided the eccentricity of Jupiter is e_0 small enough.

Key ingredients to construct the NHIL are the separatrix map associated to homoclinic channels to a normally hyperbolic invariant cylinder and an isolating block construction. Some of the necessary non-degeneracy conditions are verified numerically.

Contents

1	Introduction	2
1.1	Main results	4
1.2	Literature	8
1.3	Stochastic Arnold diffusion	8
	Acknowledgements	10
2	The a priori chaotic framework	10
2.1	A good system of coordinates and a time reparameterization	10
2.2	The invariant cylinder and the associated homoclinic channels	12
3	The separatrix map for the circular and elliptic problems	15
3.1	Derivation of the separatrix map: Proof of Theorems 3.1 and 3.2	18
3.2	The first order of the separatrix map: Proof of Proposition 3.3	26

^{*}Universitat de Barcelona, guardia@ub.edu

[†]ISTA, vadim.kaloshin@gmail.com

[‡]Universitat Politècnica de Catalunya, p.martin@upc.edu

[§]Universitat Politècnica de Catalunya, pablo.roldan@upc.edu

4	The normally hyperbolic invariant lamination	28
4.1	Existence of the normally hyperbolic invariant lamination	28
4.2	Dynamics on the normally hyperbolic invariant lamination	31
4.3	The NHIL for the circular problem: Proof of Theorem 4.4	32
4.4	The NHIL for the elliptic problem: Proof of Theorem 4.5	43
A	Numerical verification of Ansatz 1	44
A.1	Equations of motion and Poincaré map	44
A.2	Periodic points and hyperbolic splittings	46
A.3	Invariant manifolds and homoclinic points	46
A.4	Numerical verification of transversality condition	49
A.5	Bounds for $T_{\mathbf{J}}$, $L_{\mathbf{J}}$, and $L_i(t, \mathbf{J})$.	51
B	Numerical verification of Ansatz 2	52
C	Numerical bounds for $\mathbf{e}(t)$ along the homoclinic channels	56

1 Introduction

The Restricted Planar Elliptic 3 Body Problem (RPE3BP) describes the motion of a body of negligible mass under the gravitational influence of two bodies (the primaries) that move on ellipses of eccentricity $e_0 \in (0, 1)$. Normalizing the mass of the system, one can assume that the bodies have mass $\mu \in (0, 1/2]$ and $1 - \mu$.

If one takes $\mu = 0.95387536 \times 10^{-3}$, the RPE3BP models the Sun-Jupiter-Asteroid dynamics. One region in the Solar system where asteroids are abundant is the Asteroid belt, which lies between the orbits of Jupiter and Mars. Since the mass of Mars is much smaller than the mass of Jupiter, its influence on the Sun-Jupiter-Asteroid system can be neglected. The distribution of the asteroids in the Asteroid belt is not uniform but rather uneven. In fact, if one considers the distribution of the Asteroids with respect to their semimajor axes, one can see that there are semimajor axes for which Asteroids are barely present (see Figure 1). These are the so-called Kirkwood gaps, which coincide with semimajor axes such that the Asteroids' period is resonant with that of Jupiter (semimajor axis and period are related through the third Kepler law). These are the so-called mean motion resonances which are, together with the secular resonances [CFG24b, CFG24a], fundamental in understanding the “shape” of our Solar system. Resonances are a major source of instabilities which can arise through different mechanisms. A possible instability mechanism to explain the presence of the Kirkwood gaps, through slow-fast models and adiabatic invariants, was proposed by Wisdom [Wis82] and Neishtadt [Nei87] (see also [NS04]) for the regime

$$\frac{\sqrt{\mu}}{e_0} \ll 1.$$

In [FGKR16], the authors proposed an Arnold diffusion mechanism creating instabilities at the 3 : 1 Kirkwood gaps for $\mu = 0.95387536 \times 10^{-3}$ and $e_0 > 0$ small enough. This Arnold diffusion mechanism makes the asteroid's eccentricity drift, which implies that the asteroid gets closer to Mars orbit in a such way that close encounters with Mars may expel the asteroid from the Asteroid belt.

The classical Arnold mechanism relies on a normally hyperbolic invariant cylinder and its stable and unstable invariant manifolds and, unfortunately, it leads to “few” diffusing orbits. If one wants a more global understanding of unstable motions one must rely on other hyperbolic objects such as

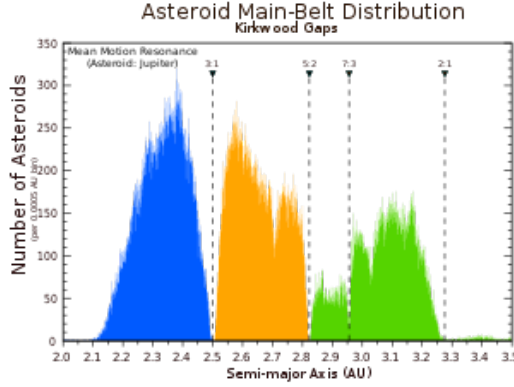


Figure 1: Distribution of asteroids in the Asteroid belt

normally hyperbolic invariant laminations (NHIL). These are hyperbolic sets which are homeomorphic to a Cantor set times a cylinder.

The purpose of this paper is to build a NHIL along the 3 : 1 mean motion resonance for the RPE3BP with $\mu = 0.95387536 \times 10^{-3}$ and $e_0 > 0$ small enough. This lamination lies in the vicinity of two homoclinic channels to the cylinder analyzed in [FGKR16]. A key ingredient to analyze this NHIL is the so-called *separatrix map*, which is an induced return map from the neighborhood of the homoclinic channels to themselves.

Both the separatrix map and the NHIL are key ingredients in the companion paper [GKMR23] to show that the Arnold diffusion orbits on the NHIL can be approximated by a 1-dimensional stochastic diffusion processes (at time scales $t \sim e_0^{-2}$), where randomness comes from the choice of initial condition according to certain measure with support at the NHIL.

The RPE3BP is a $2\frac{1}{2}$ degree of freedom Hamiltonian system given by

$$\mathcal{H}_\mu(y, x, t; e_0) = \frac{\|y\|^2}{2} - \frac{1 - \mu}{\|x + \mu x_0(t; e_0)\|} - \frac{\mu}{\|x - (1 - \mu)x_0(t; e_0)\|}, \quad (1)$$

where $x, y \in \mathbb{R}^2$ are the position and momentum of the Asteroid, $\|\cdot\|$ is the Euclidean distance and x_0 is the normalized position of the primaries (or “fictitious body”) at time t , so that the Sun and Jupiter have respective positions $-\mu x_0(t; e_0)$ and $(1 - \mu)x_0(t; e_0)$. Without loss of generality one can assume that x_0 has semi-major axis 1 and period 2π , and then it can be written as

$$x_0(t; e_0) = r(t; e_0)(\cos f(t; e_0), \sin f(t; e_0))$$

where $r(t; e_0)$ is the distance between the primaries, given by

$$r(t; e_0) = \frac{1 - e_0^2}{1 + e_0 \cos f(t; e_0)},$$

and $f(\cdot; e_0) : \mathbb{T} \rightarrow \mathbb{T}$ is the mean anomaly which satisfies $f(0; e_0) = 0$ and

$$\frac{df}{dt} = \frac{(1 + e_0 \cos f)^2}{(1 - e_0^2)^{3/2}}.$$

For $e_0 \geq 0$ the RPE3BP has two and a half degrees of freedom. When $e_0 = 0$, the primaries describe uniform circular motions around their center of mass (indeed $f(t; 0) = t$). This system is often called

the *Restricted Planar Circular 3 Body Problem* and in what follows is abbreviated RPC3BP. In a frame rotating with the primaries, this system becomes autonomous and hence has only two degrees of freedom. Its energy in the rotating frame is a first integral, called *the Jacobi integral* or *the Jacobi constant*. It is defined by

$$J(y, x) = \frac{\|y\|^2}{2} - \frac{1 - \mu}{\|x + \mu(1, 0)\|} - \frac{\mu}{\|x - (1 - \mu)(1, 0)\|} - (x_1 y_2 - x_2 y_1). \quad (2)$$

If Jupiter performs circular motion, since the system has only two degrees of freedom, KAM invariant tori are 2-dimensional and separate the 3-dimensional energy surfaces (see [Arn63, SM95]). This prevents the existence of Arnold diffusion. On the contrary, the elliptic problem in rotating coordinates, which (identifying \mathbb{R}^2 with \mathbb{C}) becomes

$$\mathcal{H}(y, x, t; e_0) = \frac{\|y\|^2}{2} - \frac{1 - \mu}{\|x + \mu x_0(t; e_0) e^{-it}\|} - \frac{\mu}{\|x - (1 - \mu) x_0(t; e_0) e^{-it}\|} - (x_1 y_2 - x_2 y_1). \quad (3)$$

is time dependent and therefore possesses a 5 dimensional phase space. Then, the existing 3-dimensional KAM tori do not prevent orbits from wandering on a 5-dimensional phase space and, therefore, Arnold diffusion is possible.

1.1 Main results

To state the main results we assume an ansatz for the RPC3BP. Roughly speaking, the ansatz states that the RPC3BP is “typical” in certain sense. More precisely, that it possesses a family of hyperbolic periodic orbits close to the 3:1 resonance with transverse homoclinic points (as happens typically at the resonances of nearly integrable 2 degrees of freedom Hamiltonian systems).

Ansatz 0. Consider the Hamiltonian of the RPC3BP (2) with $\mu = 0.95387536 \times 10^{-3}$. In every energy level $\mathbf{J} \in [\mathbf{J}_-, \mathbf{J}_+]$:

- There exists a hyperbolic periodic orbit $\lambda_{\mathbf{J}}$ of period $T_{\mathbf{J}}$ with

$$9\mu < |T_{\mathbf{J}} - 2\pi| < 15\mu, \quad (4)$$

such that its osculating semimajor axis satisfies

$$\left| a_{\mathbf{J}}(t) - 3^{-2/3} \right| < 30\mu$$

for all $t \in [0, T_{\mathbf{J}}]$. The periodic orbit and its period depend analytically on \mathbf{J} .

- The stable and unstable invariant manifolds of every $\lambda_{\mathbf{J}}$, $W^s(\lambda_{\mathbf{J}})$ and $W^u(\lambda_{\mathbf{J}})$, intersect transversally at two primary homoclinic points. Moreover, these homoclinic points depend analytically on \mathbf{J} and their orbits are confined to the interval

$$\left| a - 3^{-2/3} \right| < 56\mu.$$

Ansatz 1 rephrases this ansatz in Delaunay coordinates, which are the ones used throughout the paper. Its validity is checked numerically in Appendix A for the Jacobi constant interval $[\mathbf{J}_-, \mathbf{J}_+] = [-1.581, -1.485]$. Regarding the estimates in (4), the exact lower and upper bounds are not important. What is crucial is that

$$0 < |T_{\mathbf{J}} - 2\pi| < \frac{\pi}{2},$$

to avoid certain resonances.

Note that if one considers the RPC3BP in the 5-dimensional extended phase space (adding time as variable), the family of periodic orbits give rise to a 3-dimensional normally hyperbolic invariant cylinder foliated by 2-dimensional invariant tori (since one adds the angle $\dot{t} = 1$). Next proposition provides a symplectic system of coordinates which straightens the cylinder, its invariant manifolds and the homoclinic channels for a suitable Poincaré map.

Proposition 1.1. *Fix an interval of Jacobi constant $[\mathbf{J}_-, \mathbf{J}_+]$ as in Ansatz 0 and $M > 0$. Then, there exists a canonical transformation*

$$\Phi : \mathcal{D} = \{(I, s, p, q, g) : I \in [I_-, I_+], (s, g) \in \mathbb{T}^2, |p|, |q| \leq M, |pq| \leq \rho\} \rightarrow (\mathbb{R}^4 \times \mathbb{T}) \cap \{J(x, y) \in [\mathbf{J}_-, \mathbf{J}_+]\},$$

where $[I_-, I_+] = [-\mathbf{J}_+, -\mathbf{J}_-]$ such that the Hamiltonian $J \circ \Phi$ induces a Poincaré map \mathcal{P}_0 from $\{g = 0\}$ to itself such that

- \mathcal{P}_0 has a normally hyperbolic invariant cylinder

$$\tilde{\Lambda}_0 = \{(I, s, p, q) : p = q = 0, I \in [I_-, I_+], s \in \mathbb{T}\}.$$

- The (local) stable invariant manifold of $\tilde{\Lambda}_0$ is $\{q = 0\}$ and the (local) unstable manifold is given by $\{p = 0\}$.
- The two homoclinic channels to the cylinder are parameterized as

$$\tilde{\mathcal{C}}_0^i = \{(I, s, p, q) = (I, s, 0, q^i(I)), I \in [I_-, I_+], s \in \mathbb{T}\}, \quad i = 1, 2 \quad (5)$$

for some smooth functions $q^i : [I_-, I_+] \rightarrow \mathbb{R}$.

This proposition is proven in full detail in [GKMR23]. To make the present paper self contained we include a description of the proof in Section 2.

Now we define the separatrix maps associated to the Poincaré map \mathcal{P}_{e_0} induced by the Hamiltonian $\mathcal{H} \circ \Phi$ (see (3)) onto the section $\{g = 0\}$. Note that the objects provided by Proposition 1.1 are persistent for $e_0 > 0$ small enough thanks to normal hyperbolicity and transversality.

Consider open neighborhoods $\mathcal{U}^i \subset \{g = 0\}$ of the homoclinic channels. Then, we define the return time functions $N^{ij} : \mathcal{U}^i \rightarrow \mathbb{Z}$ as

$$N^{ij}(z) = \min \{n > 0 : \mathcal{P}_{e_0}^n(z) \in \mathcal{U}^j\}. \quad (6)$$

Note that for a lot of points N^{ij} may not be defined. On the contrary, in the domains where they are finite, open non-empty sets which we denote by $\mathcal{U}^{ij} \subset \mathcal{U}^i$, $i, j \in \{1, 2\}$, defined as

$$\mathcal{U}^{ij} = \{z \in \mathcal{U}^i : N^{ij}(z) < \infty\},$$

one can consider the separatrix maps

$$\mathcal{SM}_{e_0}^{ij} : \mathcal{U}^{ij} \rightarrow \mathcal{U}^j \quad \text{as} \quad \mathcal{SM}_{e_0}^{ij}(z) = \mathcal{P}_{e_0}^{N^{ij}(z)}(z). \quad (7)$$

Note that N^{ij} is locally constant. Thus, in suitable open subsets of \mathcal{U}^{ij} these maps are smooth.

To derive formulas for the separatrix maps in Theorem 1.3 below, we restrict them to strictly smaller domains $\mathcal{U}_\rho^{ij} \subset \mathcal{U}^{ij}$ defined as follows. Fix $\delta > 0$ small and $\kappa > 1$, we define the subsets

$$\mathcal{U}_\rho^{ij} \subset \{(I, s, p, q) \in \mathcal{U}^{ij} : I \in [I_- + \delta, I_+ - \delta], s \in \mathbb{T}, \rho^\kappa \leq p \leq \rho, |q - q^i(I)| \leq \rho\}, \quad i, j = 1, 2, \quad (8)$$

where q^i are the homoclinic channels introduced in (5).

Theorem 1.3 below provides the expansion of the separatrix map of the elliptic problem up to order 2 in e_0 and we analyze which s -harmonics each term has. To this end, we introduce the following notation.

Definition 1.2. For every smooth function f that is 2π -periodic in s , we define $\mathcal{N}(f)$ as the set of integers $k \in \mathbb{Z}$ such that the k -th harmonic of f (possibly depending on other variables) is non-zero.

Next theorem summarizes Theorem 3.1, that produces the separatrix map associated to the circular problem, and Theorem 3.2, where the separatrix map of the elliptic problem is written as a perturbation of the one of the circular problem.

Theorem 1.3. Assume Ansatz 0 and fix $\delta > 0$, $\kappa > 1$, $M > 0$. There exists $0 < \rho \ll 1$ and $e_0^* > 0$ such that for any $e_0 \in (0, e_0^*)$, there exists a system of coordinates $(\widehat{I}, \widehat{s}, \widehat{p}, \widehat{q})$ on

$$\mathcal{D} = \{(I, s, p, q, g) : I \in [I_- + \delta, I_+ - \delta], (s, g) \in \mathbb{T}^2, |p|, |q| \leq M, |pq| \leq \rho\},$$

satisfying

$$(\widehat{I}, \widehat{s}, \widehat{p}, \widehat{q}) = (I, s, p, q) + \mathcal{O}(e_0),$$

such that, on the domain \mathcal{U}_ρ^{ij} introduced in (8), which satisfies $\mathcal{U}_\rho^{ij} \subset \mathcal{D}$, the separatrix map $\mathcal{SM}_{e_0}^{ij} : \mathcal{U}_\rho^{ij} \rightarrow \mathcal{U}^j$ in (7), is well defined. Moreover, dropping the hats in the coordinates, the separatrix map $\mathcal{SM}_{e_0}^{ij} = (\mathcal{F}_{I, e_0}^{ij}, \mathcal{F}_{s, e_0}^{ij}, \mathcal{F}_{p, e_0}^{ij}, \mathcal{F}_{q, e_0}^{ij})$ is as follows.

- The (I, s) components are given by

$$\begin{pmatrix} \mathcal{F}_{I, e_0}^{ij} \\ \mathcal{F}_{s, e_0}^{ij} \end{pmatrix} = \begin{pmatrix} \mathcal{F}_{I, 0}^{ij} + e_0 \mathcal{F}_{I, 1}^{ij} + e_0^2 \mathcal{F}_{I, 2}^{ij} + \mathcal{O}_{C^2}(e_0^3 \log^3 \rho) \\ \mathcal{F}_{s, 0}^{ij} + e_0 \mathcal{F}_{s, 1}^{ij} + \mathcal{O}_{C^2}(e_0^2 \log^3 \rho) \end{pmatrix},$$

where

$$\begin{pmatrix} \mathcal{F}_{I, 0}^{ij} \\ \mathcal{F}_{s, 0}^{ij} \end{pmatrix} = \begin{pmatrix} I \\ s + \alpha_i(I) + (\nu(I) + \partial_I F(I, pq)) N^{ij}(I, p, q) + D^i(I, p, q) \end{pmatrix},$$

F and ν are the functions introduced in Lemma 2.3, N^{ij} is the return time introduced in (6), which is locally constant and satisfies $N^{ij}(I, p, q) \sim |\log \rho|$ and D^i is of the form

$$D^i(I, p, q) = a_{10}^i(I)p + a_{01}^i(I)(q - q^i(I)) + \mathcal{O}_2(p, q - q^i(I)).$$

and

$$\mathcal{F}_{z, k}^{ij} = \mathcal{M}_i^{z, k}(I, s) + \mathcal{M}_{i, pq}^{z, k}(I, s, p, q), \quad z = I, s, \quad k = 1, 2,$$

where the functions $\mathcal{M}_i^{z, k}$ and $\mathcal{M}_{i, pq}^{z, k}$ are C^2 and satisfy

$$\mathcal{M}_i^{I, l} = \mathcal{O}_{C^2}(1), \quad \mathcal{M}_i^{s, 1} = \mathcal{O}_{C^2}(\log \rho), \quad \mathcal{M}_{i, pq}^{I, l} = pq \mathcal{O}_{C^2}(1), \quad \mathcal{M}_{i, pq}^{s, 1} = pq \mathcal{O}_{C^2}(\log \rho)$$

and

$$\mathcal{N}(\mathcal{M}_i^{z, 1}) = \mathcal{N}(\mathcal{M}_{i, pq}^{z, 1}) = \{\pm 1\}, \quad z = I, s \quad \text{and} \quad \mathcal{N}(\mathcal{M}_i^{I, 2}) = \mathcal{N}(\mathcal{M}_{i, pq}^{I, 2}) = \{0, \pm 2\}.$$

- The (p, q) components are of the form

$$\begin{pmatrix} \mathcal{F}_{p, e_0}^{ij} \\ \mathcal{F}_{q, e_0}^{ij} \end{pmatrix} = \begin{pmatrix} \mathcal{F}_{p, 0}^{ij} + e_0 \mathcal{F}_{p, 1}^{ij} + \mathcal{O}_{C^2}(e_0^2 \log \rho) \\ \mathcal{F}_{q, 0}^{ij} + e_0 \mathcal{F}_{q, 1}^{ij} + \mathcal{O}_{C^2}(e_0^2 \log \rho) \end{pmatrix},$$

where

$$\begin{pmatrix} \mathcal{F}_{p,0}^{ij} \\ \mathcal{F}_{q,0}^{ij} \end{pmatrix} = \begin{pmatrix} e^{-\Theta^i(I,p,q)N^{ij}} & 0 \\ 0 & e^{\Theta^i(I,p,q)N^{ij}} \end{pmatrix} \left[\begin{pmatrix} p_0^i(I) \\ 0 \end{pmatrix} + \begin{pmatrix} b_{10}^i(I) & b_{01}^i(I) \\ c_{10}^i(I) & c_{01}^i(I) \end{pmatrix} \begin{pmatrix} p \\ q - q^i(I) \end{pmatrix} + \mathcal{O}_2(p, q - q^i(I)) \right],$$

with

$$\Theta^i(I, p, q) = \partial_2 F(I_*^i(I, p, q), p_*^i(I, p, q), q_*^i(I, p, q)),$$

where I_*^i, p_*^i, q_*^i are the images of the gluing map given in Lemma 3.8 and F is given by Lemma 2.3. Moreover, the functions a_*^i, b_*^i, c_*^i and p_0^i satisfy

$$b_{10}^i c_{01}^i - b_{01}^i c_{10}^i = 1, \quad a_{10}^i = c_{10}^i \partial_I p_0^i, \quad a_{01}^i = c_{01}^i \partial_I p_0^i \quad (9)$$

and

$$c_{01}^i \neq 0. \quad (10)$$

The functions $\mathcal{F}_{p,1}^{ij}, \mathcal{F}_{q,1}^{ij}$ satisfy $\mathcal{F}_{p,1}^{ij}, \mathcal{F}_{q,1}^{ij} = \mathcal{O}_{C^2}(\log \rho)$ and $\mathcal{N}(\mathcal{F}_{p,1}^{ij}) = \mathcal{N}(\mathcal{F}_{q,1}^{ij}) = \{\pm 1\}$.

Proposition 3.3 below rewrites certain terms appearing in the separatrix maps in terms of Melnikov-type integrals. This is necessary to verify certain non-degeneracy conditions (see Ansatz 2 below) which are crucial in the companion paper [GKMR23].

The separatrix map given by Theorem 1.3 is used to prove the existence of a normally hyperbolic invariant lamination. That is a (weakly) invariant set which is homeomorphic to

$$\Sigma \times [I_- + \delta, I_+ - \delta] \times \mathbb{T}, \quad \text{where } \Sigma = \{0, 1\}^{\mathbb{Z}},$$

and is normally hyperbolic (see Definition 4.3).

Theorem 1.4. Fix $0 < \rho \ll 1$ and consider ρ -neighborhoods B_ρ^j of the homoclinic channels given in Proposition 1.1. Then, for $0 \leq e_0 \ll 1$, the separatrix map \mathcal{SM}_{e_0} given in Theorem 1.3 has a NHIL denoted by \mathcal{L}_{e_0} which satisfies $\mathcal{L}_{e_0} \subset B_\rho^1 \cup B_\rho^2$. That is,

- The set \mathcal{L}_{e_0} is weakly invariant: there exists an embedding

$$L_{e_0} : \Sigma \times [I_- + \delta, I_+ - \delta] \times \mathbb{T} \rightarrow B_\rho^1 \cup B_\rho^2 \quad L_{e_0}(\omega, I, s) = (I, s, P_{e_0}(\omega, I, s), Q_{e_0}(\omega, I, s))$$

and functions β, S_{e_0} and J_{e_0} , which are C^3 in (I, s, e_0) and ϑ -Hölder in ω , for some $\vartheta \in (0, 1)$ independent of ρ , such that

$$\begin{aligned} \mathcal{SM}_{e_0}(I, s, P_{e_0}(\omega, I, s), Q_{e_0}(\omega, I, s)) \\ = (\mathcal{I}_{e_0}(\omega, I, s), \mathcal{S}_{e_0}(\omega, I, s), P_{e_0} \circ \mathcal{F}_{\text{inn}}(\omega, I, s), Q_{e_0} \circ \mathcal{F}_{\text{inn}}(\omega, I, s)) \end{aligned}$$

with

$$\mathcal{F}_{\text{inn}}(\omega, I, s) = (\sigma\omega, \mathcal{I}_{e_0}(\omega, I, s), \mathcal{S}_{e_0}(\omega, I, s)), \quad (11)$$

where $\sigma : \Sigma \rightarrow \Sigma$ is the Bernoulli shift and

$$\begin{aligned} \mathcal{I}_{e_0}(\omega, I, s) &= I + J_{e_0}(\omega, I, s) \\ \mathcal{S}_{e_0}(\omega, I, s) &= s + \beta(\omega, I) + S_{e_0}(\omega, I, s). \end{aligned}$$

- The set \mathcal{L}_{e_0} is normally hyperbolic.

Moreover, there exists $\zeta' > \zeta_* > 0$ such that

$$\rho^{\zeta'} \lesssim \inf_{z \in \mathcal{L}_0, z' \in \tilde{\mathcal{C}}_0^i, i=1,2} \text{dist}(z, z') \leq \sup_{z \in \mathcal{L}_0, z' \in \tilde{\mathcal{C}}_0^i, i=1,2} \text{dist}(z, z') \lesssim \rho^{\zeta_*}.$$

This theorem is proven in two steps in Section 4. First, we prove Theorem 4.4, which provides the existence of the NHIL for the circular problem ($e_0 = 0$). Note that when $e_0 = 0$, I is a constant of motion. Then, Ansatz 0 and Birkhoff-Smale Theorem leads to the existence of a Smale horseshoe for each I for the circular problem, that depends regularly on I (see Section 4.3 for the detailed construction). This gives rise to a Normally Hyperbolic Invariant Lamination in the extended phase space. Then, in Theorem 4.5, we prove the existence of the NHIL for the elliptic problem as a regular perturbation of the NHIL of the circular one. The dynamics of the NHIL is given by the separatrix map provided by Theorem 1.3.

1.2 Literature

As already mentioned and explained in more detail in Section 1.3 below, Theorems 1.3 and 1.4 are key steps to show that at certain time scales the Arnold diffusion orbits at mean motion resonances behave as a diffusion process. We refer to the companion paper [GKMR23] for references both on the connection between Arnold diffusion and Ito processes and on the astronomical motivations of this work. We focus here on the previous literature on the analysis of separatrix maps and the use of NHILs in Arnold diffusion.

The analysis of separatrix maps was initiated by Zaslavsky and Filonenko [ZF68] for near-integrable Hamiltonian systems of one-and-a-half degrees of freedom and independently by Shilnikov [Shi65] for the unfoldings of some bifurcations. It was first used in the study of Arnold diffusion by Treschev in [Tre02] (see also [Pif06, PT07, GKZ16]). In proving Theorem 1.3, we follow closely the tools developed in [Tre02]. However, note that [Tre02] deals with a priori unstable Hamiltonian systems and therefore the separatrix map can be described rather globally in the stochastic zone. On the contrary, in the present paper we are dealing with an a priori chaotic model and therefore we just analyze the separatrix map in suitable neighborhoods of two homoclinic channels, more in the spirit of the seminal Shilnikov paper [Shi65] and as happens in [Pif06]. Furthermore, since in the companion paper we want to analyze stochastic behavior at time scales $t \sim e_0^{-2}$, in Theorem 1.3 we analyze the asymptotic expansion of the separatrix map up to order 2 in e_0 (as was done in [GKZ16]).

Normally Hyperbolic Invariant Laminations were first constructed by Hirsch, Pugh and Shub in [HPS77] and first used in Arnold diffusion phenomena by Gelfreich and Turaev in [GT08]. They have also been used to obtain optimal stability time estimates by Bounemoura and Pennamen [BP12] and more recently to relate Arnold diffusion and diffusive processes for a priori unstable nearly integrable Hamiltonian systems in [KZ15]. The proof in the present paper relies on the isolating block argument developed in [KZ15].

1.3 Stochastic Arnold diffusion

Theorems 1.3 and 1.4 are key steps in proving the stochastic diffusive behavior of certain Arnold diffusion orbits. Roughly speaking, [GKMR23] shows that Arnold diffusion orbits behave as an Ito diffusion at time scales $t \sim e_0^{-2}$, where randomness comes from the choice of initial condition according to a measure whose support lies on a normally hyperbolic invariant lamination (see Theorems 1.1 and 1.2 in [GKMR23] for the precise statements).

The proof is achieved through a perturbative analysis. We start with the Hamiltonian of the 2 body problem

$$\mathcal{H}_0(y, x) = \frac{\|y\|^2}{2} - \frac{1}{\|x\|},$$

and we perform two perturbations:

- From the 2 body problem Hamiltonian \mathcal{H}_0 to the circular Hamiltonian

$$\mathcal{H}_{\text{circ},\mu}(y, x, t) = \frac{\|y\|^2}{2} - \frac{1 - \mu}{\|x + \mu x_0(t, 0)\|} - \frac{\mu}{\|x - (1 - \mu)x_0(t, 0)\|}.$$

- From the circular Hamiltonian $\mathcal{H}_{\text{circ},\mu}$ to the elliptic Hamiltonian \mathcal{H}_μ (see (1)).

Let us explain the main steps of the proof of the main results in [GKMR23] and what is the contribution of the present paper to them.

1. For the 2 body problem the Kirkwood gap 3 : 1 is defined by the semimajor axis $a = 3^{-2/3}$, where $2a = \mathcal{H}_0^{-1}$. For each eccentricity $e \in [0, 1)$, there is a one parameter family of periodic orbits, each represented by an ellipse with semimajor axis a and eccentricity e . It turns out that, at the Kirkwood gap, e is an implicit function of \mathbf{J} .
2. Consider the Hamiltonian of the circular problem $\mathcal{H}_{\text{circ},\mu}$, which is an $O(\mu)$ -perturbation of \mathcal{H}_0 (recall that we are taking $\mu = 0.95387536 \times 10^{-3}$). Ansatz 0, which is verified numerically in Appendix A, assumes that
 - (a) There exists a family of saddle periodic orbits $p_{\mathbf{J}}$ of the RPC3BP at the 3 : 1 mean motion resonance parametrized by the Jacobi constant $\mathbf{J} \in [\mathbf{J}_-, \mathbf{J}_+]$ and
 - (b) For values $\mathbf{J} \in [\mathbf{J}_-, \mathbf{J}_+]$, the associated stable and unstable invariant manifolds $W^s(p_{\mathbf{J}})$ and $W^u(p_{\mathbf{J}})$ intersect transversally (within the Jacobi constant level) at two distinct homoclinic orbits. Each transverse intersection gives rise to a homoclinic channel.
3. For each homoclinic channel, we determine a collection of open sets $\{\mathcal{U}_n\}_{n \geq n_0}$ for some n_0 large and such that the separatrix map \mathcal{SM}_{e_0} is well defined and consists of n iterates of the Poincaré map onto de section $\{g = 0\}$, when restricted to \mathcal{U}_n . This is shown in Theorem 1.3, which also provides its e_0 -expansion, and proven in Section 3.
4. We prove that the separatrix map \mathcal{SM}_{e_0} restricted to these open sets $\{\mathcal{U}_n\}_n$ is partially hyperbolic and, using an isolating block technique, construct a normally hyperbolic lamination Λ . The existence of this lamination is provided by Theorem 1.4 and proven in Section 4.
5. We derive a normal form for the dynamics of \mathcal{SM}_{e_0} restricted to the lamination Λ such that it is conjugate to a skew shift model. This is done in Lemma 5.1 and Proposition 5.7 of [GKMR23]. This normal form requires certain non-degeneracy conditions which are provided by Ansatz 2 below and verified numerically in Appendix B.
6. To prove stochastic diffusive behavior for the skew shift model, we analyze first a “reduced model”: a Lie group (circle) extension of hyperbolic maps, for which one can prove decay of correlations and central limit theorems for certain measures. For some of these measures (called Type 2 in [GKMR23]) these properties were proven in [FMT03] and for others (called Type 1 in [GKMR23]) are proven in Theorem 5.4 of [GKMR23].
7. Last step is to prove the convergence to the Itô process through a martingale analysis. Such analysis is provided by Lemma 5.10 in [GKMR23].

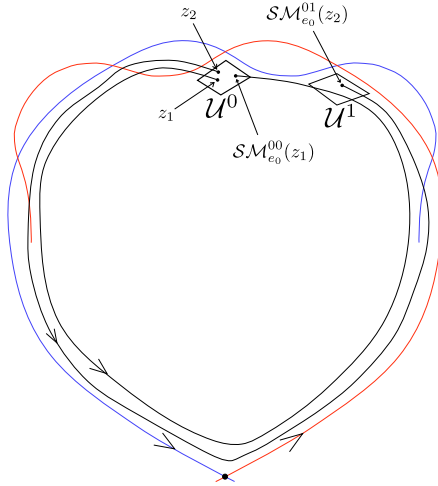


Figure 2: The separatrix map, defined on open sets in \mathcal{U}_0 and \mathcal{U}_1 , close to the two homoclinic channels.

Acknowledgements

This work was partially supported by the grant PID-2021-122954NB-100 and PID2021-123968NB-100 funded by MCIN/AEI/10.13039/501100011033 and “ERDF A way of making Europe. M. G. is supported by the Catalan Institution for Research and Advanced Studies via an ICREA Academia Prize 2019. V.K. is also partially supported by the ERC Advanced Grant SPERIG (# 885707). P. M. is also partially supported by PID2024-158570NB-I00. This work is also supported by the Spanish State Research Agency through the Severo Ochoa and María de Maeztu Program for Centers and Units of Excellence in R&D(CEX2020-001084-M).

2 The a priori chaotic framework

2.1 A good system of coordinates and a time reparameterization

In this section we reproduce Section 2 of [GKMR23] and we write the RPE3BP Hamiltonian \mathcal{H}_μ , defined in (1) in the classical Delaunay coordinates (L, ℓ, G, \hat{g}, t) , which are defined as follows. Let the polar coordinates r and φ be defined as

$$q = (r \cos \varphi, r \sin \varphi),$$

we introduce,

- L as the square of the semimajor axis of the instantaneous ellipse, which satisfies

$$-\frac{1}{2L^2} = \frac{\|p\|^2}{2} - \frac{1}{\|q\|}.$$

- $G = q \times p$ is the angular momentum. The eccentricity of the ellipse is defined through L and G by

$$\mathbf{e} = \sqrt{1 - \frac{G^2}{L^2}}.$$

- \hat{g} is the argument of the pericenter.
- ℓ is the mean anomaly defined as follows. The true anomaly v is the angle of the body with respect to the perihelion measured from the focus of the ellipse. That is, $\varphi = v + \hat{g}$. From v , one can compute the eccentric anomaly u by

$$\tan \frac{v}{2} = \sqrt{\frac{1+e}{1-e}} \tan \frac{u}{2}$$

and from it the mean anomaly ℓ by the Kepler equation

$$\ell = u - e \sin u.$$

In these coordinates, the Hamiltonian (1) becomes of the form

$$\hat{H}(L, \ell, G, \hat{g} - t, t) = -\frac{1}{2L^2} + \mu \Delta H_{\text{circ}}(L, \ell, G, \hat{g} - t, \mu) + \mu e_0 \Delta H_{\text{ell}}(L, \ell, G, \hat{g} - t, t, \mu, e_0), \quad (12)$$

where $e_0 \in (0, 1)$ is the primaries' eccentricity. Define the new angle $g = \hat{g} - t$ (the argument of the pericenter, measured in the rotating frame) and a new variable I conjugate to time t . Then we have

$$H(L, \ell, G, g, I, t) = -\frac{1}{2L^2} - G + \mu \Delta H_{\text{circ}}(L, \ell, G, g, \mu) + \mu e_0 \Delta H_{\text{ell}}(L, \ell, G, g, t, \mu, e_0) + I. \quad (13)$$

Without loss of generality we can restrict our study to $H = 0$.

We consider the RPE3BP as a perturbation of the circular one, i.e. $e_0 = 0$,

$$H_{\text{circ}}(L, \ell, G, g) = -\frac{1}{2L^2} - G + \mu \Delta H_{\text{circ}}(L, \ell, G, g, \mu). \quad (14)$$

Now we perform a Poincaré-Cartan reduction so that g becomes the new time. To this end, it is enough to consider a Hamiltonian K such that¹

$$H(L, \ell, -K(L, \ell, I, t, g), g, I, t) = 0.$$

Note that it can be rewritten as

$$K(L, \ell, I, t, g) = -\frac{1}{2L^2} - I + \mu \Delta K_{\text{circ}}(L, \ell, I, g) + \mu e_0 \Delta K_{\text{ell}}(L, \ell, I, t, g; e_0). \quad (15)$$

We also define

$$K_{\text{circ}}(L, \ell, I, g) = -\frac{1}{2L^2} - I + \mu \Delta K_{\text{circ}}(L, \ell, I, g). \quad (16)$$

It can be easily checked that the Hamiltonian equations associated to (15), coincide with

$$\begin{aligned} \frac{d}{ds} \ell &= \frac{\partial_L H}{-1 + \mu \partial_G \Delta H_{\text{circ}} + \mu e_0 \partial_G \Delta H_{\text{ell}}} & \frac{d}{ds} L &= -\frac{\partial_\ell H}{-1 + \mu \partial_G \Delta H_{\text{circ}} + \mu e_0 \partial_G \Delta H_{\text{ell}}} \\ \frac{d}{ds} g &= 1 & \frac{d}{ds} G &= -\frac{\partial_g H}{-1 + \mu \partial_G \Delta H_{\text{circ}} + \mu e_0 \partial_G \Delta H_{\text{ell}}} \\ \frac{d}{ds} t &= \frac{1}{-1 + \mu \partial_G \Delta H_{\text{circ}} + \mu e_0 \partial_G \Delta H_{\text{ell}}} & \frac{d}{ds} I &= -\frac{\mu e_0 \partial_t \Delta H_{\text{ell}}}{-1 + \mu \partial_G \Delta H_{\text{circ}} + \mu e_0 \partial_G \Delta H_{\text{ell}}} \end{aligned} \quad (17)$$

¹Note that we change the order of the variables so that the new time g is at the end.

and, in particular, when $e_0 = 0$, the equations associated to K_{circ} are given by

$$\begin{aligned} \frac{d}{ds}\ell &= \frac{\partial_L H_{\text{circ}}}{-1 + \mu\partial_G \Delta H_{\text{circ}}} & \frac{d}{ds}L &= -\frac{\partial_\ell H_{\text{circ}}}{-1 + \mu\partial_G \Delta H_{\text{circ}}} \\ \frac{d}{ds}g &= 1 & \frac{d}{ds}G &= -\frac{\partial_g H_{\text{circ}}}{-1 + \mu\partial_G \Delta H_{\text{circ}}} \\ \frac{d}{ds}t &= \frac{1}{-1 + \mu\partial_G \Delta H_{\text{circ}}} & \frac{d}{ds}I &= 0, \end{aligned} \tag{18}$$

whose right hand side is t independent.

2.2 The invariant cylinder and the associated homoclinic channels

We now describe the invariant objects that we consider and also define further changes of coordinates in suitable neighborhoods of them. Relying on numerical computations in Appendix A we assume the following ansatz, which is a rephrasing on Ansatz 0 in Delaunay coordinates.

Ansatz 1. *Consider the Hamiltonian (14) with $\mu = 0.95387536 \times 10^{-3}$. In every energy level $\mathbf{J} \in [\mathbf{J}_-, \mathbf{J}_+]$:*

- *There exists a hyperbolic periodic orbit $\lambda_{\mathbf{J}} = (L_{\mathbf{J}}(t), \ell_{\mathbf{J}}(t), G_{\mathbf{J}}(t), g_{\mathbf{J}}(t))$ of period $T_{\mathbf{J}}$ with*

$$9\mu < |T_{\mathbf{J}} - 2\pi| < 15\mu, \tag{19}$$

such that

$$\left| L_{\mathbf{J}}(t) - 3^{-1/3} \right| < 19\mu$$

for all $t \in [0, T_{\mathbf{J}}]$. The periodic orbit and its period depend analytically on \mathbf{J} ².

- *The stable and unstable invariant manifolds of every $\lambda_{\mathbf{J}}$, $W^s(\lambda_{\mathbf{J}})$ and $W^u(\lambda_{\mathbf{J}})$, intersect transversally at two primary homoclinic points. Moreover, these homoclinic points depend analytically on \mathbf{J} and their orbits are confined in the interval*

$$\left| L - 3^{-1/3} \right| < 42\mu.$$

This ansatz is similar (in fact stronger) to that in [FGKR16]. Later we impose an additional Ansatz (see Ansatz 2). In Appendix A we check that it is satisfied in the Jacobi constant interval $[\mathbf{J}_-, \mathbf{J}_+] = [-1.581, -1.485]$.

Ansatz 1 and the fact that the right hand side of the (18) is t independent, implies that there exist analytic functions (ℓ_0, L_0) such that the (ℓ, L, g, G) components of (18) have a periodic orbit for each

$$I_0 \in [I_-, I_+] = [-\mathbf{J}_+, -\mathbf{J}_-].$$

that can be parameterized as

$$\begin{aligned} \ell &= \ell_0(I, g) \\ L &= L_0(I, g). \end{aligned} \tag{20}$$

²The analyticity with respect to \mathbf{J} is just a consequence of the analyticity of the Hamiltonian (14).

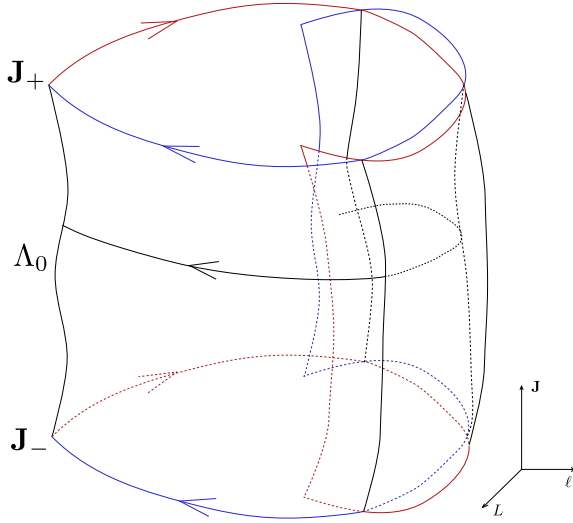


Figure 3: The periodic orbits provided by Ansatz 1 give rise to a normally hyperbolic invariant cylinder, as stated in Corollary 2.1. It possesses two transverse homoclinic channels.

Corollary 2.1. *Assume Ansatz 1 holds. The system (18) with $\mu = 0.95387536 \times 10^{-3}$, associated to K_{circ} , has an analytic normally hyperbolic³ invariant 3-dimensional cylinder Λ_0 , which is foliated by 2-dimensional invariant tori.*

The cylinder Λ_0 has stable and unstable invariant manifolds, denoted $W^s(\Lambda_0)$ and $W^u(\Lambda_0)$. In the invariant planes $I = I_0$, for every $I_0 \in [I_-, I_+]$ the manifolds $W^s(\Lambda_0)$ and $W^u(\Lambda_0)$ intersect transversally at two homoclinic channels \mathcal{C}_0^1 and \mathcal{C}_0^2 .

The next two lemmas, proven in [GKMR23], perform changes of coordinates to Hamiltonian K_{circ} . The first of them places the periodic orbits at the origin and the second one is the classical Moser Normal Form [Mos56] in a neighborhood around them.

Lemma 2.2. *There exists an analytic g -time dependent symplectic change of coordinates $(\widehat{L}, \widehat{\ell}, I, \widehat{t}, g) = \Psi(L, \ell, t, I, g)$, of the form*

$$\begin{aligned}\widehat{L} &= L - L_0(I, g) \\ \widehat{\ell} &= \ell - \ell_0(I, g) \\ I &= I \\ \widehat{t} &= t + T(L, \ell, I, g)\end{aligned}$$

and periodic in g such that the periodic orbit (20) is translated to $(\widehat{L}, \widehat{\ell}, I) = (0, 0, I)$ and the function T satisfies

$$T(L_0(I, g), \ell_0(I, g), I, g) = 0. \quad (21)$$

Lemma 2.3. *Consider the Hamiltonian K_{circ} in (16) and the change of coordinates Ψ introduced in Lemma 2.2. Then, there exists an analytic g -time dependent symplectic change of coordinates*

³See Definition 4.1 for the precise definition of Normally Hyperbolic Invariant Manifold.

$(I, s, p, q, g) = \Upsilon(\widehat{L}, \widehat{\ell}, \widehat{I}, \widehat{t}, g)$ of the form

$$\begin{aligned} I &= I & p &= P(\widehat{L}, \widehat{\ell}, \widehat{I}, g) \\ s &= \widehat{t} + B(\widehat{L}, \widehat{\ell}, \widehat{I}) & q &= Q(\widehat{L}, \widehat{\ell}, \widehat{I}, g), \end{aligned}$$

such that

$$B(0, 0, \widehat{I}, g) = 0$$

and the Hamiltonian $K_{\text{circ}} \circ \Psi^{-1} \circ \Upsilon^{-1}$ is of the form

$$\mathcal{K}_0(I, p, q) = K_{\text{circ}} \circ \Psi^{-1} \circ \Upsilon^{-1}(I, p, q) = E(I) + F(I, pq), \quad (22)$$

where the frequency

$$\nu(I) = \partial_I E(I) \quad (23)$$

satisfies

$$\frac{9}{2\pi}\mu \leq |\nu(I) - 1| \leq \frac{15}{2\pi}\mu \quad (24)$$

and F satisfies $F(I, pq) = \lambda(I)pq + \mathcal{O}_2(pq)$, where $\lambda(I)$ is the positive eigenvalue of the periodic orbit $(p, q) = (0, 0)$ given by Ansatz 1.

The next corollary rephrases Corollary 2.1 in the new system of coordinates.

Corollary 2.4. *Assume Ansatz 1 holds. Then the Hamiltonian (22) with $\mu = 0.95387536 \times 10^{-3}$ has an analytic normally hyperbolic invariant 3-dimensional cylinder*

$$\Lambda_0 = \{(p, q) = (0, 0), I \in [I_-, I_+], (g, s) \in \mathbb{T}^2\},$$

which is foliated by 2-dimensional invariant tori.

Moreover, for every $I_0 \in [I_-, I_+]$, in the invariant planes $I = I_0$, the invariant manifolds $W^s(\Lambda_0)$ and $W^u(\Lambda_0)$ intersect transversally at two homoclinic channels \mathcal{C}_0^1 and \mathcal{C}_0^2 . Their intersection with $\{g = 0\}$ are parameterized as

$$(I, s, p, q) = (I, s, 0, q^1(I)) \quad \text{and} \quad (I, s, p, q) = (I, s, 0, q^2(I)) \quad (25)$$

for some smooth functions $q^i : [I_-, I_+] \rightarrow \mathbb{R}$ and $s \in \mathbb{T}$, respectively.

To analyze the elliptic problem for $e_0 > 0$ small enough, we start by expressing the elliptic Hamiltonian perturbation ΔK_{ell} in (15) in the new coordinates. We define

$$\Delta \mathcal{K}_{\text{ell}} = \Delta K_{\text{ell}} \circ \Psi^{-1} \circ \Upsilon^{-1}, \quad (26)$$

where Ψ and Υ are the symplectic changes of coordinates introduced in Lemmas 2.2 and 2.3 respectively. We define the transformed elliptic Hamiltonian

$$\mathcal{K} = K \circ \Psi^{-1} \circ \Upsilon^{-1} = \mathcal{K}_0 + \mu e_0 \Delta \mathcal{K}_{\text{ell}} \quad (27)$$

(see (22)).

Classical perturbation theory ensures the persistence of the structures provided by Corollary 2.4 for $e_0 > 0$ small enough. In particular, we denote by Λ_{e_0} the perturbed cylinder, which is e_0 -close to the cylinder Λ_0 defined in Corollary 2.4. Analogously, we can define the cylinder for the Poincaré map \mathcal{P}_{e_0} associated to this Hamiltonian and the section $\{g = 0\}$, given by $\widetilde{\Lambda}_{e_0} = \Lambda_{e_0} \cap \{g = 0\}$. (Recall

that changes performed in Lemmas 2.2 and 2.3 have not modified g and thus the section is defined independently of the system of coordinates).

By Corollary 2.1, the Poincaré map \mathcal{P}_0 of the RPC3BP has transverse homoclinic channels

$$\tilde{\mathcal{C}}_0^i = \mathcal{C}_0^i \cap \{g = 0\}, \quad i = 1, 2, \quad (28)$$

for $I \in [I_-, I_+]$. By a transversality argument, for any predetermined $\delta > 0$ and $e_0 > 0$ small enough, the elliptic problem also possesses transverse homoclinic channels $\tilde{\mathcal{C}}_{e_0}^i$, $i = 1, 2$ in slightly smaller domains $I \in [I_- + \delta, I_+ - \delta]$, which are $\mathcal{O}(e_0)$ -close to $\tilde{\mathcal{C}}_0^i$. This is summarized in the next theorem.

Theorem 2.5. *Assume Ansatz 1 holds. Let \mathcal{P}_{e_0} be the Poincaré map associated to the Hamiltonian \mathcal{K} in (27) and the section $\{g = 0\}$. For any $\delta > 0$, there exists $e_0^* > 0$ such that for $e_0 \in (0, e_0^*)$ the map \mathcal{P}_{e_0} has a normally hyperbolic locally invariant manifold $\tilde{\Lambda}_{e_0}$, which is e_0 -close in the C^1 -topology to the unperturbed cylinder $\tilde{\Lambda}_0 = \Lambda_0 \cap \{g = 0\}$ of the circular problem and can be written as a graph over it. Namely, there exists a function $\mathcal{G}_{e_0} : [I_- + \delta, I_+ - \delta] \times \mathbb{T} \rightarrow \mathbb{R}^3 \times \mathbb{T}$ such that*

$$\tilde{\Lambda}_{e_0} = \{\mathcal{G}_{e_0}(I, s) : (I, s) \in [I_- + \delta, I_+ - \delta] \times \mathbb{T}\}.$$

Moreover, in the region $I \in [I_- + \delta, I_+ - \delta]$ the invariant manifolds $W^u(\tilde{\Lambda}_{e_0})$ (resp. $W^s(\tilde{\Lambda}_{e_0})$) intersect transversally along homoclinic channels $\tilde{\mathcal{C}}_{e_0}^i$, $i = 1, 2$ which are e_0 -close to the homoclinic channels $\tilde{\mathcal{C}}_0^i$, $i = 1, 2$ respectively.

3 The separatrix map for the circular and elliptic problems

We devote this section to prove Theorem 1.3. We first split it in two. Theorem 3.1 below provides formulas for $\mathcal{SM}_{e_0}^{ij}$ with $e_0 = 0$ (that is for the RPC3BP). Then, in Theorem 3.2, we give formulas for $\mathcal{SM}_{e_0}^{ij}$ for $0 < e_0 \ll 1$. Finally Proposition 3.3 rewrites certain terms in the separatrix maps in terms of Melnikov-type integrals. This is crucial to verify numerically that they satisfy certain non-degeneracy conditions (see Ansatz 2 below).

Theorem 3.1. *Assume Ansatz 1 and fix $\delta > 0$, $\kappa > 1$. There exists $0 < \rho \ll 1$ such that, on the domain \mathcal{U}_ρ^{ij} in (8), the separatrix map $\mathcal{SM}_0^{ij} : \mathcal{U}_\rho^{ij} \rightarrow \mathcal{U}^j$ in (7) is well defined and its components $\mathcal{SM}_0^{ij} = (\mathcal{F}_{I,0}^{ij}, \mathcal{F}_{s,0}^{ij}, \mathcal{F}_{p,0}^{ij}, \mathcal{F}_{q,0}^{ij})$ have the following form.*

- The (I, s) components are given by

$$\begin{pmatrix} \mathcal{F}_{I,0}^{ij} \\ \mathcal{F}_{s,0}^{ij} \end{pmatrix} = \begin{pmatrix} I \\ s + \alpha_i(I) + (\nu(I) + \partial_I F(I, pq))N^{ij}(I, p, q) + D^i(I, p, q) \end{pmatrix},$$

where F and ν are the functions introduced in Lemma 2.3, N^{ij} is the return time introduced in (6), which is locally constant and satisfies

$$N^{ij}(I, p, q) \sim |\log \rho|$$

and D^i is of the form

$$D^i(I, p, q) = a_{10}^i(I)p + a_{01}^i(I)(q - q^i(I)) + \mathcal{O}_2(p, q - q^i(I)).$$

- The (p, q) components are of the form

$$\begin{pmatrix} \mathcal{F}_{p,0}^{ij} \\ \mathcal{F}_{q,0}^{ij} \end{pmatrix} = \begin{pmatrix} e^{-\Theta^i(I,p,q)N^{ij}} & 0 \\ 0 & e^{\Theta^i(I,p,q)N^{ij}} \end{pmatrix} \left[\begin{pmatrix} p_0^i(I) \\ 0 \end{pmatrix} + \begin{pmatrix} b_{10}^i(I) & b_{01}^i(I) \\ c_{10}^i(I) & c_{01}^i(I) \end{pmatrix} \begin{pmatrix} p \\ q - q^i(I) \end{pmatrix} + \mathcal{O}_2(p, q - q^i(I)) \right],$$

with

$$\Theta^i(I, p, q) = \partial_2 F(I_*^i(I, p, q), p_*^i(I, p, q), q_*^i(I, p, q)), \quad (29)$$

where I_*^i, p_*^i, q_*^i are the images of the gluing map given in Lemma 3.8 and F is given by Lemma 2.3.

Moreover, the functions a_*^i, b_*^i, c_*^i and p_0^i satisfy

$$b_{10}^i c_{01}^i - b_{01}^i c_{10}^i = 1, \quad a_{10}^i = c_{10}^i \partial_I p_0^i, \quad a_{01}^i = c_{01}^i \partial_I p_0^i \quad (30)$$

and

$$c_{01}^i \neq 0. \quad (31)$$

Theorem 3.2. Assume Ansatz 1 and fix $\delta > 0, \kappa > 1, M > 0$. There exists $0 < \rho \ll 1$ and $e_0^* > 0$ such that for any $e_0 \in (0, e_0^*)$, there exists a system of coordinates $(\widehat{I}, \widehat{s}, \widehat{p}, \widehat{q})$ on

$$\mathcal{D} = \{(I, s, p, q, g) : I \in [I_- + \delta, I_+ - \delta], (s, g) \in \mathbb{T}^2, |p|, |q| \leq M, |pq| \leq \rho\},$$

satisfying

$$(\widehat{I}, \widehat{s}, \widehat{p}, \widehat{q}) = (I, s, p, q) + \mathcal{O}(e_0),$$

such that, on the domain \mathcal{U}_ρ^{ij} introduced in (8), which satisfies $\mathcal{U}_\rho^{ij} \subset \mathcal{D}$, the separatrix map $\mathcal{SM}_{e_0}^{ij} : \mathcal{U}_\rho^{ij} \rightarrow \mathcal{U}^j$ in (7), is well defined. Moreover, dropping the hats in the coordinates, the separatrix map $\mathcal{SM}_{e_0}^{ij} = (\mathcal{F}_{I,e_0}^{ij}, \mathcal{F}_{s,e_0}^{ij}, \mathcal{F}_{p,e_0}^{ij}, \mathcal{F}_{q,e_0}^{ij})$ is as follows.

- The (I, s) components are given by⁴

$$\begin{pmatrix} \mathcal{F}_{I,e_0}^{ij} \\ \mathcal{F}_{s,e_0}^{ij} \end{pmatrix} = \begin{pmatrix} \mathcal{F}_{I,0}^{ij} + e_0 \mathcal{F}_{I,1}^{ij} + e_0^2 \mathcal{F}_{I,2}^{ij} + \mathcal{O}_{C^2}(e_0^3 \log^3 \rho) \\ \mathcal{F}_{s,0}^{ij} + e_0 \mathcal{F}_{s,1}^{ij} + \mathcal{O}_{C^2}(e_0^2 \log^3 \rho) \end{pmatrix},$$

where $\mathcal{F}_{I,0}^{ij}, \mathcal{F}_{s,0}^{ij}$ are the functions introduced in Theorem 3.1 and

$$\begin{aligned} \mathcal{F}_{I,1}^{ij} &= \mathcal{M}_i^{I,1}(I, s) + \mathcal{M}_{i,pq}^{I,1}(I, s, p, q) \\ \mathcal{F}_{I,2}^{ij} &= \mathcal{M}_i^{I,2}(I, s) + \mathcal{M}_{i,pq}^{I,2}(I, s, p, q) \\ \mathcal{F}_{s,1}^{ij} &= \mathcal{M}_i^{s,2}(I, s) + \mathcal{M}_{i,pq}^{s,1}(I, s, p, q), \end{aligned}$$

where $\mathcal{M}_i^{*,*}$ are C^2 functions which satisfy

$$\mathcal{M}_i^{I,l} = \mathcal{O}_{C^2}(1), \quad \mathcal{M}_i^{s,1} = \mathcal{O}_{C^2}(\log \rho), \quad \mathcal{M}_{i,pq}^{I,l} = pq \mathcal{O}_{C^2}(1), \quad \mathcal{M}_{i,pq}^{s,1} = pq \mathcal{O}_{C^2}(\log \rho)$$

and

$$\mathcal{N}(\mathcal{M}_i^{z,1}) = \mathcal{N}(\mathcal{M}_{i,pq}^{z,1}) = \{\pm 1\}, \quad z = I, s \quad \text{and} \quad \mathcal{N}(\mathcal{M}_i^{I,2}) = \mathcal{N}(\mathcal{M}_{i,pq}^{I,2}) = \{0, \pm 2\}.$$

⁴In the estimates of the errors below, note that the power in the logarithms could be more accurate. Indeed, the C^0 norm of the errors is $\mathcal{O}(e_0^3 \log \rho)$ and the C^1 norm is $\mathcal{O}(e_0^3 \log^2 \rho)$. Since, we consider ρ fixed and take e_0 arbitrarily small, these logarithms do not play role.

- The (p, q) components are of the form

$$\begin{pmatrix} \mathcal{F}_{p, e_0}^{ij} \\ \mathcal{F}_{q, e_0}^{ij} \end{pmatrix} = \begin{pmatrix} \mathcal{F}_{p, 0}^{ij} + e_0 \mathcal{F}_{p, 1}^{ij} + \mathcal{O}_{C^2}(e_0^2 \log \rho) \\ \mathcal{F}_{q, 0}^{ij} + e_0 \mathcal{F}_{q, 1}^{ij} + \mathcal{O}_{C^2}(e_0^2 \log \rho) \end{pmatrix},$$

where $\mathcal{F}_{p, 0}^{ij}, \mathcal{F}_{q, 0}^{ij}$ are the functions introduced in Theorem 3.1 and the functions $\mathcal{F}_{p, 1}^{ij}, \mathcal{F}_{q, 1}^{ij}$ satisfy $\mathcal{F}_{p, 1}^{ij}, \mathcal{F}_{q, 1}^{ij} = \mathcal{O}_{C^2}(\log \rho)$ and $\mathcal{N}(\mathcal{F}_{p, 1}^{ij}) = \mathcal{N}(\mathcal{F}_{q, 1}^{ij}) = \{\pm 1\}$.

These theorems are proven in Section 3.1. The main improvement on [Tre02, Pif06] is to perform a second order analysis in e_0 of the separatrix map.

For the analysis in the companion paper [GKMR23], we need explicit formulas for the functions $\mathcal{M}_i^{I, 1}$ and $\alpha_i(I)$ in terms of the original system (17) (see Ansatz 2 below). Indeed, they will Melnikov-type integrals defined through the functions ΔH_{circ} and ΔH_{ell} introduced in (12). In [FGKR16] it was checked that they satisfy

$$\mathcal{N}(\Delta H_{\text{circ}}) = \{0\} \quad \text{and} \quad \mathcal{N}(\Delta H_{\text{ell}}|_{e_0=0}) = \{\pm 1\}. \quad (32)$$

We need to introduce some more notation. Since the right hand side of (18) does not depend on t , one can consider it for the coordinates (ℓ, L, g, G) treating I as a constant. Denote by Φ_0^{circ} its flow. Ansatz 1 implies that, for each value $I \in [I^-, I^+]$, this flow has a periodic orbit with two transverse homoclinic orbits. We denote the time-parameterization of this periodic orbit by $\lambda_I(s)$ and those of the two homoclinic orbits by $\gamma_I^i(s)$ with $i = 1, 2$. Moreover, since \dot{t} in (18) only depends on (ℓ, L, g, G, I) , it can be integrated on the periodic orbit to obtain

$$t = t_0 + \tilde{\lambda}_I(s), \quad \tilde{\lambda}_I(s) = \int_0^s \frac{1}{-1 + \mu \partial_G \Delta H_{\text{circ}}(\lambda_I(\sigma))} d\sigma$$

and analogously on the homoclinic orbits to obtain analogously $t = t_0 + \tilde{\gamma}_I^i(s)$.

Proposition 3.3. *The functions $\alpha_i(I)$ and $\mathcal{M}_i^{I, 1}(I, s)$ introduced in Theorems 3.1 and 3.2 respectively satisfy the following.*

- $\alpha_i(I)$ can be written as $\alpha_i(I) = \alpha_i^+(I) - \alpha_i^-(I)$ with

$$\alpha_i^\pm(I) = \mu \lim_{N \rightarrow \pm\infty} \left(\int_0^{2\pi N} \frac{(\partial_G \Delta H_{\text{circ}}) \circ \gamma_I^i(\sigma)}{-1 + \mu (\partial_G \Delta H_{\text{circ}}) \circ \gamma_I^i(\sigma)} d\sigma + 2\pi N \nu(I) \right) \quad (33)$$

where ν is the function defined in (23).

- The function $\mathcal{M}_i^{I, 1}(I, s)$ satisfies $\mathcal{N}(\mathcal{M}_i^{I, 1}(I, s)) = \{\pm 1\}$ and can be written as

$$\mathcal{M}_i^{I, 1}(I, s) = B_i(I) e^{is} + \overline{B_i}(I) e^{-is}$$

with $B_i = B_i^{\text{in}} + B_i^{\text{out}}$ where

$$B_i^{\text{in}}(I) = i\mu \frac{1 - e^{i\alpha_i(I)}}{1 - e^{i2\pi\nu(I)}} \int_0^{2\pi} \frac{\Delta H_{\text{ell}}^{1,+} \circ \lambda_I(\sigma)}{-1 + \mu \partial_G \Delta H_{\text{circ}} \circ \lambda_I(\sigma)} e^{i\tilde{\lambda}_I(\sigma)} d\sigma. \quad (34)$$

$$B_i^{\text{out}}(I) = -i\mu \lim_{T \rightarrow +\infty} \int_0^T \left(\frac{\Delta H_{\text{ell}}^{1,+} \circ \gamma_I^i(\sigma)}{-1 + \mu \partial_G \Delta H_{\text{circ}} \circ \gamma_I^i(\sigma)} e^{i\tilde{\gamma}_I^i(\sigma)} \right. \\ \left. - \frac{\Delta H_{\text{ell}}^{1,+} \circ \lambda_I(\sigma)}{-1 + \mu \partial_G \Delta H_{\text{circ}} \circ \lambda_I(\sigma)} e^{i(\tilde{\lambda}_I(\sigma) + \alpha_i^+(I))} \right) d\sigma \quad (35) \\ + i\mu \lim_{T \rightarrow -\infty} \int_0^T \left(\frac{\Delta H_{\text{ell}}^{1,+} \circ \gamma_I^i(\sigma)}{-1 + \mu \partial_G \Delta H_{\text{circ}} \circ \gamma_I^i(\sigma)} e^{i\tilde{\gamma}_I^i(\sigma)} \right. \\ \left. - \frac{\Delta H_{\text{ell}}^{1,+} \circ \lambda_I(\sigma)}{-1 + \mu \partial_G \Delta H_{\text{circ}} \circ \lambda_I(\sigma)} e^{i(\tilde{\lambda}_I(\sigma) + \alpha_i^-(I))} \right) d\sigma,$$

where $\Delta H_{\text{ell}}^{1,+}$ is defined by $\Delta H_{\text{ell}}^1(I, s) = \Delta H_{\text{ell}}^{1,+}(I) e^{is} + \Delta H_{\text{ell}}^{1,-}(I) e^{-is}$, with $\Delta H_{\text{ell}}^1 = \Delta H_{\text{ell}}|_{e_0=0}$ (see (32)).

This proposition is proved in Section 3.2.

3.1 Derivation of the separatrix map: Proof of Theorems 3.1 and 3.2

We devote this section to prove Theorems 3.1 and 3.2, by providing formulas for the separatrix maps of the circular and elliptic problems. Note that both theorems are proven at the same time. To prove both theorems we follow the approach in [Tre02, GKZ16] adapted to an a priori chaotic setting and to the features of the RPE3BP (in particular, to the harmonic structure of the expansion in e_0 of the Hamiltonian (36)).

The proof is achieved in three steps:

1. We perform a normal form to the elliptic Hamiltonian (36) in a neighborhood of the normally hyperbolic invariant cylinder and we extend it along its stable and unstable invariant manifolds. Note that the normal form transformation becomes multivaluated when extended to the homoclinic channels. This is done in Section 3.1.1.
2. We analyze the flow of the normal form Hamiltonian (see Section 3.1.2).
3. We analyze the gluing maps which relate the two extensions of the normal form along the stable and unstable invariant manifolds (see Section 3.1.3).

These three steps lead to the formulas of the separatrix map provided in Theorems 3.1 and 3.2.

3.1.1 A normal form for the elliptic Hamiltonian

To perform a normal form procedure, the first step is to expand the elliptic Hamiltonians \mathcal{K} in (27) in powers of the parameter e_0 . Consider the elliptic Hamiltonian perturbation ΔK_{ell} expressed in Delaunay coordinates (see (15)) and expand it in powers of e_0 ,

$$\Delta K_{\text{ell}}(L, \ell, g, I, t; e_0) = K_1(L, \ell, g, I, t) + e_0 K_2(L, \ell, g, I, t) + \mathcal{O}(e_0^2).$$

In [FGKR16], it is shown that nontrivial harmonics of K_1 and K_2 satisfy the following

$$\mathcal{N}(K_1) = \{\pm 1\}, \quad \mathcal{N}(K_2) \subset \{0, \pm 1, \pm 2\}$$

(see Definition 1.2).

Lemma 3.4. *The Hamiltonian \mathcal{K} in (27) is of the form*

$$\mathcal{K}(I, s, p, q, g) = \mathcal{K}_0(I, p, q, g) + e_0 \mathcal{K}_1(I, s, p, q, g) + e_0^2 \mathcal{K}_2(I, s, p, q, g) + \mathcal{O}(e_0^3), \quad (36)$$

where \mathcal{K}_0 is the Hamiltonian introduced in Lemma 2.3 and $\mathcal{K}_i = K_i \circ \Psi^{-1} \circ \Upsilon^{-1}$ satisfy

$$\mathcal{N}(\mathcal{K}_1) = \{\pm 1\}, \quad \mathcal{N}(\mathcal{K}_2) \subset \{0, \pm 1, \pm 2\}.$$

Proof. This lemma is a direct consequence of the particular form of the changes obtained in Lemmas 2.2 and 2.3. \square

We perform two steps of normal form to the Hamiltonian (36). This normal form extends the Moser coordinates to the region where $|qp|$ is small and straightens the invariant manifolds up to errors $\mathcal{O}(e_0^3)$. The normal form procedure follows the same lines as the one in [GKZ16]. Nevertheless, it has some differences since we do not have resonances and therefore it can be performed globally in a compact domain of the form

$$\mathcal{D}_{\rho, \delta, \mathbf{M}} = \{(I, s, p, q, g) : I \in [I_- + \delta, I_+ - \delta], (s, g) \in \mathbb{T}^2, |p|, |q| \leq \mathbf{M}, |pq| \leq \rho\}. \quad (37)$$

Proposition 3.5. *Fix $\mathbf{M}_2 > \mathbf{M}_1$ and $\delta > 0$. Consider the Hamiltonian \mathcal{K} given by Lemma 3.4. Then, there exists $\rho^* > 0$ such that for any $\rho \in (0, \rho^*)$ there exists a symplectic transformation*

$$\Phi : \mathcal{D}_{\rho/2, 2\delta, \mathbf{M}_1} \rightarrow \mathcal{D}_{\rho, \delta, \mathbf{M}_2}$$

such that

1. *The Hamiltonian $\mathcal{K} \circ \Phi$ is of the form*

$$\mathcal{K} \circ \Phi(\widehat{I}, \widehat{s}, \widehat{p}, \widehat{q}, \widehat{g}) = E(\widehat{I}) + F_0(\widehat{I}, \widehat{p}\widehat{q}) + e_0^2 F_1(\widehat{I}, \widehat{p}\widehat{q}) + \mathcal{O}(e_0^3).$$

2. *The changes of coordinates Φ is of the form*

$$\begin{aligned} I &= \widehat{I} + e_0 M_1^I + e_0^2 M_2^I + \mathcal{O}(e_0^3) \\ s &= \widehat{s} + e_0 M_1^s + e_0^2 M_2^s + \mathcal{O}(e_0^3) \\ p &= \widehat{p} + e_0 M_1^p + e_0^2 M_2^p + \mathcal{O}(e_0^3) \\ q &= \widehat{q} + e_0 M_1^q + e_0^2 M_2^q + \mathcal{O}(e_0^3) \end{aligned}$$

where each M_*^z is a C^2 function and, for $z = I, p, q, s$, satisfies

$$\begin{aligned} M_1^z &= \mathcal{O}(1) \quad \text{and} \quad \mathcal{N}(M_1^z) = \{\pm 1\} \\ M_2^z &= \mathcal{O}(1) \quad \text{and} \quad \mathcal{N}(M_2^z) \subset \{0, \pm 1, \pm 2\}. \end{aligned}$$

The proof of this proposition is deferred to the end of this section (Section 3.1.5). It follows the approach in [Tre02], but it presents significant differences. Indeed, there the normal form procedure only removes the first order in e_0 and pq whereas in the present paper we remove completely the terms up to errors of order $\mathcal{O}(e_0^3)$.

Corollary 3.6. *The inverse change Φ^{-1} is of the same form, that is*

$$\begin{aligned}\widehat{I} &= I - e_0 M_1^I + e_0^2 \widetilde{M}_2^I + \mathcal{O}(e_0^3) \\ \widehat{s} &= s - e_0 M_1^s + e_0^2 \widetilde{M}_2^s + \mathcal{O}(e_0^3) \\ \widehat{p} &= p - e_0 M_1^p + e_0^2 \widetilde{M}_2^p + \mathcal{O}(e_0^3) \\ \widehat{q} &= q - e_0 M_1^q + e_0^2 \widetilde{M}_2^q + \mathcal{O}(e_0^3),\end{aligned}$$

where the functions \widetilde{M}_2^z satisfy the same properties as M_2^z .

3.1.2 The flow in the normal form variables

The equations associated to the Hamiltonian given in Proposition 3.5 are

$$\begin{aligned}\dot{I} &= \mathcal{O}(e_0^3) \\ \dot{s} &= \nu(I) + \partial_I F_0(I, pq) + e_0^2 \partial_I F_1(I, pq) + \mathcal{O}(e_0^3) \\ \dot{p} &= -(\partial_2 F_0(I, pq) + e_0^2 \partial_2 F_1(I, pq) + \mathcal{O}(e_0^3)) p + \mathcal{O}(e_0^3) \\ \dot{q} &= (\partial_2 F_0(I, pq) + e_0^2 \partial_2 F_1(I, pq)) q + \mathcal{O}(e_0^3)\end{aligned}$$

and $\frac{d}{d\bar{g}}(pq) = \mathcal{O}(e_0^3)$.

Fix $0 < \rho \ll 1$ and $M > 1$ and introduce the domain

$$U_* = \{(I, s, p, q) : I \in [I_- + \delta, I_+ - \delta], M^{-1} < |p| < M, M e_0 \leq |pq| \leq \rho\}. \quad (38)$$

Lemma 3.7. *Suppose that for some $(I^*, s^*, p^*, q^*) \in U_*$ and final time $\bar{g} \in \mathbb{R}$,*

$$M^{-1} \leq |q^*| e^{\partial_2 F_0(I^*, p^* q^*) \bar{g}} \leq M.$$

Then,

$$\begin{aligned}I(\bar{g}) &= I^* + \mathcal{O}(e_0^3) \bar{g} \\ s(\bar{g}) &= s^* + (\nu(I^*) + \partial_I F_0(I^*, p^* q^*) + e_0^2 \partial_I F_1(I^*, p^* q^*)) \bar{g} + \mathcal{O}(e_0^3) \bar{g}^2 \\ p(\bar{g}) &= p^* e^{-(P_0 + e_0^2 P_1^*) \bar{g}} (1 + \mathcal{O}(e_0^3) \bar{g}) + \mathcal{O}(e_0^3) \\ q(\bar{g}) &= q^* e^{(P_0 + e_0^2 P_1^*) \bar{g}} (1 + \mathcal{O}(e_0^3) \bar{g}) \\ p(\bar{g})q(\bar{g}) &= p^* q^* + \mathcal{O}(e_0^3) \bar{g},\end{aligned}$$

where $P_0^* = \partial_2 F_0(I^*, p^* q^*)$ and $P_1^* = \partial_2 F_1(I^*, p^* q^*)$.

The proof of this lemma can be found in [GKZ16]. Even though there it is only valid for points ε -away from the invariant manifolds, one can easily check that the proof also applies to the larger domain U_* in (38).

3.1.3 The gluing maps

The Moser normal form coordinates obtained in Lemma 2.3 can be extended along the stable and unstable invariant manifolds of the cylinder. Note that this extension is multivaluated. Indeed, when propagating the coordinates along the stable and unstable invariant manifolds, we reach domains

where the invariant manifolds intersect. In this overlapping domain, we have “stable” Moser coordinates (Moser coordinates propagated along the stable manifold) and “unstable” Moser coordinates. Following Treschev [Tre02], we call gluing map to the diffeomorphism which expresses the stable Moser coordinates in terms of the unstable ones.

We devote this section to analyze these gluing maps. We first analyze them in the original Moser normal form coordinates. We compute them in neighborhoods of the homoclinic channels. Indeed, since we are in an *a priori* chaotic setting instead of *a priori* unstable, the gluing maps can be only defined in suitable small neighborhoods of homoclinic points and not in a whole fundamental domain (as happened in [Tre02] and [GKZ16]). These gluing maps are e_0 -independent since they are defined by the Moser normal form associated to the circular problem given by Lemma 2.3.

The second step in this section is to express the gluing maps in the normal form variables obtained in Proposition 3.5. They depend on e_0 since the change of coordinates given by Proposition 3.5 does.

Since the change to Moser normal form given in Lemma 2.3 does not modify the variable g , we can study the gluing maps restricted to the section $\{g = 0\}$. We define thus ρ -neighborhoods of the homoclinic channels $\tilde{\mathcal{C}}_0^i$ in (28),

$$\mathcal{D}_\rho^i = \{I \in [I_- + \delta, I_+ - \delta], s \in \mathbb{T}, |p| \leq \rho, |q - q^i(I)| \leq \rho\} \quad \text{for } 0 < \rho \ll 1 \quad \text{and } i = 1, 2$$

(see (25)). We define the gluing maps \mathcal{G}_0^i associated to the Moser normal form coordinates in Lemma 2.3 in the domains \mathcal{D}_ρ^i .

Lemma 3.8. *Fix $0 < \rho \ll 1$ and consider the section $\{g = 0\}$. Then, the gluing map restricted to this section,*

$$\mathcal{G}_0^i : \mathcal{D}_\rho^i \rightarrow \mathbb{R} \times \mathbb{T} \times \mathbb{R}^2,$$

denoted by $(I^, s^*, p^*, q^*) = \mathcal{G}_0(I, s, p, q)$ is analytic and of the form*

$$\begin{aligned} I^* &= I \\ s^* &= s + \alpha_i(I) + a_{10}^i(I)p + a_{01}^i(I)(q - q^i(I)) + \mathcal{O}_2(p, q - q^i(I)) \\ p^* &= p_0^i(I) + b_{10}^i(I)p + b_{01}^i(I)(q - q^i(I)) + \mathcal{O}_2(p, q - q^i(I)) \\ q^* &= c_{10}^i(I)p + c_{01}^i(I)(q - q^i(I)) + \mathcal{O}_2(p, q - q^i(I)). \end{aligned}$$

Moreover, the coefficients a_{kl}^i , b_{kl}^i , c_{kl}^i are analytic functions and satisfy formulas (30) and (31).

Proof. The particular form and (30) is just a consequence of Lemma 2.3, the fact that it is symplectic and that I is a first integral. Then, it just remains to do a Taylor expansion around the homoclinic channel $(p, q) = (0, q^i(I))$.

Property (31) is a consequence of the transversality of the invariant manifolds at the homoclinic channel $\tilde{\mathcal{C}}_0^i = \mathcal{C}_0^i \cap \{g = 0\}$ given by Corollary 2.1. \square

Next step is to express the gluing maps in the coordinates obtained in Proposition 3.5. To simplify notation, we define the matrices

$$B^i(I) = \begin{pmatrix} b_{10}^i(I) & b_{01}^i(I) \\ c_{10}^i(I) & c_{01}^i(I) \end{pmatrix}, \quad i = 1, 2, \quad (39)$$

which, by (30), are invertible and satisfy $\det B^i = 1$.

Lemma 3.9. Consider the section $\{g = 0\}$, the change of coordinates Φ obtained in Proposition 3.5 and the gluing maps \mathcal{G}_0^i , $i = 1, 2$, obtained in Lemma 3.8. Then, the maps

$$\tilde{\mathcal{G}}_{e_0}^i = \Phi^{-1} \circ \mathcal{G}_0^i \circ \Phi : \mathcal{D}_\rho^i \rightarrow \mathbb{R} \times \mathbb{T} \times \mathbb{R}^2,$$

with $\rho \ll 1$, are of the form

$$\tilde{\mathcal{G}}_{e_0}^i = \mathcal{G}_0^i + e_0 \mathcal{G}_1^i + e_0^2 \mathcal{G}_2^i + \mathcal{O}(e_0^3),$$

where

- \mathcal{G}_0^i are the maps given in Lemma 3.8.
- \mathcal{G}_1^i satisfy $\mathcal{N}(\mathcal{G}_1^i) = \{\pm 1\}$ and are of the form

$$\mathcal{G}_1^i(I, s, p, q) = \begin{pmatrix} \mathcal{M}_i^{I,1}(I, s) + \mathcal{M}_{i,pq}^{I,1}(I, s, p, q) \\ \tilde{\mathcal{M}}_i^{s,1}(I, s) + \tilde{\mathcal{M}}_{i,pq}^{s,1}(I, s, p, q) \\ \mathcal{M}_i^{p,1}(I, s) + \mathcal{M}_{i,pq}^{p,1}(I, s, p, q) \\ \mathcal{M}_i^{q,1}(I, s) + \mathcal{M}_{i,pq}^{q,1}(I, s, p, q) \end{pmatrix}$$

for some functions $\mathcal{M}_*^{1,i}$ such that $\mathcal{M}_*^{1,i} = \mathcal{O}_{C^2}(1)$ with respect to e_0 and ρ . Moreover

$$\begin{aligned} \mathcal{M}_i^{I,1}(I, s) &= M_1^I(I, s, 0, q^i(I)) - M_1^I(I, s + \alpha_i(I), p_0^i(I), 0) \\ \tilde{\mathcal{M}}_i^{s,1}(I, s) &= M_1^s(I, s, 0, q^i(I)) - M_1^s(I, s + \alpha_i(I), p_0^i(I), 0) + (\alpha^i)'(I) M_1^I(I, s, 0, q^i(I)) \\ &\quad + a_{10}^i(I) M_p^{I,i}(I, s, 0, q^i(I)) + a_{01}^i(I) M_q^I(I, s, 0, q^i(I)) \\ \begin{pmatrix} \mathcal{M}_i^{p,1}(I, s) \\ \mathcal{M}_i^{q,1}(I, s) \end{pmatrix} &= B^i(I) \begin{pmatrix} M_1^p(I, s, 0, q^i(I)) \\ M_1^q(I, s, 0, q^i(I)) \end{pmatrix} - \begin{pmatrix} M_1^p(I, s + \alpha_i(I), p_0^i(I), 0) \\ M_1^q(I, s + \alpha_i(I), p_0^i(I), 0) \end{pmatrix} \\ &\quad + p_0^{i'}(I) \begin{pmatrix} M_1^I(I, s, 0, q^i(I)) \\ 0 \end{pmatrix}. \end{aligned}$$

Finally,

$$\mathcal{M}_{i,pq}^{*,1}(I, s) = \mathcal{O}(pq).$$

- \mathcal{G}_2^i satisfy $\mathcal{N}(\mathcal{G}_2^i) = \{0, \pm 1, \pm 2\}$, are of the same form as \mathcal{G}_1^i and the associated functions satisfy the same estimates.

Proof. The proof of this lemma is a direct consequence of applying the change of coordinates obtained in Lemma 3.13 to the gluing map defined in Lemma 3.8. \square

3.1.4 Formulas for the separatrix maps

In this section we obtain formulas for the separatrix map \mathcal{SM}^{ij} which go from suitable domains close to the homoclinic channel i to suitable domains close to the homoclinic channel j and thus we prove Theorem 3.2. To simplify the notation, we omit the dependence on the channels given by i and j .

Consider the flow $\Phi_{e_0}^g$ analyzed in Lemma 3.7 and the gluing maps $\tilde{\mathcal{G}}_{e_0}$ analyzed in Lemma 3.9. We compose them and we obtain the following formula for the separatrix map. This lemma completes the proof of Theorem 3.2.

Lemma 3.10. Consider the section $\{g = 0\}$. Then, the map $\mathcal{F} = \Phi_{e_0}^{\bar{g}} \circ \tilde{\mathcal{G}}_{e_0} : \{g = 0\} \rightarrow \{g = 0\}$ is given by

$$\mathcal{F}(I, s, p, q) = (\mathcal{F}_I(I, s, p, q), \mathcal{F}_s(I, s, p, q), \mathcal{F}_p(I, s, p, q), \mathcal{F}_q(I, s, p, q))$$

as follows.

- For the (I, s) components,

$$\begin{aligned} \mathcal{F}_I &= I + e_0 (\mathcal{M}^{I,1}(I, s) + \mathcal{M}_{pq}^{I,1}(I, s, p, q)) + e_0^2 (\mathcal{M}^{I,2}(I, s) + \mathcal{M}_{pq}^{I,2}(I, s, p, q)) + \mathcal{O}(e_0^3) \bar{g} \\ \mathcal{F}_s &= s + \alpha(I) + (\nu(I) + \partial_I F(I, pq)) \bar{g} + D(I, p, q) + e_0 (\mathcal{M}^{s,1}(I, s) + \mathcal{M}_{pq}^{s,1}(I, s, p, q)) + \mathcal{O}(e_0^2) \bar{g} \end{aligned}$$

where the functions $\mathcal{M}^{I,*}$ have been introduced in Lemma 3.9,

$$\begin{aligned} D(I, p, q) &= a_{10}(I)p + a_{01}(I)(q - q(I)) + \mathcal{O}(p, q - q(I)), \\ \mathcal{M}^{s,1}(I, s) &= \tilde{\mathcal{M}}^{s,1}(I, s) + \bar{g}\nu'(I)\mathcal{M}^{I,1}(I, s), \end{aligned}$$

and $\mathcal{M}_{pq}^{s,1}$ satisfies $\mathcal{M}_{pq}^{s,1} = \mathcal{O}(\bar{g})$.

- For the (p, q) components,

$$\begin{pmatrix} \mathcal{F}_p \\ \mathcal{F}_q \end{pmatrix} = \begin{pmatrix} \mathcal{F}_p^0 + e_0 \mathcal{F}_p^1 + \mathcal{O}(e_0^2) \bar{g} \\ \mathcal{F}_q^0 + e_0 \mathcal{F}_q^1 + \mathcal{O}(e_0^2) \bar{g} \end{pmatrix}$$

with

$$\begin{pmatrix} \mathcal{F}_p^0 \\ \mathcal{F}_q^0 \end{pmatrix} = \begin{pmatrix} e^{-\Theta(I,p,q)\bar{g}} & 0 \\ 0 & e^{\Theta(I,p,q)\bar{g}} \end{pmatrix} \left[\begin{pmatrix} p_0(I) \\ 0 \end{pmatrix} + \begin{pmatrix} b_{10}(I) & b_{01}(I) \\ c_{10}(I) & c_{01}(I) \end{pmatrix} \begin{pmatrix} p \\ q - 1 \end{pmatrix} + \mathcal{O}_2(p, q - q(I)) \right]$$

with

$$\Theta(I, p, q) = \partial_2 F(I^*(I, p, q), p^*(I, p, q)q^*(I, p, q)), \quad (40)$$

where I^*, p^*, q^* are the images of the gluing map given in Lemma 3.8 and F is given by Proposition 3.5.

Moreover, the functions $\mathcal{F}_p^1, \mathcal{F}_q^1$ satisfy $\mathcal{F}_p^1, \mathcal{F}_q^1 = \mathcal{O}_{C^2}(\bar{g})$ and $\mathcal{N}(\mathcal{F}_p^1) = \mathcal{N}(\mathcal{F}_q^1) = \{\pm 1\}$ and

Note that in this lemma \bar{g} is not a free parameter but is related to the distance of the original point to the stable invariant manifold. This relation is more explicitly stated in Section 4. The proof of this lemma is a direct consequence of the composition of the maps obtained in Lemmas 3.7 and 3.9.

3.1.5 The normal form: Proof of Proposition 3.5

We perform the change of coordinates by the Lie Method. We consider the expansion of the Hamiltonian \mathcal{K} given in Lemma 3.4 and we perform successive changes to remove successive orders (in e_0 and qp).

We consider a Hamiltonian $e_0 W_1$ and call Φ_1 the time-one map associated to the flow of $e_0 W_1$. This change is symplectic. Moreover,

$$\begin{aligned} \mathcal{K} \circ \Phi_1 &= \mathcal{K}_0 + e_0 (\mathcal{K}_1 + \{\mathcal{K}_0, W_1\}) \\ &\quad + e_0^2 (\{\mathcal{K}_1, W_1\} + \{\{\mathcal{K}_0, W_1\}, W_1\} + \mathcal{K}_2) + \mathcal{O}(e_0^3). \end{aligned}$$

We look for suitable W_1 such that

$$\mathcal{K}_1 + \{\mathcal{K}_0, W_1\} = 0. \quad (41)$$

To compute W_1 , we write the Hamiltonian \mathcal{K}_1 defined in Lemma 3.4, in the following way

$$\mathcal{K}_1(I, s, p, q, g) = \sum_{j \geq 0} (pq)^j \left(\mathcal{K}_1^j(I, s, g) + \mathcal{K}_1^{j,p}(I, s, p, g) + \mathcal{K}_1^{j,q}(I, s, q, g) \right)$$

where

$$\begin{aligned} \mathcal{K}_1^j(I, s, g) &= \frac{1}{(j!)^2} \partial_p^j \partial_q^j \mathcal{K}_1(I, s, 0, 0, g) \\ \mathcal{K}_1^{j,p}(I, s, p, g) &= \frac{1}{(j!)^2} \left(\partial_p^j \partial_q^j \mathcal{K}_1(I, s, p, 0, g) - \partial_p^j \partial_q^j \mathcal{K}_1(I, s, 0, 0, g) \right) \\ \mathcal{K}_1^{j,q}(I, s, q, g) &= \frac{1}{(j!)^2} \left(\partial_p^j \partial_q^j \mathcal{K}_1(I, s, 0, q, g) - \partial_p^j \partial_q^j \mathcal{K}_1(I, s, 0, 0, g) \right). \end{aligned} \quad (42)$$

The analyticity of \mathcal{K}_1 implies that this series is convergent in $\mathcal{D}_{\rho, \delta, M}$ in (37) for any given $M > 0, \delta > 0$ and taking $\rho > 0$ small enough (depending on M) and that in $\mathcal{D}_{\rho, \delta, M}$,

$$|\mathcal{K}_1^{j,*}| \leq C, \quad * = \emptyset, q, p, \quad (43)$$

for some $C > 0$ independent of ρ and j .

The next lemma contains the first step of the normal form. In the next two lemmas we denote by $\{\cdot, \cdot\}_{(q,p)}$, the Poisson bracket with respect to the conjugate variables (q, p) .

Lemma 3.11. *Fix $M' > M$ and $\delta' < \delta$. Then, for $\rho > 0$ small enough, there exists a change of coordinates $\Phi_1 : \mathcal{D}_{3\rho/4, \delta, M} \rightarrow \mathcal{D}_{\rho, \delta', M'}$ such that*

$$\|\Phi_1 - \text{Id}\|_{C^0} \leq \mathcal{O}(e_0)$$

and the Hamiltonian $\mathcal{K} \circ \Phi_1$ is of the form

$$\mathcal{K} \circ \Phi_1(\widehat{I}, \widehat{s}, \widehat{p}, \widehat{q}, \widehat{g}) = A(\widehat{I}) + F(\widehat{I}, \widehat{q}\widehat{p}) + e_0^2 \widetilde{\mathcal{K}}_2 + \mathcal{O}(e_0^3),$$

and $\widetilde{\mathcal{K}}_2$ satisfies $\mathcal{N}(\widetilde{\mathcal{K}}_2) \subset \{0, \pm 1, \pm 2\}$.

Proof. We build a function $W_1(I, s, p, q, g)$ which is a solution of equation (41), which can be rewritten as

$$(\nu(I) + \partial_I F(I, pq)) \partial_s W_1 + \partial_g W_1 + \{F(I, pq), W_1\}_{(p,q)} + \mathcal{K}_1 = 0. \quad (44)$$

We take

$$W_1(I, s, p, q, g) = \sum_{j \geq 0} (pq)^j \left(W_1^j(I, s, g) + W_1^{j,p}(I, s, p, g) + W_1^{j,q}(I, s, q, g) \right). \quad (45)$$

Then, it can be easily checked that solving equation (44) is equivalent to solving the equations

$$(\nu(I) + \partial_I F(I, pq)) \partial_s W_1^{j,*} + \partial_g W_1^{j,*} + \{F(I, pq), W_1^{j,*}\}_{(q,p)} + \mathcal{K}_1^{(j,*)} = 0, \quad * = \emptyset, q, p,$$

(note in particular that $\{F(I, pq), (pq)^j W\}_{(p,q)} = (pq)^j \{F(I, pq), W\}_{(p,q)}$).

Each equation is solved as follows. For W_1^j , we just have

$$(\nu(I) + \partial_I F(I, pq)) \partial_s W_1^j + \partial_g W_1^j + \mathcal{K}_1^j = 0. \quad (46)$$

Thus, we invert the operator

$$\widetilde{\partial} := (\nu(I) + \partial_I F(I, pq)) \partial_s + \partial_g \quad (47)$$

by using the Fourier expansion and inverting for each Fourier coefficient. Note that this operator can be inverted globally since thanks to Lemma 3.4, the Hamiltonians $\mathcal{K}_1^{(j)}$ do not have strong resonances. Indeed, Lemma 3.4 implies that these functions only have harmonics $(k_1, k_2) \in \mathbb{Z}^2$ with $k_1 = \pm 1$. Then, by (24), taking $k_1 = \pm 1$, $k_2 \in \mathbb{Z}$ and $\rho > 0$ small enough,

$$|k_1(\nu(I) + \partial_I F(I, pq)) + k_2| \geq 8\mu.$$

Therefore, using also (43), the functions W_1^j satisfy that, in $\mathcal{D}_{\rho, \delta', M'}$,

$$|W_1^j| = |\tilde{\partial}^{-1} \mathcal{K}_1^{(1)}| \leq C$$

for some $C > 0$ independent of j and ρ .

For the others, we use the characteristics method to obtain

$$\begin{aligned} W_1^{j,p} &= - \int_0^{+\infty} \mathcal{K}_1^{j,p}(I, s + (\nu(I) + \partial_I F(I, pq))g', pe^{-\partial_2 F(I, pq)g'}, g + g') dg', \\ W_1^{j,q} &= - \int_{-\infty}^0 \mathcal{K}_1^{j,q}(I, s + (\nu(I) + \partial_I F(I, pq))g', qe^{\partial_2 F(I, pq)g'}, g + g') dg' \end{aligned}$$

which also satisfy

$$\|W_1^{j,p}\|_{C^2}, \|W_1^{j,q}\|_{C^2} \leq C$$

in $\mathcal{D}_{\rho, \delta', M'}$, for some $C > 0$ independent of j and ρ .

Then, the series (45) is convergent for ρ small enough and we can define the change of coordinates Φ_1 as the time 1 map associated to the flow given by the Hamiltonian $e_0 W_1$. Then, one can easily see that it satisfies the statements of the lemma and that $\mathcal{N}(W_1) = \{\pm 1\}$.

Finally, one can easily see that

$$\tilde{\mathcal{K}}_2 = \{\mathcal{K}_1, W_1\} + \{\{\mathcal{K}_0, W_1\}, W_1\} + \mathcal{K}_2$$

where \mathcal{K}_2 is Hamiltonian defined in Lemma 3.4. Then, $\mathcal{N}(\tilde{\mathcal{K}}_2) = \{0, \pm 1, \pm 2\}$. □

Now we eliminate the e_0^2 -terms proceeding as in Lemma 3.11.

Lemma 3.12. *Fix $M'' > M'$ and $\delta'' < \delta'$. Then, for $\rho > 0$ small enough, there exists a change of coordinates $\Phi_2 : \mathcal{D}_{\rho/2, \delta', M'} \rightarrow \mathcal{D}_{3\rho/4, \delta'', M''}$ such that*

$$\|\Phi_2 - \text{Id}\|_{C^2} \leq \mathcal{O}(e_0^2)$$

and the Hamiltonian $\mathcal{K} \circ \Phi_1$ is of the form

$$\mathcal{K} \circ \Phi_1 \circ \Phi_2(\hat{I}, \hat{s}, \hat{p}, \hat{q}, \hat{g}) = A(\hat{I}) + F(\hat{I}, \hat{q}\hat{p}) + e_0^2 F_2(\hat{I}, \hat{q}\hat{p}) + \mathcal{O}(e_0^3).$$

Proof. We construct the change Φ_2 as the time 1 map associated to the flow of a Hamiltonian $e_0^2 W_2$. We consider the Hamiltonian $\mathcal{K} \circ \Phi_1$ obtained in Lemma 3.11 and we proceed as in the proof of Lemma 3.11 by looking for a function W_2 satisfying

$$\tilde{\mathcal{K}}_2 + \{\mathcal{K}_0, W_2\} = 0.$$

This equation can be solved as in Lemma 3.11. Indeed, by Lemma 3.11, $\tilde{\mathcal{K}}_2$ has only harmonics $\{0, \pm 1, \pm 2\}$. Then, by (24), and $k_1 = 0, \pm 1, \pm 2$ and $k_2 \in \mathbb{Z}$ with $k_1 k_2 \neq 0$,

$$|k_1(\nu(I) + \partial_I F(I, pq)) + k_2| \geq 18\mu.$$

Thus, proceeding as in Lemma 3.11 one can deduce the statements of Lemma 3.12. □

To complete the proof of Proposition 3.5, we need more precise information of the change of coordinates. Define

$$\Phi = \Phi_1 \circ \Phi_2 : (\widehat{I}, \widehat{s}, \widehat{p}, \widehat{q}, \widehat{g}) \longmapsto (I, s, p, q, g).$$

Lemma 3.13. *The change Φ is of the form*

$$\begin{aligned} I &= \widehat{I} + e_0 M_1^I + e_0^2 M_2^I + \mathcal{O}(e_0^3) \\ s &= \widehat{s} + e_0 M_1^s + e_0^2 M_2^s + \mathcal{O}(e_0^3) \\ p &= \widehat{p} + e_0 M_1^p + e_0^2 M_2^p + \mathcal{O}(e_0^3) \\ q &= \widehat{q} + e_0 M_1^q + e_0^2 M_2^q + \mathcal{O}(e_0^3) \end{aligned}$$

where

$$M_1^I = \partial_s W_1, \quad M_1^s = -\partial_I W_1, \quad M_1^p = -\partial_q W_1 \quad \text{and} \quad M_1^q = \partial_p W_1,$$

and W_1 is the function defined in Lemma 3.11. Moreover,

$$\mathcal{N}(M_1^z) = \{\pm 1\}, \quad M_2^z = \mathcal{O}(1) \quad \text{and} \quad \mathcal{N}(M_2^z) = \{0, \pm 1, \pm 2\} \quad z = I, p, q, s. \quad (48)$$

The inverse change is of the same form, that is

$$\begin{aligned} \widehat{I} &= I - e_0 M_1^I + e_0^2 \widetilde{M}_2^I + \mathcal{O}(e_0^3) \\ \widehat{s} &= s - e_0 M_1^s + e_0^2 \widetilde{M}_2^s + \mathcal{O}(e_0^3) \\ \widehat{p} &= p - e_0 M_1^p + e_0^2 \widetilde{M}_2^p + \mathcal{O}(e_0^3) \\ \widehat{q} &= q - e_0 M_1^q + e_0^2 \widetilde{M}_2^q + \mathcal{O}(e_0^3) \end{aligned}$$

and

$$\widetilde{q\widehat{p}} = qp - e_0 M_1^r + e_0^2 \widetilde{M}_2^r + \mathcal{O}(e_0^3).$$

The terms \widetilde{M}_2^z satisfy the same properties as M_2^z given in (48).

The proof of this lemma is analogous to the proof of Lemma 4.4 in [GKZ16]

3.2 The first order of the separatrix map: Proof of Proposition 3.3

The derivation of the formulas for $\alpha_i(I)$ follows the same lines as for the analogous terms in [Tre02]. Indeed, the homoclinic orbits $\gamma_I^i(\sigma)$ considered in Proposition 3.3 are asymptotic to the periodic orbit $\lambda_I(\sigma)$. Note that, if we choose parameterizations that such that both satisfy $g = g_0 + \sigma$, one has that $\|\gamma_I^i(\sigma) - \lambda_I(\sigma)\| \rightarrow 0$ as $\sigma \rightarrow \pm\infty$ (recall that λ_I and γ_I^i only contain the components (ℓ, L, g, I)). This convergence does not take place in the t component since there may be a time shift. Indeed, the parameterization for the t component is of the form

$$t = t_0 + \lambda_I(\sigma), \quad t = t_0 + \gamma_I^i(\sigma) \quad \text{with} \quad \lambda_I(0) = \gamma_I^i(0).$$

Then, one can easily see (see [FGKR16] for all the details) that the functions $\alpha_{\pm}^i(I)$ introduced in (33) satisfy

$$\alpha_{\pm}^i(I) = \lim_{\sigma \rightarrow \pm\infty} (\gamma_I^i(\sigma) - \lambda_I(\sigma)). \quad (49)$$

Now we prove that these functions are those appearing in the formulas for the gluing map introduced in Lemma 3.8. The first step is to point out that the shifts $\alpha_{\pm}^i(I)$ in the t variable as defined in (49) do

not change after applying the changes of coordinates from Lemmas 2.2 and 2.3. Indeed, the functions B and T involved in those changes vanish on the periodic orbits and therefore they tend to zero when evaluated at the homoclinic orbits with $\sigma \rightarrow \pm\infty$.

Now we analyze the Moser normal form Hamiltonian (22). The periodic orbit in Moser coordinates is just

$$I = I_0, \quad s^{\text{PO}} = s_0^{\text{PO}} + \nu(I)\sigma, \quad p^{\text{PO}}(\sigma) = 0, \quad q^{\text{PO}}(\sigma) = 0, \quad g = g_0 + \sigma,$$

and the homoclinic orbit γ_I^i with initial condition at the fixed homoclinic point has become the following two orbits, depending whether we extend the Moser coordinates along the stable or the unstable invariant manifolds,

$$\begin{aligned} I = I, \quad s^+ = s_0^+ + \nu(I)\sigma, \quad p^+(\sigma) = 0, \quad q^+(\sigma) = q^i(I)e^{\lambda(I)\sigma}, \quad g = g_0 + \sigma \\ I = I, \quad s^- = s_0^- + \nu(I)\sigma, \quad p^-(\sigma) = p_0^i(I)e^{-\lambda(I)\sigma}, \quad q^-(\sigma) = 0, \quad g = g_0 + \sigma. \end{aligned}$$

By definition, we have that $s_0^\pm - s_0^{\text{PO}} = \alpha_i^\pm(I)$. The gluing map \mathcal{G}_0^i maps one trajectory to the other. Thus, if we call $\mathcal{G}_{0,s}^i$ to the s -component of the gluing map, we have

$$\mathcal{G}_{0,s}^i(I, s, 0, q^i(I)) = s + \alpha_i(I).$$

The proof of the first statement of Proposition 3.3 follows by applying fundamental theorem of calculus.

Now we derive the formulas for B^i . To simplify notation we omit the dependence on i in all functions below. We rely on the definition of the function $\mathcal{M}^{I,1}$ in Lemma 3.9, that is

$$\mathcal{M}^{I,1}(I, s) = M_1^I(I, s, 0, q(I), 0) - M_1^I(I, s + \alpha(I), p_0(I), 0, 0),$$

where M_1^I is the function introduced in Proposition 3.5.

We look for formulas for this function. To this end, we need to go into the proof of Proposition 3.5 in Section 3.1.5. As stated in Lemma 3.13, the function M_1^I is defined as $M_1^I = \partial_s W_1$ where W_1 is the function introduced in the proof of Lemma 3.11 as the sum

$$W_1 = W_1^0 + W_1^{0,p} + W_1^{0,q} + \mathcal{O}(pq),$$

(see (45)). Following this sum, we can split $\mathcal{M}^{I,1}$ as a sum and analyze the first three terms.

We start with the first one. As explained in the proof of Lemma 3.11, $W_1^0 = W_1^0(I, s, g)$. Then, the first term is given by

$$\mathcal{M}^{I,1}(I, s) = \partial_s W_1^0(I, s, 0) - \partial_s W_1^0(I, s + \alpha(I), 0)$$

To look for formulas for this term, we use that, as explained in the proof of Lemma 3.11, W_1^0 satisfies

$$\nu(I)\partial_s W_1^0(I, s, g) + \partial_g W_1^0(I, s, g) + \mathcal{K}_1^{(0)} = 0.$$

Note that this equation is just (46) with $pq = 0$.

Since $\mathcal{N}(\mathcal{K}_1^{(0)}) = \mathcal{N}(\mathcal{K}_1)$, Lemma 3.4 implies $\mathcal{N}(\mathcal{K}_1^{(0)}) = \{\pm 1\}$ and the same happens for W_1^0 . Writing W_1^0 as

$$W_1^0(I, s, g) = A(I, g)e^{is} + \bar{A}(I, g)e^{-is}$$

we know that A satisfies

$$i\nu(I)A(I, g) + \partial_g A(I, g) + \mathcal{K}_1^{(0)}(I, g) = 0,$$

which has a unique solution periodic in g , which is given by

$$A(I, g) = A_0(I)e^{-i\nu(I)g} - e^{-i\nu(I)g} \int_0^g \mathcal{K}_1^{(0)}(I, \sigma)e^{i\nu(I)\sigma} d\sigma$$

with

$$A_0(I) = \frac{1}{1 - e^{2\pi i\nu(I)}} \int_0^{2\pi} \mathcal{K}_1^{(0)}(I, \sigma)e^{i\nu(I)\sigma} d\sigma.$$

Therefore

$$\mathcal{M}^{I,1}(I, s) = \mathcal{M}^{I,1,+}(I)e^{is} + \overline{\mathcal{M}^{I,1,+}(I)}e^{-is}$$

with

$$\mathcal{M}^{I,1,+}(I) = iA_0(I) \left(1 - e^{i\alpha(I)}\right) = \frac{1 - e^{i\alpha(I)}}{1 - e^{2\pi i\nu(I)}} \int_0^{2\pi} \mathcal{K}_1^{(0)}(I, \sigma)e^{i\nu(I)\sigma} d\sigma.$$

Now it only remains to write the integral in terms of the original coordinates. Note that we are integrating the Hamiltonian \mathcal{K} at $p = q = 0$, that is, along the periodic orbit. The Moser normal form change of coordinates (Lemma 2.3) is the identity on the periodic orbit. Thus, undoing the change of coordinates done at Lemma 2.2, one can see that

$$\mathcal{M}^{I,1,+}(I) = i \frac{1 - e^{i\alpha(I)}}{1 - e^{2\pi i\nu(I)}} \int_0^{2\pi} \frac{\Delta H_{\text{ell}}^{1,+} \circ \lambda_I(\sigma)}{-1 + \mu \partial_G \Delta H_{\text{circ}} \circ \lambda_I(\sigma)} e^{i\tilde{\lambda}_I(\sigma)} d\sigma,$$

where $\lambda_I(\sigma)$, $\tilde{\lambda}_I(\sigma)$ and $\Delta H_{\text{ell}}^{1,+}$ are the functions used in Proposition 3.3. This is just the function B_{in} introduced in Proposition 3.3. The function B_{out} can be obtained by analyzing the functions $W_1^{0,p}$ and $W_1^{0,q}$ and interpreting them as Menikov functions. This derivation follows exactly the same lines as the analogous derivation in [Tre02].

4 The normally hyperbolic invariant lamination

4.1 Existence of the normally hyperbolic invariant lamination

In this section we construct a Normally Hyperbolic Invariant Lamination for RPE3BP. We do it in two steps. First we analyze the Poincaré map associated to the circular problem (14). This system is autonomous and hence I is a constant of motion. Therefore building the lamination is reduced to proving the existence of a horseshoe at each level $I = \text{constant}$ and showing its regularity with respect to I . We prove its existence by an isolating block technique. As a second step, we show the existence of the NHIL for (the Poincaré map of) the elliptic problem (13) with $0 < e_0 \ll 1$. This is a regular perturbation problem and therefore the existence of the lamination is a consequence of normal hyperbolicity.

A normally hyperbolic invariant lamination generalizes the concepts of hyperbolic sets and normally hyperbolic invariant manifolds. Here we will consider a less general definition than that of [HPS77], which will be enough for our purposes. It follows the ideas in [KZ15].

First, we define normally hyperbolic invariant manifold.

Definition 4.1. *Given a C^1 map F on a manifold M , we say that that a submanifold $N \subset M$ is normally hyperbolic for the map F if it is F -invariant and one can split $T_N M$ into three invariant subbundles,*

$$T_x M = T_x N \oplus E_x^s \oplus E_x^u, \quad \text{for all } x \in N$$

which satisfy

$$\begin{aligned} \|DF^n(x)|_{E^s}\| &\leq C\lambda^n && \text{for } n \geq 0 \\ \|DF^n(x)|_{E^u}\| &\leq C\lambda^{|n|} && \text{for } n \leq 0 \\ \|DF^n(x)|_{TN}\| &\leq C\eta^{|n|} && \text{for } n \in \mathbb{N} \end{aligned}$$

for some $C > 0$, $\lambda < 1$ and $\eta \geq 1$ such that $\eta\lambda < 1$.

The concept of normally hyperbolic invariant lamination is a generalization of this definition. To this end, we define the following.

Definition 4.2. Let $\Sigma = \{0, 1\}^{\mathbb{Z}}$. We define the Bernoulli shift $\sigma : \Sigma \rightarrow \Sigma$ as $(\sigma\omega)_k = \omega_{k+1}$.

Definition 4.3. Consider a C^1 map F on a manifold M . We say that a closed set Ξ is a normally hyperbolic lamination if

$$\Xi = \bigcup_{\omega \in \Sigma} \Xi_\omega$$

where Ξ_ω are C^1 manifolds which satisfy $F(\Xi_\omega) = \Xi_{\sigma\omega}$ and is normally hyperbolic in the following sense. There exist constants $C > 0$, $\lambda < 1$ and $\eta \geq 1$ satisfying $\eta\lambda < 1$ and subbundles E^s and E^u such that for any $\omega \in \Sigma$ and $x \in \Xi_\omega$,

$$T_x M = T_x \Xi_\omega \oplus E_x^s \oplus E_x^u$$

which are invariant and satisfy

$$\begin{aligned} \|DF^n(x)|_{E^s}\| &\leq C\lambda^n && \text{for } n \geq 0 \\ \|DF^n(x)|_{E^u}\| &\leq C\lambda^{|n|} && \text{for } n \leq 0 \\ \|DF^n(x)|_{T\Xi_\omega}\| &\leq C\eta^{|n|} && \text{for } n \in \mathbb{N}. \end{aligned}$$

Finally, we say that Ξ is a normally hyperbolic lamination weakly invariant under F if there exist a neighborhood U of Ξ such that, if there exist $x \in \Xi$ such that $F(x) \notin \Xi$ implies $F(x) \notin U$.

The next two theorems prove the existence of such objects. First, Theorem 4.4 for the RPC3BP (Hamiltonian (14)) and then Theorem 4.5 for the RPE3BP with $0 < e_0 \ll 1$ (Hamiltonian (13)).

Theorem 4.4. Fix $0 < \rho \ll 1$ and consider ρ -neighborhoods B_ρ^i of the homoclinic channels $\{\tilde{\mathcal{C}}_0^i\}_{I \in \mathcal{I}}$ (see (28)) of the Poincaré map of the circular problem (14). Then, the separatrix maps \mathcal{SM}_0 associated to this problem given in Theorem 3.2 (with $e_0 = 0$) have a NHIL denoted by \mathcal{L}_0 satisfying $\mathcal{L}_0 \subset B_\rho^1 \cup B_\rho^2$. That is,

- The set \mathcal{L}_0 is invariant: there exists an embedding

$$L_0 : \Sigma \times \mathbb{T} \times \mathcal{I} \rightarrow B_\rho^1 \cup B_\rho^2 \quad L_0(\omega, I, s) = (P_0(\omega, I), Q_0(\omega, I), I, s)$$

and a function $\beta(\omega, I)$, which are C^3 in I and ϑ -Hölder in ω , for some $\vartheta \in (0, 1)$ independent of ρ , such that

$$\mathcal{SM}_0(I, s, P_0(\omega, I), Q_0(\omega, I)) = (I, s + \beta(\omega, I), P_0(\sigma\omega, I), Q_0(\sigma\omega, I)).$$

- The set \mathcal{L}_0 is normally hyperbolic.

Moreover, there exists $\zeta' > \zeta_* > 0$ such that

$$\rho^{\zeta'} \lesssim \inf_{z \in \mathcal{L}_0, z' \in \tilde{\mathcal{C}}_0^i, i=1,2} \text{dist}(z, z') \leq \sup_{z \in \mathcal{L}_0, z' \in \tilde{\mathcal{C}}_0^i, i=1,2} \text{dist}(z, z') \lesssim \rho^{\zeta_*}.$$

This theorem is proven in Section 4.3.

For $e_0 > 0$ small enough the NHIL persists for the Hamiltonian system associated to (13) and it is smooth with respect to e_0 .

Theorem 4.5. Fix $0 < \rho \ll 1$ and consider ρ -neighborhoods B_ρ^j of the homoclinic channels $\{\tilde{\mathcal{C}}_{e_0}^i\}_{I \in \mathcal{I}}$ (see Theorem 4.5) of the Poincaré map of the elliptic problem (13). Then, the separatrix maps \mathcal{SM}_{e_0} associated to this problem given in Theorem 3.2 have a NHIL denoted by \mathcal{L}_{e_0} which is e_0 -close to the NHIL \mathcal{L}_0 obtained in Theorem 4.4 and satisfies $\mathcal{L}_{e_0} \subset B_\rho^1 \cup B_\rho^2$. That is,

- The set \mathcal{L}_{e_0} is invariant: there exists an embedding

$$L_{e_0} : \Sigma \times \mathbb{T} \times \mathcal{I} \rightarrow B_\rho^1 \cup B_\rho^2 \quad L_{e_0}(\omega, I, s) = (I, s, P_{e_0}(\omega, I, s), Q_{e_0}(\omega, I, s))$$

and functions $S_{e_0}(\omega, I, s)$ and $J_{e_0}(\omega, I, s)$, which are C^3 in (I, s, e_0) and ϑ -Hölder in ω , for some $\vartheta \in (0, 1)$ independent of ρ , such that

$$\begin{aligned} \mathcal{SM}_{e_0}(I, s, P_{e_0}(\omega, I, s), Q_{e_0}(\omega, I, s)) \\ = (\mathcal{I}_{e_0}(\omega, I, s), \mathcal{S}_{e_0}(\omega, I, s), P_{e_0} \circ \mathcal{F}_{\text{inn}}(\omega, I, s), Q_{e_0} \circ \mathcal{F}_{\text{inn}}(\omega, I, s)) \end{aligned} \quad (50)$$

with

$$\mathcal{F}_{\text{inn}}(\omega, I, s) = (\sigma\omega, \mathcal{I}_{e_0}(\omega, I, s), \mathcal{S}_{e_0}(\omega, I, s))$$

and

$$\begin{aligned} \mathcal{I}_{e_0}(\omega, I, s) &= I + J_{e_0}(\omega, I, s) \\ \mathcal{S}_{e_0}(\omega, I, s) &= s + \beta(\omega, I) + S_{e_0}(\omega, I, s). \end{aligned}$$

- The set \mathcal{L}_{e_0} is normally hyperbolic.

Moreover,

- There exists $\zeta' > \zeta_* > 0$ such that

$$\rho^{\zeta'} \lesssim \inf_{z \in \mathcal{L}_0, z' \in \tilde{\mathcal{C}}_0^i, i=1,2} \text{dist}(z, z') \leq \sup_{z \in \mathcal{L}_0, z' \in \tilde{\mathcal{C}}_0^i, i=1,2} \text{dist}(z, z') \lesssim \rho^{\zeta_*}.$$

- The functions P_{e_0}, Q_{e_0} are of the form

$$(P_{e_0}, Q_{e_0}) = (P_0, Q_0) + e_0(P_1, Q_1) + \mathcal{O}(e_0^2) \quad \text{with} \quad \mathcal{N}(P_1) = \mathcal{N}(Q_1) = \{\pm 1\},$$

where (P_0, Q_0) are the functions obtained in Theorem 4.4.

- The functions S_{e_0} and J_{e_0} are of the form

$$\begin{aligned} J_{e_0} &= e_0 J_1 + e_0^2 J_2 + \mathcal{O}(e_0^3) \quad \text{with} \quad \mathcal{N}(J_1) = \{\pm 1\}, \mathcal{N}(J_2) = \{0, \pm 2\}, \\ S_{e_0} &= e_0 S_1 + \mathcal{O}(e_0^2) \quad \text{with} \quad \mathcal{N}(S_1) = \{\pm 1\} \end{aligned}$$

and⁵

$$J_1(\omega, I, s) = \mathcal{M}_{\omega_0}^{I,1}(I, s) + \mathcal{M}_{\omega, pq}^{I,1}(I, s),$$

where the right hand side functions are defined in Theorem 3.2

⁵Note that in the formula below we are abusing notation. The leading term in the order e_0 in the separatrix map, $\mathcal{M}_i^{I,1}$, only depends on (I, s) and the homoclinic channel, which now is labeled by ω_0 . On the contrary, $\mathcal{M}_{i, pq}^{I,1}(I, s, p, q)$ introduced in Theorem 3.2 depends also on p and q . When pull backed to the invariant lamination, this implies that the corresponding term depends on the full ω . Accordingly, we denote this term by $\mathcal{M}_{\omega, pq}^{I,1}(I, s)$.

4.2 Dynamics on the normally hyperbolic invariant lamination

Theorem 4.5 induces a map on the invariant lamination constructed, which can be further analyzed by relying on the formulas of the separatrix map obtained in Theorem 3.2. Let us define the induce a map as

$$\begin{aligned} \mathcal{F} : \Sigma \times \mathbb{T} \times [I_-, I_+] &\longrightarrow \Sigma \times \mathbb{T} \times \mathbb{R} \\ (\omega, s, I) &\mapsto (\sigma\omega, \mathcal{F}_\omega(s, I)) \end{aligned} \quad (51)$$

By Theorem 4.5, the leaves of the NHIL, which are cylinders with boundaries, are localized ρ^{ζ^*} -close to the homoclinic channels. Since both e_0 and ρ are taken small, $e_0 \ll \rho$, we have “good” expansions on the separatrix maps restricted into the weakly invariant lamination.

Lemma 4.6. *The separatrix map obtained in Theorem 3.2 induces a map \mathcal{F} of the form (51) on the lamination obtained in Theorem 4.5 with*

$$\mathcal{F}_\omega : \begin{pmatrix} I \\ s \end{pmatrix} \rightarrow \begin{pmatrix} I + e_0 \mathcal{A}_\omega(I, s) + e_0^2 \mathcal{B}_\omega(I, s) + \mathcal{O}_\omega(e_0^{2+a}) \\ s + \beta_\omega(I) + e_0 \mathcal{D}_\omega(I, s) + \mathcal{O}_\omega(e_0^{1+a}) \end{pmatrix} \quad (52)$$

where β_ω satisfies

$$\beta_\omega(I) = \beta_{\omega_0}^0(I) + \eta_\omega(I), \quad \beta_{\omega_0}^0(I) = \nu(I)\bar{g} + \alpha_{\omega_0}(I) \quad (53)$$

and the other functions satisfy $\mathcal{N}(\mathcal{A}_\omega) = \mathcal{N}(\mathcal{D}_\omega) = \{\pm 1\}$ and $\mathcal{N}(\mathcal{B}_\omega) = \{0, \pm 2\}$,

$$\begin{aligned} \mathcal{A}_\omega(I, s) &= \mathcal{M}_{\omega_0}^{I,1}(I, s) + \mathcal{R}_\omega^{I,1}(I, s) \\ \mathcal{B}_\omega(I, s) &= \mathcal{M}_{\omega_0}^{I,2}(I, s) + \mathcal{R}_\omega^{I,2}(I, s) \\ \mathcal{D}_\omega(I, s) &= \widetilde{\mathcal{M}}_{\omega_0}^s(I, s, \bar{g}) + \mathcal{R}_\omega^s(I, s). \end{aligned} \quad (54)$$

which satisfy

$$\mathcal{N}(\mathcal{A}_\omega) = \mathcal{N}(\mathcal{D}_\omega) = \{\pm 1\} \quad \text{and} \quad \mathcal{N}(\mathcal{B}_\omega) = \{\pm 0, \pm 2\}.$$

The functions $\mathcal{M}_{\omega_0}^*$ and α_{ω_0} are those introduced in Theorem 3.2 (see also Proposition 3.3). ν is defined in (23) and the time \bar{g} is independent of e_0 and satisfies $\bar{g} \sim |\log \rho|$. Moreover, the remainders in formulas (53) and (54) satisfy the following estimates.

$$\begin{aligned} \|\mathcal{R}_\omega^{I,j}\|_{\Sigma \times \mathbb{T} \times [I_-, I_+]} &\lesssim \rho^{\zeta^*} \\ \|\eta_\omega\|_{\Sigma \times \mathbb{T} \times [I_-, I_+]}, \|\mathcal{R}_\omega^s\|_{\Sigma \times \mathbb{T} \times [I_-, I_+]} &\lesssim \rho^{\zeta^*} |\log \rho|. \end{aligned}$$

Moreover, there exists $\vartheta \in (0, 1)$, such that the functions $\mathcal{R}_\omega^{I,j}$, \mathcal{R}_ω^s , η_ω are ϑ -Hölder with respect to ω .

Since $\rho \ll 1$, the formula for β_ω in (53) implies that each of the maps encounter many resonances, which are $|\log \rho|^{-1}$ -close. Nevertheless, they will not play any role in the random map analysis since, thanks to Ansatz 2 below, the maps have different twist condition and therefore they are not simultaneously resonant.

Ansatz 2 is crucial in the analysis of the stochastic behavior of the map \mathcal{F}_ω , done in the companion paper [GKMR23]. We include it here, even though it is not used in the present paper, since we verify it numerically in Appendix B.

Ansatz 2. *The following is satisfied.*

- The functions α_i , $i = 1, 2$ defined in Proposition 3.3, satisfy

$$|\alpha_i(I)| \leq 100\mu \quad \text{for all } I \in [I_-, I_+].$$

- For all $I \in [I_-, I_+]$, we have

$$\alpha_1(I) - \alpha_2(I) \neq 0.$$

- We define the first order of a certain variance, given by

$$\sigma_0^2(I) = 2\mathbb{E}_\omega \left| \mathcal{M}_{\omega_0}^{I,1}(J) - \mathbb{E}_\omega \mathcal{M}_{\omega_0}^{I,1}(I) \frac{1 - e^{i\beta_{\omega_0}^0(I)}}{1 - \mathbb{E}_\omega \left(e^{i\beta_{\omega_0}^0(I)} \right)} \right|^2, \quad (55)$$

where \mathbb{E}_ω is the expectation with respect to the Bernoulli measure on Σ . We assume that it satisfies

$$\sigma_0^2(I) \neq 0 \quad \text{for all } I \in [I_-, I_+].$$

We devote the rest of the section to prove Theorems 4.4 and 4.5. They are proven in Sections 4.3 and 4.4 respectively.

4.3 The NHIL for the circular problem: Proof of Theorem 4.4

We first analyze the existence of laminations for the circular problem. Its existence will be a consequence of [BKZ16] (Appendix A, see also Theorem A.4 in [KZ15]) which uses the isolating block method. In this section we check that our system satisfies the hypotheses of that theorem, namely, we obtain suitable *blocks* by finding their *centers* and then check the isolating block conditions, that is, existence of contracting and expanding directions and cone conditions.

4.3.1 Linearization of the separatrix map of the circular problem

Theorem 3.1 provides formulas for the four separatrix maps we are considering, \mathcal{SM}_0^{ij} , $i, j = 1, 2$. To simplify notation, we denote the return time (6) as

$$\bar{g} = 2\pi N^{ij}(I, s, p, q),$$

We consider the (p, q) expansion of the separatrix map of the circular problem $\mathcal{F}_0^{ij} = \mathcal{SM}_0^{ij}$. We recall that

$$\mathcal{F}_0^{ij} = \left(\mathcal{F}_{I,0}^{ij}, \mathcal{F}_{s,0}^{ij}, \mathcal{F}_{p,0}^{ij}, \mathcal{F}_{q,0}^{ij} \right) \quad (56)$$

with

$$\begin{aligned} \mathcal{F}_{I,0}^{ij} &= I \\ \mathcal{F}_{s,0}^{ij} &= s + \alpha_i(I) + (\nu(I) + \partial_I F(I, pq))\bar{g} + a_{10}^i(I)p + a_{01}^i(I)(q - q^i(I)) + \mathcal{O}_2(p, q - q^i(I)) \end{aligned}$$

and

$$\begin{aligned} \begin{pmatrix} \mathcal{F}_{p,0}^{ij} \\ \mathcal{F}_{q,0}^{ij} \end{pmatrix} &= \begin{pmatrix} e^{-\Theta^i(I, s, p, q)\bar{g}} p_0^i(I) \\ 0 \end{pmatrix} \\ &+ \begin{pmatrix} e^{-\Theta^i(I, s, p, q)\bar{g}} b_{10}^i(I) & e^{-\Theta^i(I, s, p, q)\bar{g}} b_{01}^i(I) \\ e^{\Theta^i(I, s, p, q)\bar{g}} c_{10}^i(I) & e^{\Theta^i(I, s, p, q)\bar{g}} c_{01}^i(I) \end{pmatrix} \begin{pmatrix} p + \mathcal{O}_2(p, q - q^i(I)) \\ q - q^i(I) + \mathcal{O}_2(p, q - q^i(I)) \end{pmatrix} \end{aligned}$$

where, using the definition of Θ^i in (29) and the gluing map given by Lemma 3.8, Θ^i is independent of s and satisfies

$$\Theta^i(I, s, p, q) = \Theta^i(I, p, q) = \lambda(I) + \lambda_2(I)p_0^i(I) (c_{10}^i(I)p + c_{01}^i(I)(q - q^i(I))) + \mathcal{O}_2(p, q - q^i(I)),$$

for some smooth function λ_2 . We remark that $\mathcal{F}_{I,0}^{ij}$, $\mathcal{F}_{s,0}^{ij} - s$, $\mathcal{F}_{p,0}^{ij}$ and $\mathcal{F}_{q,0}^{ij}$ do not depend on s .

Lemma 4.7. *The differential of \mathcal{F}_0^{ij} satisfies*

$$D\mathcal{F}_0^{ij} = \begin{pmatrix} 1 & 0 & 0 & 0 \\ \dot{\alpha}_i - a_{01}^i \dot{q}^i + \dot{\nu} \bar{g} + \mathcal{O}_1 \bar{g} & 1 & \dot{\lambda} \bar{g} + a_{10}^i + \mathcal{O}_1 \bar{g} & a_{01}^i + \mathcal{O}_1 \bar{g} \\ e^{-\Theta^i \bar{g}} (A_1^i + \mathcal{O}_1 \bar{g} + \mathcal{O}_1) & 0 & e^{-\Theta^i \bar{g}} (-\lambda_2 (p_0^i)^2 c_{10}^i \bar{g} + b_{10}^i + \mathcal{O}_1 \bar{g}) & e^{-\Theta^i \bar{g}} (-\lambda_2 (p_0^i)^2 c_{01}^i \bar{g} + b_{01}^i + \mathcal{O}_1 \bar{g}) \\ e^{\Theta^i \bar{g}} (-c_{01}^i \dot{q}^i + \mathcal{O}_1 \bar{g}) & 0 & e^{\Theta^i \bar{g}} (c_{10}^i + \mathcal{O}_1 \bar{g}) & e^{\Theta^i \bar{g}} (c_{01}^i + \mathcal{O}_1 \bar{g}) \end{pmatrix},$$

where $\mathcal{O}_1 = \mathcal{O}_1(p, q - q^i(I))$, $\mathcal{O}_2 = \mathcal{O}_2(p, q - q^i(I))$,

$$A_1^i = p_0^i - b_{01}^i \dot{q}^i - \partial_I \Theta^i p_{0\bar{g}}^i$$

and \dot{a}_{mn}^i denotes the derivative of a_{mn}^i with respect to I .

Proof. To prove the lemma, it is enough to take derivatives in the formulas of the separatrix map in (56). \square

Now we can analyze the eigenvectors and eigenvalues of the matrix $D\mathcal{F}_0^{ij}$. Recall that, by Theorem 4.4, the function c_{01}^i satisfies $c_{01}^i \neq 0$. We assume

$$c_{01}^i > 0$$

One can proceed analogously if one assumes $c_{01}^i < 0$.

The proofs of the following two lemmas are straightforward.

Lemma 4.8. *Take \bar{g} big enough. The matrix*

$$\mathcal{B}_0^{ij} = \begin{pmatrix} e^{-\Theta^i \bar{g}} (-\lambda_2 (p_0^i)^2 c_{10}^i \bar{g} + b_{10}^i + \mathcal{O}_1 \bar{g}) & e^{-\Theta^i \bar{g}} (-\lambda_2 (p_0^i)^2 c_{01}^i \bar{g} + b_{01}^i + \mathcal{O}_1 \bar{g}) \\ e^{\Theta^i \bar{g}} (c_{10}^i + \mathcal{O}_1 \bar{g}) & e^{\Theta^i \bar{g}} (c_{01}^i + \mathcal{O}_1 \bar{g}) \end{pmatrix}$$

has eigenvalues $\mu^{ij}, (\mu^{ij})^{-1} \in \mathbb{R}$ with

$$\mu^{ij} = e^{\Theta^i \bar{g}} (c_{01}^i + \mathcal{O}_1 \bar{g}) + \mathcal{O}(e^{-\Theta^i \bar{g}}) \gg 1.$$

Let w_1^{ij}, w_2^{ij} be two eigenvectors associated to these eigenvalues. They can be chosen to satisfy

$$w_1^{ij} = \begin{pmatrix} e^{-2\Theta^i \bar{g}} \frac{-\lambda_2 (p_0^i)^2 c_{01}^i \bar{g} + b_{01}^i}{c_{01}^i} \left(1 + \mathcal{O}_1 + \mathcal{O}(e^{-2\Theta^i \bar{g}})\right) \\ 1 \end{pmatrix} \quad w_2^{ij} = \begin{pmatrix} 1 \\ -\frac{c_{10}^i}{c_{01}^i} + \mathcal{O}_1 + \mathcal{O}(e^{-\Theta^i \bar{g}}) \end{pmatrix}. \quad (57)$$

Lemma 4.9. *Take \bar{g} big enough. Then, the matrix $D\mathcal{F}_0^{ij}$ has as eigenvalues*

$$\lambda_1^{ij} = \mu^{ij} = e^{\Theta^i \bar{g}} (c_{01}^i + \mathcal{O}_1 \bar{g}) + \mathcal{O}(e^{-\Theta^i \bar{g}}) \gg 1, \quad \lambda_2^{ij} = (\lambda_1^{ij})^{-1}.$$

The associated eigenvectors can be chosen to be

$$v_1^{ij} = \begin{pmatrix} 0 \\ \frac{e^{-\Theta^i \bar{g}}}{c_{01}^i} \left(a_{01}^i + \mathcal{O}_1 \bar{g} + \mathcal{O} \left(e^{-\Theta^i \bar{g}} \right) \right) \\ w_{11}^{ij} \\ w_{21}^{ij} \end{pmatrix}, \quad v_2^{ij} = \begin{pmatrix} 0 \\ -\lambda \bar{g} - a_{10}^i + \frac{c_{10}^i}{c_{01}^i} a_{01}^i + \mathcal{O}_1 \bar{g} + \mathcal{O} \left(e^{-\Theta^i \bar{g}} \right) \\ w_{12}^{ij} \\ w_{22}^{ij} \end{pmatrix},$$

where w_1^{ij} and w_2^{ij} are the eigenvectors obtained in Lemma 4.8.

Remark 4.10. The matrix $D\mathcal{F}_0^{ij}$ has also an eigenvalue equal to 1 with an associated Jordan Block and eigenvector $v_2 = (0, 1, 0, 0)^T$. Nevertheless, it is not used in the isolating block construction.

Remark 4.11. Since $\mathcal{F}_0^{ij} - (0, s, 0, 0)$ does not depend on s , neither $D\mathcal{F}_0^{ij}$ nor its eigenvectors, v_1^{ij} and v_2^{ij} , depend on s .

4.3.2 Center of the blocks

We compute the center of the isolating blocks for the separatrix map of the circular problem, given in (56). We have certain freedom to choose the distance of the center from the homoclinic points. We will use this freedom later.

Recall that for the circular problem, the function Θ^i satisfies

$$\Theta^i(I, p, q) = \lambda(I) + \mathcal{O}(p, q - q^i(I)), \quad (58)$$

where $\lambda(I) > 0$ has been defined in Lemma 2.3. We fix $I^* \in [I_-, I_+]$ and we define $\lambda^* = \lambda(I^*)$ for some $I^* \in \mathcal{I}$. We define the function

$$\zeta(I) = \frac{\lambda(I)}{\lambda^*}. \quad (59)$$

We start by computing the center of the blocks for \mathcal{F}_0^{11} and \mathcal{F}_0^{22} .

Lemma 4.12. Fix $(I, s) \in [I_-, I_+] \times \mathbb{T}$ and $0 < \rho \ll 1$ such that

$$\frac{|\log \rho|}{\lambda^*} \in \mathbb{Z}.$$

Consider the separatrix map in (56). Then, the equation

$$\begin{aligned} p &= \mathcal{F}_{p,0}^{ii}(I, s, p, q) \\ q &= \mathcal{F}_{q,0}^{ii}(I, s, p, q) \end{aligned}$$

has a solution of the form $(p_*^{ii}(I), q_*^{ii}(I)) = (p_{\text{circ}}^{ii}(I) \rho^{\zeta(I)}, q^i(I) + q_{\text{circ}}^{ii}(I) \rho^{\zeta(I)})$ with

$$\begin{aligned} p_{\text{circ}}^{ii}(I) &= p_0^i(I) + \mathcal{O} \left(\rho^{\zeta(I)} \log \rho \right) \\ q_{\text{circ}}^{ii}(I) &= \frac{1}{c_{01}^i(I)} \left(q^i(I) - c_{10}^i(I) p_0^i(I) \right) + \mathcal{O} \left(\rho^{\zeta(I)} \log \rho \right). \end{aligned}$$

Moreover, the time \bar{g} needed to achieve this transition is given by

$$\bar{g} = \frac{|\log \rho|}{\lambda^*}.$$

The proof is straightforward setting up a fixed point argument.

The curve $(p_*^{ii}(I), q_*^{ii}(I))$ defines the parameterization of the center of the blocks for all $s \in \mathbb{T}$. That is, the centers do not depend on s . This is due to the particular form of the circular problem. Note also that when I varies, the distance of the center of the block with respect to the homoclinic point changes. This is due to the dependence on I of the eigenvalue $\lambda(I)$.

The same happens for the center of the blocks of \mathcal{F}_0^{12} and \mathcal{F}_0^{21} .

Lemma 4.13. *Fix $i, j = 1, 2$ with $i \neq j$, $(I, s) \in [I_-, I_+] \times \mathbb{T}$ and $0 < \rho \ll 1$ such that*

$$\frac{|\log \rho|}{\lambda^*} \in \mathbb{Z}.$$

Consider the separatrix map in (56). Then, the equation

$$\begin{aligned} p &= \mathcal{F}_{p,0}^{ji} \circ \mathcal{F}_0^{ij}(I, s, p, q) \\ q &= \mathcal{F}_{q,0}^{ji} \circ \mathcal{F}_0^{ij}(I, s, p, q) \end{aligned}$$

has a solution of the form $(p_^{ij}(I), q_*^{ij}(I)) = (p_{\text{circ}}^{ij}(I)\rho^{\zeta(I)}, q^i(I) + q_{\text{circ}}^{ij}(I)\rho^{\zeta(I)})$ with*

$$\begin{aligned} p_{\text{circ}}^{ij}(I) &= p_0^j(I) + \mathcal{O}\left(\rho^{\zeta(I)} \log \rho\right) \\ q_{\text{circ}}^{ij}(I) &= \frac{1}{c_{01}^i(I)}(q^j(I) - c_{10}^j(I)p_0^j(I)) + \mathcal{O}\left(\rho^{\zeta(I)} \log \rho\right). \end{aligned}$$

Moreover, the time \bar{g} needed to to achieve this transition is given by

$$\bar{g} = 2 \frac{|\log \rho|}{\lambda^*}.$$

The proof is a direct consequence of applying a fix point argument.

4.3.3 Isolating block conditions

To prove the existence of the lamination, we need to define the blocks and prove that they satisfy the cone conditions given in [BKZ16, KZ15] (explained below).

In Lemma 4.8, we have computed the eigenvalues of the $D\mathcal{F}_0^{ij}$. Using the notation in (59) and Lemma 4.12 and taking into account that, from now on, $e^{\Theta^i \bar{g}} = \rho^{\zeta(I)}$, we have that the hyperbolic eigenvalues are $\lambda_1^{ij} = \mu^{ij}$ and $\lambda_2^{ij} = (\mu^{ij})^{-1}$ with

$$\mu^{ij} = \frac{c_{01}^i}{\rho^{\zeta(I)}} \left(1 + \mathcal{O}\left(\rho^{\zeta(I)}\right)\right).$$

We also consider the eigenvectors of $D\mathcal{F}_0^{ij}$ given by Lemma 4.9 based at the center of the blocks computed in Lemma 4.12. Thus, we define

$$v_k^{ij}(I) = v_k(I, p_*^{ij}(I), q_*^{ij}(I)) \quad k = 1, 2.$$

Using (30), (59) and Lemma 4.9, we have

$$v_1(I) = \begin{pmatrix} 0 \\ \mathcal{O}(\rho^{\zeta(I)}) \\ \mathcal{O}(\rho^{2\zeta(I)} \log \rho) \\ 1 \end{pmatrix}, \quad v_2(I) = \begin{pmatrix} 0 \\ -\lambda \bar{g} - a_{10}^i + \frac{c_{10}^i}{c_{01}^i} a_{01} + \mathcal{O}(\rho^{\zeta(I)} \log \rho) \\ 1 \\ -\frac{c_{10}^i}{c_{01}^i} + \mathcal{O}(\rho^{\zeta(I)}) \end{pmatrix}. \quad (60)$$

We fix $\delta > 0$, which will be defined in terms of ρ later. Then, we consider the blocks

$$\begin{aligned} \Pi_{ij}^{s,\kappa} = \left\{ (I, s, p, q) = (I, s, p_*^{ij}(I), q_*^{ij}(I)) + cv_1^{ij}(I) + dv_2^{ij}(I) : \right. \\ \left. I \in [I_-, I_+], s \in \mathbb{T}, |c| \leq \kappa\delta^2, |d| \leq \kappa\delta \right\}. \end{aligned} \quad (61)$$

These blocks are parallelograms centered at the points computed in Lemma 4.12 with sides in the direction of the eigenvectors obtained in Lemma 4.9. The superscript s refers to the fact that this blocks are stretched along the stable eigenvector v_2^{ij} . We introduce

$$\partial^s \Pi_{ij}^{s,\kappa} = \{(I, s, p, q) \in \Pi_{ij}^{s,\kappa} : |c| = \kappa\delta^2\}. \quad (62)$$

Analogously, we can define the unstable blocks

$$\begin{aligned} \Pi_{ij}^{u,\kappa} = \left\{ (I, s, p, q) = (I, s, p_*^{ij}(I), q_*^{ij}(I)) + cv_1^{ij}(I) + dv_2^{ij}(I) : \right. \\ \left. I \in [I_-, I_+], s \in \mathbb{T}, |c| \leq \kappa\delta, |d| \leq \kappa\delta^2 \right\}, \end{aligned} \quad (63)$$

which are stretched along the unstable eigenvector v_1 , and

$$\partial^s \Pi_{ij}^{u,\kappa} = \{(I, s, p, q) \in \Pi_{ij}^{u,\kappa} : |d| = \kappa\delta^2\}. \quad (64)$$

One can define a system of coordinates adapted to these blocks. Define the map

$$\Psi^{ij} : (I, s, c, d) \mapsto (I, s, p_*^{ij}(I), q_*^{ij}(I)) + cv_1^{ij}(I)^\top + dv_2^{ij}(I)^\top. \quad (65)$$

Since, in view of Lemma 4.9, the vectors $(1, 0, 0, 0)^\top$, $(0, 1, 0, 0)^\top$, v_1^{ij} and v_2^{ij} are linearly independent, we have that Ψ^{ij} is a diffeomorphism from $\Pi_{ij}^{\sigma,\kappa}$ onto its image for c and d small enough (that is, if δ is small enough). As a matter of fact, since $\Psi_I^{ij}(I, s, c, d) = I$, it is a diffeomorphism for all (c, d) . We introduce its inverse

$$\Phi^{ij} = (\Psi^{ij})^{-1} : (I, s, p, q) \mapsto (I_0(I, s, p, q), s_0(I, s, p, q), c^{ij}(I, s, p, q), d^{ij}(I, s, p, q)). \quad (66)$$

We express the separatrix map and the blocks in this new system of coordinates. That is,

$$F_0 = \Phi^{ij} \circ \mathcal{F}_0 \circ (\Phi^{ij})^{-1}. \quad (67)$$

We also define

$$P_{ij}^{\sigma,\kappa} = \Phi^{ij} \left(\Pi_{ij}^{\sigma,\kappa} \right), \quad \sigma = u, s \quad (68)$$

and

$$\partial^u P_{ij}^{s,\kappa} = \Phi^{ij} \left(\partial^u \Pi_{ij}^{s,\kappa} \right) \quad \text{and} \quad \partial^s P_{ij}^{u,\kappa} = \Phi^{ij} \left(\partial^s \Pi_{ij}^{u,\kappa} \right). \quad (69)$$

Let $\pi_j(z)$ denote the projection onto the j -component of z .

Lemma 4.14. *Let $\delta = \rho^\zeta$ be small enough. There exist $\kappa, \kappa_1, \kappa_2 > 0$ such that, if $z \in \partial^u P_{ij}^{s,\kappa}$,*

$$|\pi_3 \circ F_0(z)| \geq \kappa_1 \rho^\zeta \quad (70)$$

and, if $z \in P_{ij}^{s,\kappa}$,

$$|\pi_4 \circ F_0(z)| \leq \kappa_2 \rho^{2\zeta}. \quad (71)$$

Moreover, $F_0(\partial^u P_{ij}^{s,\kappa})$ is homotopically equivalent to $\partial^u P_{ij}^{s,\kappa}$.

Proof. In what follows, we assume $\kappa < 1$. Given $(I, s, c, d) \in P_{ij}^{s, \kappa}$, we write $(I, \tilde{s}, \tilde{p}, \tilde{q}) = (\Phi^{ij})^{-1}(I, s, c, d)$. Let

$$z^{ij}(I) = (I, s, p_*^{ij}(I), q_*^{ij}(I)) = (\Phi^{ij})^{-1}(I, s, 0, 0)$$

be the center of the corresponding block. Along the proof, we denote $F_0(\tilde{z}) = \tilde{z}^+$ and $\mathcal{F}_0(z) = z^+$. By Lemma 4.12, $F_0(I, s, 0, 0) = (I^+, s^+, 0, 0) = (I, s^+, 0, 0)$ that is, $\pi_{3,4} \circ F_0(I, s, 0, 0) = (0, 0)$. Introducing

$$\Delta(I, s, c, d) = \int_0^1 \left[D\mathcal{F}_0(z^{ij} + u(cv_1^{ij} + dv_2^{ij})) - D\mathcal{F}_0(z^{ij}) \right]_{|(I,s)} du \quad (72)$$

we have that

$$\begin{aligned} & \mathcal{F}_0 \circ (\Phi^{ij})^{-1}(I, s, c, d) \\ &= \mathcal{F}_0 \circ (\Phi^{ij})^{-1}(I, s, 0, 0) + \mathcal{F}_0 \circ (\Phi^{ij})^{-1}(I, s, c, d) - \mathcal{F}_0 \circ (\Phi^{ij})^{-1}(I, s, 0, 0) \\ &= \mathcal{F}_0 \circ (\Phi^{ij})^{-1}(I, s, 0, 0) + \int_0^1 D\mathcal{F}_0(z^{ij} + u(cv_1^{ij} + dv_2^{ij}))_{|(I,s)} du (cv_1^{ij} + dv_2^{ij})_{|(I,s)} \\ &= \mathcal{F}_0 \circ (\Phi^{ij})^{-1}(I, s, 0, 0) + D\mathcal{F}_0(z^{ij})(cv_1^{ij} + dv_2^{ij})_{|(I,s)} + \Delta(I, s, c, d)(cv_1^{ij} + dv_2^{ij})_{|(I,s)} \\ &= z^{ij}(I^+, s^+) + c\lambda_1^{ij}v_1^{ij}(I^+, s^+) + d\lambda_2^{ij}v_2^{ij}(I^+, s^+) + \mathcal{E}^{ij}(I, s) \end{aligned}$$

where

$$\begin{aligned} \mathcal{E}^{ij}(I, s) &= \mathcal{F}_0 \circ (\Phi^{ij})^{-1}(I, s, 0, 0) - z^{ij}(I^+, s^+) + c\lambda_1^{ij}(v_1^{ij}(I^+, s^+) - v_1^{ij}(I, s)) \\ &\quad + d\lambda_2^{ij}(v_2^{ij}(I^+, s^+) - v_2^{ij}(I, s)) + \Delta(I, s, c, d)(cv_1^{ij} + dv_2^{ij})_{|(I,s)}. \end{aligned} \quad (73)$$

We claim that

$$\begin{aligned} |\mathcal{E}_I^{ij}| &= 0, \\ |\mathcal{E}_s^{ij}| &\leq \mathcal{O}(\rho^{2\zeta(I)} \log \rho), \\ |\mathcal{E}_p^{ij}| &\leq \mathcal{O}(\rho^{3\zeta(I)} \log \rho), \\ |\mathcal{E}_q^{ij}| &\leq \kappa^2 \mathcal{O}(\rho^{\zeta(I)}). \end{aligned} \quad (74)$$

Indeed, introducing

$$\begin{aligned} \mathcal{E}_1 &= \mathcal{F}_0 \circ (\Phi^{ij})^{-1}(I, s, 0, 0) - z^{ij}(I^+, s^+), \\ \mathcal{E}_2 &= c\lambda_1^{ij}(v_1^{ij}(I^+, s^+) - v_1^{ij}(I, s)) + d\lambda_2^{ij}(v_2^{ij}(I^+, s^+) - v_2^{ij}(I, s)), \\ \mathcal{E}_3 &= \Delta(I, s, c, d)(cv_1^{ij} + dv_2^{ij})_{|(I,s)}, \end{aligned}$$

we have that $\mathcal{E}^{ij} = \mathcal{E}_1 + \mathcal{E}_2 + \mathcal{E}_3$ and

1. by Lemmas 4.12 and 4.13 and taking into account that $I^+ = I$, $\mathcal{E}_1 = 0$,
2. since $I^+ = I$ and v_1^{ij}, v_2^{ij} only depend on I , $\mathcal{E}_2 = 0$,
3. since $cv_1^{ij} + dv_2^{ij} = \kappa(0, \mathcal{O}(\rho^{\zeta(I)} \log \rho), \mathcal{O}(\rho^{\zeta(I)}), \mathcal{O}(\rho^{\zeta(I)}))$ and taking into account the expression of \mathcal{F}_0 given by Theorem 3.1,

$$\Delta(I, s, c, d) = \kappa \begin{pmatrix} 0 & 0 & 0 & 0 \\ \mathcal{O}(\rho^{\zeta(I)} \log \rho) & 0 & \mathcal{O}(\rho^{\zeta(I)} \log \rho) & \mathcal{O}(\rho^{\zeta(I)} \log \rho) \\ \mathcal{O}(\rho^{2\zeta(I)} \log \rho) & 0 & \mathcal{O}(\rho^{2\zeta(I)} \log \rho) & \mathcal{O}(\rho^{2\zeta(I)} \log \rho) \\ \mathcal{O}(\log \rho) & 0 & \tilde{\mathcal{A}} & \tilde{\mathcal{B}} \end{pmatrix},$$

where, using that $\partial_p \Theta = \lambda_2 p_0 c_{10} + \mathcal{O}_1$, $\partial_q \Theta = \lambda_2 p_0 c_{01} + \mathcal{O}_1$ and the expressions for v_1^{ij} and v_2^{ij} given by Lemma 4.9,

$$\tilde{\mathcal{A}}, \tilde{\mathcal{B}} = \mathcal{O}(1),$$

which implies that

$$\Delta(I, s, c, d)(cv_1^{ij} + dv_2^{ij})|_{(I, s)} = \kappa^2 \left(0, \mathcal{O}(\rho^{2\zeta(I)} \log \rho), \mathcal{O}(\rho^{3\zeta(I)} \log \rho), \mathcal{O}(\rho^{\zeta(I)}) \right).$$

Combining 1), 2) and 3) we obtain the bound (74).

Hence,

$$\begin{aligned} F_0(I, s, c, d) &= \Phi^{ij} \circ \mathcal{F}_0 \circ \Psi^{ij}(I, s, c, d) \\ &= \Phi^{ij}(z^{ij}(I^+, s^+) + c\lambda_1^{ij}v_1^{ij}(I^+, s^+) + d\lambda_2^{ij}v_2^{ij}(I^+, s^+) + \mathcal{E}^{ij}(I, s)) \\ &= (I^+, s^+, c\lambda_1^{ij}, d\lambda_2^{ij}) + \tilde{\mathcal{E}}^{ij}, \end{aligned} \quad (75)$$

where

$$\begin{aligned} \tilde{\mathcal{E}}^{ij} &= \Phi^{ij}(z^{ij}(I^+, s^+) + c\lambda_1^{ij}v_1^{ij}(I^+, s^+) + d\lambda_2^{ij}v_2^{ij}(I^+, s^+) + \mathcal{E}^{ij}(I, s)) \\ &\quad - \Phi^{ij}(z^{ij}(I^+, s^+) + c\lambda_1^{ij}v_1^{ij}(I^+, s^+) + d\lambda_2^{ij}v_2^{ij}(I^+, s^+)) \\ &= \int_0^1 D\Phi^{ij}(z^{ij}(I^+, s^+) + c\lambda_1^{ij}v_1^{ij}(I^+, s^+) + d\lambda_2^{ij}v_2^{ij}(I^+, s^+) + u\mathcal{E}^{ij}(I, s)) du \mathcal{E}^{ij}(I, s). \end{aligned} \quad (76)$$

Since Φ^{ij} is invertible, $I^+ = I$, z^{ij} , v_k^{ij} , λ_k^{ij} depend only on I and $\pi_I v_k^{ij} = 0$, we have that, for $u \in [0, 1]$,

$$\begin{aligned} z^{ij}(I^+, s^+) + c\lambda_1^{ij}v_1^{ij}(I^+, s^+) + d\lambda_2^{ij}v_2^{ij}(I^+, s^+) + u\mathcal{E}^{ij}(I, s) \\ = z^{ij}(I) + c\lambda_1^{ij}v_1^{ij}(I) + d\lambda_2^{ij}v_2^{ij}(I) + u\mathcal{E}^{ij}(I, s) = z^{ij}(I) + \tilde{c}v_1^{ij}(I) + \tilde{d}v_2^{ij}(I), \end{aligned}$$

for some (\tilde{c}, \tilde{d}) . But, using the bound (74), we deduce that

$$\tilde{c} - c\lambda_1^{ij} = \mathcal{O}(\rho^{\zeta(I)}), \quad \tilde{d} - d\lambda_2^{ij} = \mathcal{O}(\rho^{3\zeta(I)} \log \rho).$$

This implies, by its definition in (65) and the formulas for the center of the blocks z^{ij} in Lemma 4.13

$$D\Psi^{ij}|_{(I, s^+, \tilde{c}, \tilde{d})} = \begin{pmatrix} 1 & 0 & 0 & 0 \\ \mathcal{O}(\rho^{2\zeta(I)} \log \rho) & 1 & \mathcal{O}(\rho^{\zeta(I)}) & \mathcal{O}(\log \rho) \\ \mathcal{O}(\rho^{2\zeta(I)} \log \rho) & 0 & \mathcal{O}(\rho^{\zeta(I)}) & 1 \\ \mathcal{O}(\rho^{\zeta(I)} \log \rho) & 0 & 1 & -c_{10}/c_{01} + \mathcal{O}(\rho^{\zeta(I)}) \end{pmatrix}. \quad (77)$$

Hence,

$$D\Phi^{ij}|_{\Psi^{ij}(I, s^+, \tilde{c}, \tilde{d})} = \begin{pmatrix} 1 & 0 & 0 & 0 \\ \mathcal{O}(\rho^{2\zeta(I)} \log^2 \rho) & 1 & \mathcal{O}(\log \rho) & \mathcal{O}(\rho^{\zeta(I)} \log \rho) \\ \mathcal{O}(\rho^{\zeta(I)} \log \rho) & 0 & c_{10}/c_{01} + \mathcal{O}(\rho^{\zeta(I)}) & 1 + \mathcal{O}(\rho^{\zeta(I)}) \\ \mathcal{O}(\rho^{2\zeta(I)} \log \rho) & 0 & 1 + \mathcal{O}(\rho^{\zeta(I)}) & \mathcal{O}(\rho^{\zeta(I)}) \end{pmatrix}. \quad (78)$$

Using these bounds on $D\Phi^{ij}|_{\Psi^{ij}(\tilde{I}, \tilde{s}^+, \tilde{c}, \tilde{d})}$, (76) and (74), we have that

$$|\tilde{\mathcal{E}}_p^{ij}| \leq \kappa^2 \mathcal{O}(\rho^{\zeta(I)}), \quad |\tilde{\mathcal{E}}_q^{ij}| \leq \kappa^2 \mathcal{O}(\rho^{2\zeta(I)}). \quad (79)$$

Now, if $z \in \partial^u P_{ij}^{s,\kappa}$, that is, $|c| = \kappa\delta^2 = \kappa\rho^{2\zeta(I)}$ and $|d| < \kappa\delta = \kappa\rho^{\zeta(I)}$,

$$\begin{aligned} |\pi_3 \circ F_0(I, s, c, d)| &\geq |c\lambda_1^{ij} - \kappa^2\mathcal{O}(\rho^{\zeta(I)})| \\ &\geq \kappa c_{01}^i \rho^{\zeta(I)} (1 + \kappa\mathcal{O}(1)). \end{aligned}$$

Hence, choosing κ such that $1 + \kappa\mathcal{O}(1) > 0$, (70) follows. Also, if $z \in P_{ij}^{s,\kappa}$, that is, $|c| = \kappa\delta^2 = \kappa\rho^{2\zeta(I)}$ and $|d| = \kappa\delta = \kappa\rho^{\zeta(I)}$,

$$|\pi_4 \circ F_0(I, s, c, d)| \leq d\lambda_2^{ij} + \kappa^2\mathcal{O}(\rho^{2\zeta(I)}) \leq \frac{\kappa}{c_{01}^i} \rho^{2\zeta(I)} (1 + \kappa\mathcal{O}(1)),$$

which proves (71).

As for $F_0(\partial^u P_{ij}^{s,\kappa})$ being homotopically equivalent to $\partial^u P_{ij}^{s,\kappa}$, we can use the same arguments as in [KZ15], considering the lift of \mathcal{F}_0 to the covering space where $P_{ij}^{s,\kappa}$ becomes simply connected. The image of its boundary, which is a hyperplane, is a slightly deformed hyperplane. \square

We also have the analogous claim for the unstable blocks. The proof follows the same lines as the proof of Lemma 4.14.

Lemma 4.15. *Let $\delta = \rho^\zeta$ be small enough. There exist $\kappa, \kappa_1, \kappa_2 > 0$ such that, if $F_0(z) \in \partial^s P_{ij}^{u,\kappa}$,*

$$|\pi_4 \circ F_0^{-1}(F_0(z))| \geq \kappa_1 \rho^{\zeta(I)} \quad (80)$$

and, if $F_0(z) \in P_{ij}^{u,\kappa}$,

$$|\pi_3 \circ F_0^{-1}(F_0(z))| \leq \kappa_2 \rho^{2\zeta(I)}. \quad (81)$$

Moreover, $F_0^{-1}(\partial^s P_{ij}^{u,\kappa})$ is homotopically equivalent to $\partial^s P_{ij}^{u,\kappa}$.

From Lemmas 4.14 and 4.15 and the isolating block argument in [KZ15], we obtain an invariant set in the intersections $\Pi_{ij}^{u,\kappa} \cap \Pi_{lk}^{s,\kappa}$, $i, j, l, k = 0, 1$. Now we check that the cone conditions are also satisfied.

Our invariant set is a subset of $\{g = 0\} \subset \mathbb{R} \times \mathbb{T} \times \mathbb{R}^2$. On its tangent space we consider the vector fields

$$\begin{aligned} e_1^c &= (1, 0, 0, \dot{q}^i)^\top, \\ e_2^c &= (0, 1, 0, 0)^\top, \\ e^u &= v_1^{ij}, \\ e^s &= v_2^{ij}, \end{aligned} \quad (82)$$

which, for each $z \in \{g = 0\}$, span $T_z\{g = 0\}$. Given $v \in T_z\{g = 0\}$, we shall identify v with its coordinates, (v^1, v^2, v^3, v^4) .

For $z \in \Pi_{ij}^{s,\kappa}$, we consider the the unstable cones

$$C_{ij}^u(z) = \{v \in T_z\{g = 0\} : |v^1| < |v^3|, |v^2| < |v^3|, |v^4| < |v^3|\}, \quad i, j = 0, 1,$$

and, for $z \in \Pi_{ij}^{u,\kappa}$, we consider the the stable cones

$$C_{ij}^s(z) = \{v \in T_z\{g = 0\} : |v^1| < |v^4|, |v^2| < |v^4|, |v^3| < |v^4|\}, \quad i, j = 0, 1.$$

We will use the standard flat norm, that is, $\|v\|^2 = |v^1|^2 + |v^2|^2 + |v^3|^2 + |v^4|^2$.

Lemma 4.16. *There exists $C > 0$ such that for all $z \in \Pi_{ij}^{s,\kappa}$ and $v \in C_{ij}^u(z)$,*

$$D\mathcal{F}_0^{ij}(z)v \in C_{ij}^u(\mathcal{F}_0^{ij}(z)) \quad \text{and} \quad \|D\mathcal{F}_0^{ij}(z)v\| \geq \frac{C}{\rho^{\zeta(I)}} \|v\|. \quad (83)$$

Assume $\inf |\dot{\lambda}| > 0$ (see also (58)). Then, for all $z^+ \in \Pi_{ij}^{u,\kappa}$ and $v \in C_{ij}^s(z^+)$,

$$D(\mathcal{F}_0^{ij})^{-1}(z^+)v \in C_{ij}^s(z) \quad \text{and} \quad \|D(\mathcal{F}_0^{ij})^{-1}(z^+)v\| \geq \frac{C}{\rho^{\zeta(I)}} \|v\|. \quad (84)$$

If $\inf |\dot{\lambda}| = 0$, then the stable cones are invariant and

$$\|D(\mathcal{F}_0^{ij})^{-1}(z^+)v\| \geq \frac{C}{\rho^{\zeta(I)} |\log \rho|} \|v\|.$$

Proof. Let $v \in C_{ij}^u(z)$. Let z^{ij} be the center of the block. In view of Lemma 4.7,

$$D\mathcal{F}_0^{ij}(z) - D\mathcal{F}_0^{ij}(z^{ij}) = \begin{pmatrix} 0 & 0 & 0 & 0 \\ \mathcal{O}(\rho^{\zeta(I)} \log \rho) & 0 & \mathcal{O}(\rho^{\zeta(I)} \log \rho) & \mathcal{O}(\rho^{\zeta(I)} \log \rho) \\ \mathcal{O}(\rho^{\zeta(I)} \log \rho) & 0 & \mathcal{O}(\rho^{\zeta(I)} \log \rho) & \mathcal{O}(\rho^{\zeta(I)} \log \rho) \\ \mathcal{O}(\log \rho) & 0 & \mathcal{O}(\log \rho) & \mathcal{O}(\log \rho) \end{pmatrix}.$$

In the basis e_1^c, e_2^c, e^u, e^s , $D\mathcal{F}_0^{ij}(z) - D\mathcal{F}_0^{ij}(z^{ij})$ becomes

$$\begin{pmatrix} 0 & 0 & 0 & 0 \\ \mathcal{O}(\log^2 \rho) & 0 & \mathcal{O}(\log^2 \rho) & \mathcal{O}(\log^2 \rho) \\ \mathcal{O}(\log \rho) & 0 & \mathcal{O}(\log \rho) & \mathcal{O}(\log \rho) \\ \mathcal{O}(\log \rho) & 0 & \mathcal{O}(\log \rho) & \mathcal{O}(\log \rho) \end{pmatrix}. \quad (85)$$

Then,

$$\begin{aligned} D\mathcal{F}_0^{ij}(z)v &= D\mathcal{F}_0^{ij}(z^{ij})v + (D\mathcal{F}_0^{ij}(z) - D\mathcal{F}_0^{ij}(z^{ij}))v \\ &= v^1 D\mathcal{F}_0^{ij}(z^{ij})e_1^c + v^2 D\mathcal{F}_0^{ij}(z^{ij})e_2^c + v^3 D\mathcal{F}_0^{ij}(z^{ij})e^u + v^4 D\mathcal{F}_0^{ij}(z^{ij})e^s \\ &\quad + (D\mathcal{F}_0^{ij}(z) - D\mathcal{F}_0^{ij}(z^{ij}))v \\ &= v^1 e_1^c + (v^2 + v^1 \mathcal{O}(\log \rho))e_2^c + (\lambda_1^{ij} v^3 + v^1 \mathcal{O}(\log \rho))e^u + (\lambda_2^{ij} v^4 + v^1 \mathcal{O}(\log \rho))e^s \\ &\quad + \mathcal{O}(\log^2 \rho)(|v^2| + |v^3| + |v^4|)e_2^c + \mathcal{O}(\log \rho)(|v^2| + |v^3| + |v^4|)e^u \\ &\quad + \mathcal{O}(\log \rho)(|v^2| + |v^3| + |v^4|)e^s. \end{aligned} \quad (86)$$

Then, it is clear that, for $\rho^{\zeta(I)}$ small enough,

$$\left| (D\mathcal{F}_0^{ij}(z)v)^3 \right| \geq \frac{c_{01}^i}{\rho^{\zeta(I)}} (|v^3| - \mathcal{O}(\rho^{\zeta(I)} \log \rho)(|v^1| + |v^2| + |v^3| + |v^4|)) \geq \frac{c_{01}^i}{2\rho^{\zeta(I)}} |v^3|, \quad (87)$$

which implies

$$\begin{aligned} |(D\mathcal{F}_0^{ij}(z)v)^1| &= |v^1| \leq |v^3| \leq |(D\mathcal{F}_0^{ij}(z)v)^3|, \\ |(D\mathcal{F}_0^{ij}(z)v)^2| &\leq \mathcal{O}(\log^2 \rho)|v^3| \leq |(D\mathcal{F}_0^{ij}(z)v)^3|, \\ |(D\mathcal{F}_0^{ij}(z)v)^4| &\leq \mathcal{O}(\log \rho)|v^3| \leq |(D\mathcal{F}_0^{ij}(z)v)^3|. \end{aligned}$$

We have proved that the unstable cone field is invariant. As for the expansion, it follows easily from (87), since

$$\|D\mathcal{F}_0^{ij}(z)v\|^2 \geq |(D\mathcal{F}_0^{ij}(z)v)^3|^2 \geq \frac{(c_{01}^i)^2}{2\rho^{2\zeta(I)}}|v^3|^2 \geq \frac{(c_{01}^i)^2}{8\rho^{2\zeta(I)}}\|v\|^2.$$

Now we study the field of stable cones. A simple computation yields

$$(D\mathcal{F}_0^{ij})^{-1} = \begin{pmatrix} 1 & 0 & 0 & 0 \\ \bar{g}^2\mathcal{O}_0 & 1 & e^{\Theta^i\bar{g}}\mathcal{O}_0 & e^{-\Theta^i\bar{g}}\mathcal{O}_0 \\ \bar{g}^2\mathcal{O}_0 & 0 & e^{\Theta^i\bar{g}}\mathcal{O}_0 & -e^{-\Theta^i\bar{g}}\mathcal{O}_0 \\ \bar{g}\mathcal{O}_0 & 0 & -e^{\Theta^i\bar{g}}\mathcal{O}_0 & e^{-\Theta^i\bar{g}}\mathcal{O}_0 \end{pmatrix}. \quad (88)$$

Let $v \in C_{ij}^s(z^+)$. Let z_+^{ij} the center of the block. In view of (88),

$$D(\mathcal{F}_0^{ij})^{-1}(z^+) - D(\mathcal{F}_0^{ij})^{-1}(z_+^{ij}) = \begin{pmatrix} 0 & 0 & 0 & 0 \\ \mathcal{O}(\rho^{\zeta(I)} \log^2 \rho) & 0 & \mathcal{O}(\log^2 \rho) & \mathcal{O}(\rho^{\zeta(I)} \log \rho^2) \\ \mathcal{O}(\rho^{\zeta(I)} \log^2 \rho) & 0 & \mathcal{O}(\log \rho) & \mathcal{O}(\rho^{\zeta(I)} \log^2 \rho) \\ \mathcal{O}(\rho^{\zeta(I)} \log \rho) & 0 & \mathcal{O}(\log \rho) & \mathcal{O}(\rho^{\zeta(I)} \log^2 \rho) \end{pmatrix}.$$

In the basis e_1^c, e_2^c, e^u, e^s , $D(\mathcal{F}_0^{ij})^{-1}(z^+) - D(\mathcal{F}_0^{ij})^{-1}(z_+^{ij})$ becomes

$$\begin{pmatrix} 0 & 0 & 0 & 0 \\ \mathcal{O}(\log^2 \rho) & 0 & \mathcal{O}(\log^2 \rho) & \mathcal{O}(\log^2 \rho) \\ \mathcal{O}(\log \rho) & 0 & \mathcal{O}(\log \rho) & \mathcal{O}(\log \rho) \\ \mathcal{O}(\log \rho) & 0 & \mathcal{O}(\log \rho) & \mathcal{O}(\log \rho) \end{pmatrix}.$$

By (88),

$$\begin{aligned} D(\mathcal{F}_0^{ij})^{-1}(z^+)v &= D(\mathcal{F}_0^{ij})^{-1}(z_+^{ij})v + (D(\mathcal{F}_0^{ij})^{-1}(z^+) - D(\mathcal{F}_0^{ij})^{-1}(z_+^{ij}))v \\ &= v^1 D(\mathcal{F}_0^{ij})^{-1}(z_+^{ij})e_1^c + v^2 D(\mathcal{F}_0^{ij})^{-1}(z_+^{ij})e_2^c + v^3 D(\mathcal{F}_0^{ij})^{-1}(z_+^{ij})e^u \\ &\quad + v^4 D(\mathcal{F}_0^{ij})^{-1}(z_+^{ij})e^s + (D(\mathcal{F}_0^{ij})^{-1}(z^+) - D(\mathcal{F}_0^{ij})^{-1}(z_+^{ij}))v \\ &= v^1 e_1^c + (v^2 + v^1 \mathcal{O}(\log^2 \rho))e_2^c + ((\lambda_1^{ij})^{-1}v^3 + v^1 \mathcal{O}(\log^2 \rho))e^u \\ &\quad + ((\lambda_2^{ij})^{-1}v^4 + v^1 \mathcal{O}(\log^2 \rho))e^s + \mathcal{O}(\log^2 \rho)(|v^2| + |v^3| + |v^4|)e_2^c \\ &\quad + \mathcal{O}(\log^2 \rho)(|v^2| + |v^3| + |v^4|)e^u + \mathcal{O}(\log^2 \rho)(|v^2| + |v^3| + |v^4|)e^s. \end{aligned}$$

Then, it is clear that, for $\rho^{\zeta(I)}$ small enough,

$$\left| (D(\mathcal{F}_0^{ij})^{-1}(z^+)v)^4 \right| \geq \frac{c_{01}^i}{\rho^{\zeta(I)}}(|v^4| - \mathcal{O}(\rho^{\zeta(I)} \log^2 \rho)(|v^1| + |v^2| + |v^3| + |v^4|)) \geq \frac{c_{01}^i}{2\rho^{\zeta(I)}}|v^4|, \quad (89)$$

which implies

$$\begin{aligned} |(D(\mathcal{F}_0^{ij})^{-1}(z^+)v)^1| &= |v^1| \leq |v^4| \leq |(D(\mathcal{F}_0^{ij})^{-1}(z^+)v)^4|, \\ |(D(\mathcal{F}_0^{ij})^{-1}(z^+)v)^2| &\leq \mathcal{O}(\log^2 \rho)|v^4| \leq |(D(\mathcal{F}_0^{ij})^{-1}(z^+)v)^4|, \\ |(D(\mathcal{F}_0^{ij})^{-1}(z^+)v)^3| &\leq \mathcal{O}(\log^2 \rho)|v^4| \leq |(D(\mathcal{F}_0^{ij})^{-1}(z^+)v)^4|. \end{aligned}$$

We have proved that the stable cone field is invariant. As for the expansion, it follows easily from (89) since

$$\|D(\mathcal{F}_0^{ij})^{-1}(z^+)v\|^2 \geq |(D(\mathcal{F}_0^{ij})^{-1}(z^+)v)^4|^2 \geq \frac{(c_{01}^i)^2}{2\rho^{2\zeta(I)}}|v^4|^2 \geq \frac{(c_{01}^i)^2}{8\rho^{2\zeta(I)}}\|v\|^2.$$

□

Lemmas 4.14, 4.15 and 4.16 imply the existence of two collections of Lipschitz graphs, W_{ij}^{uc} and W_{ij}^{sc} . The normally hyperbolic lamination \mathcal{L}_0 is then $W_{ij}^c = W_{ij}^{uc} \cap W_{ij}^{sc}$. Now, for each $x \in W_{ij}^c$, the sequence $\{(\mathcal{F}_0^{ij})^k(x)\}_{k \in \mathbb{Z}}$ defines a unique sequence $\tilde{\omega} = (\tilde{\omega}_k)$, $k \in \mathbb{Z}$, $\tilde{\omega}_k \in \{00, 01, 10, 11\}$, by the relation $(\mathcal{F}_0^{ij})^k(x) \in \Pi_{\tilde{\omega}_k}^{s,k}$. Notice that not all sequences are possible: if $\tilde{\omega}_k = (\tilde{\omega}_k^1, \tilde{\omega}_k^2)$, then $\tilde{\omega}_{k+1}^1 = \tilde{\omega}_k^2$. Let $\tilde{\Sigma} \subset \Sigma_{\{00,01,10,11\}}$ be the subset of possible sequences in the space of sequences of four symbols. Let $\Sigma_{\{0,1\}}$ the space of sequences of two symbols. We endow $\Sigma_{\{00,01,10,11\}}$ and $\Sigma_{\{0,1\}}$ with the product topology. It is clear that the map $h : \tilde{\Sigma} \rightarrow \Sigma_{\{0,1\}}$ defined by

$$h(\dots, \omega_{-1}^1, \omega_{-1}^2, \omega_0^1, \omega_0^2, \omega_1^1, \omega_1^2, \dots) = (\dots, \omega_{-1}^1, \omega_0^1, \omega_1^1, \dots)$$

is a homeomorphism with the given topology. That is, we can use sequences of two symbols to label each leaf of the lamination. By construction, the action of \mathcal{F}_0^{ij} on the lamination commutes with the action of the Bernoulli shift on $\Sigma_{\{0,1\}}$.

We claim that each leaf of the lamination, $L_0(\omega, \cdot) : \mathcal{I} \times \mathbb{T} \rightarrow B_\rho^1 \cup B_\rho^2$ is in fact C^r , for any r , if ρ is small enough. To prove the claim, we consider the splitting $E^c \oplus E^u \oplus E^s$ of $T_{B_\rho^1 \cup B_\rho^2}(\mathcal{I} \times \mathbb{T} \times \mathbb{R}^2)$, where $E_x^c = \langle e_1^c(x), e_2^c(x) \rangle$, $E_x^u = \langle e^u(x) \rangle$ and $E_x^s = \langle e^s(x) \rangle$, where $\langle v_1, \dots, v_n \rangle$ denotes the subspace spanned by v_1, \dots, v_n and the vector fields e_1^c, e_2^c, e^u, e^s were introduced in (82), with the Riemannian metric associated to the standard norm. Let π^* denote the projection onto E^* . Proceeding in the same way as in (86) and taking into account (85), there exists a constant $C > 0$ such that for all $v^{sc} \in E^{sc}$, $v^u \in E^u$, $v^{uc} \in E^{uc}$ and $v^s \in E^s$

$$\begin{aligned} \|\pi^{sc} D\mathcal{F}_0^{ij}(x)v^{sc}\| &\leq C|\log \rho|^2 \|v^{sc}\|, & \|\pi^u D\mathcal{F}_0^{ij}(x)v^u\| &\geq \frac{C}{\rho^{\zeta(I)}} \|v^u\|, \\ \|\pi^u D\mathcal{F}_0^{ij}(x)v^{sc}\| &\leq C|\log \rho|^2 \|v^{sc}\|, & \|\pi^{sc} D\mathcal{F}_0^{ij}(x)v^u\| &\leq C|\log \rho|^2 \|v^u\|, \\ \|\pi^{uc} (D\mathcal{F}_0^{ij})^{-1}(x)v^{uc}\| &\leq C|\log \rho|^2 \|v^{uc}\|, & \|\pi^s (D\mathcal{F}_0^{ij})^{-1}v^s\| &\geq \frac{C}{\rho^{\zeta(I)}} \|v^s\|, \\ \|\pi^s D\mathcal{F}_0^{ij}(x)v^{uc}\| &\leq C|\log \rho|^2 \|v^{uc}\|, & \|\pi^{uc} D\mathcal{F}_0^{ij}(x)v^s\| &\leq C|\log \rho|^2 \|v^s\|. \end{aligned}$$

Then the standard theory of normally hyperbolic laminations ensures that the leaves are C^r if, for all $0 \leq k \leq r$,

$$(C|\log \rho|^2)^k \frac{\rho^{\zeta(I)}}{C^2 |\log \rho|^2} < 1.$$

Hence, for any fixed r , taking ρ small enough, follows the claim.

We only need to check the Hölder dependence of the leaves with respect to ω . To do so, for a fixed $a > 1$, we consider in the space of sequences $\Sigma_{\{0,1\}}$ the distance

$$d_a(\omega, \omega') = \sum_{k \in \mathbb{Z}} \frac{|\omega_k - \omega'_k|}{a^{|k+1|}}.$$

Then, applying directly the arguments in [KZ15], we have that

$$\|L_0(\omega, \cdot) - L_0(\omega', \cdot)\|_{C^r} \leq C_r d_a(\omega, \omega')^{\prod_{j=1}^r \varphi_j},$$

with

$$\varphi_j = \frac{\log(C/\rho^{\zeta(I)}) - \log(C|\log \rho|^2)}{\log b_j - \log(C|\log \rho|^2)}$$

and $b_j = C_j \|\mathcal{F}_0^{ij}\|_{C^{j+3}}^{j+3}$. Since $\|\mathcal{F}_0^{ij}\|_{C^{j+3}}^{j+3} = \mathcal{O}(\rho^{-(j+3)\zeta(I)})$, $\varphi_j \approx 1/(j+3)$.

4.4 The NHIL for the elliptic problem: Proof of Theorem 4.5

Normal Hyperbolicity implies that the NHIL given by Theorem 4.4 for the circular problem persists for $e_0 > 0$ small enough and depends smoothly on e_0 [HPS77]. Moreover, it can be parameterized by an embedding L_{e_0} , which is regular with respect to (e_0, I, s) , is Hölder with respect to ω and is e_0 -close to the embedding L_0 given in Theorem 4.4. The embedding L_{e_0} satisfies the invariance equation (50). It only remains to prove the claim on the functions J_{e_0} , S_{e_0} , P_{e_0} and Q_{e_0} . To do so, we write

$$\begin{aligned} \mathcal{SM}_{e_0} &= \mathcal{SM}_0 + e_0 \mathcal{SM}_1 + e_0^2 \mathcal{SM}_2 + \mathcal{O}(e_0^3), \\ L_{e_0} &= L_0 + e_0 \tilde{L}_1 + e_0^2 \tilde{L}_2 + \mathcal{O}(e_0^3), \\ \mathcal{F}_{\text{inn}} &= \mathcal{F}_0 + e_0 F_1 + e_0^2 F_2 + \mathcal{O}(e_0^3), \end{aligned}$$

where \mathcal{SM}_{e_0} and \mathcal{SM}_0 denote the separatrix map for the elliptic and circular problem, respectively, L_{e_0} and L_0 are their corresponding laminations and \mathcal{F}_{inn} and \mathcal{F}_0 are their inner maps. The invariance equation (50) implies that the functions \tilde{L}_1 , \tilde{L}_2 , F_1 and F_2 have to satisfy

$$DSM_0 \circ L_0 \tilde{L}_1 - \tilde{L}_1 \circ \mathcal{F}_0 = DL_0 \circ \mathcal{F}_0 F_1 - SM_1 \circ L_0 \quad (90)$$

$$\begin{aligned} DSM_0 \circ L_0 \tilde{L}_2 - \tilde{L}_2 \circ \mathcal{F}_0 &= DL_0 \circ \mathcal{F}_0 F_2 + \frac{1}{2} D^2 L_0 \circ \mathcal{F}_0 F_1^2 + D\tilde{L}_1 \circ \mathcal{F}_0 F_1 \\ &\quad - \frac{1}{2} D^2 \mathcal{SM}_0 \circ L_0 \tilde{L}_1^2 - DSM_1 \circ L_0 \tilde{L}_1 - SM_2 \circ L_0. \end{aligned} \quad (91)$$

Since L_{e_0} is a graph over (I, s) , $\pi_{I,s} \circ \tilde{L}_i = 0$, $i = 1, 2$, where $\pi_{I,s}$ denotes the projection onto the (I, s) variables and $\pi_{I,s} \circ DL_0 \circ \mathcal{F}_0 = \text{Id}$. Moreover, since I is invariant for \mathcal{SM}_0 , we have that $\pi_I DSM_0 \circ L_0 \tilde{L}_1 = 0$. Hence, by the expression of SM_1 given by Theorem 3.2, the projection onto the I variable of equation (90) gives

$$J_1 = \pi_I F_1 = \mathcal{M}_i^{I,1} + \mathcal{M}_{i,pq}^{I,1},$$

which, since $\mathcal{N}(\mathcal{M}_i^{I,1}), \mathcal{N}(\mathcal{M}_{i,pq}^{I,1}) = \{\pm 1\}$, proves the claim for J_1 .

By Theorem 4.4, the projection onto the (p, q) variables of L_0 does not depend on s and $\mathcal{F}_0(\omega, I, s) = (I, s + \beta(\omega, I))$. Hence, the projection onto the (p, q) variables of (90) reads

$$\left(\begin{array}{cc} \partial_p \mathcal{F}_{p,0} & \partial_q \mathcal{F}_{p,0} \\ \partial_p \mathcal{F}_{q,0} & \partial_q \mathcal{F}_{q,0} \end{array} \right)_{|L_0(I,s)} \begin{pmatrix} P_1 \\ Q_1 \end{pmatrix}_{|(I,s)} - \begin{pmatrix} P_1 \\ Q_1 \end{pmatrix}_{|(I,s+\beta(\omega,I))} = \begin{pmatrix} \partial_I P_0 J_1 \\ \partial_I Q_0 J_1 \end{pmatrix}_{|(I,s)} - \begin{pmatrix} F_{p,1} \\ F_{q,2} \end{pmatrix}_{|(I,s)}.$$

The right hand side of the above equation has only harmonics ± 1 . Since $\pi_{p,q} \circ DSM_0 \circ L_0 \circ \pi_{p,q}$ is hyperbolic and does not depend on s , it follows that $\mathcal{N}(P_1) = \mathcal{N}(Q_1) = \{\pm 1\}$.

Since the projection onto the s -variable of (90) is

$$\partial_p \mathcal{F}_{s,0} \circ L_0 P_1 + \partial_q \mathcal{F}_{s,0} \circ L_0 Q_1 = S_1 - F_{s,1} \circ L_0,$$

the function $\mathcal{F}_{s,0}$ does not depend on s and $\mathcal{N}(F_{s,1}) = \{\pm 1\}$, the same claim holds for S_1 .

Finally, regarding the e_0^2 -term of the I component, it is enough to take into account (91). We have that $\pi_I DL_0 \circ \mathcal{F}_0 F_2 = J_2$ and, then, using that $\pi_I \tilde{L}_2 = \pi_I DSM_0 \circ L_0 \tilde{L}_2 = 0$,

$$J_2 = -\pi_I \left(\frac{1}{2} D^2 L_0 \circ \mathcal{F}_0 F_1^2 + DL_1 \circ \mathcal{F}_0 F_1 - \frac{1}{2} D^2 \mathcal{SM}_0 \circ L_0 \tilde{L}_1^2 - DSM_1 \circ L_0 \tilde{L}_1 - SM_2 \circ L_0 \right).$$

The claim follows from the fact that neither $D^2 L_0$ nor $D^2 \mathcal{SM}_0$ depend on s and $\mathcal{N}(F_1) = \mathcal{N}(\tilde{L}_1) = \mathcal{N}(DSM_1) = \mathcal{N}(SM_2) = \{\pm 1\}$.

A Numerical verification of Ansatz 1

A.1 Equations of motion and Poincaré map

Consider the restricted planar circular three body problem (RPC3BP) in rotating Cartesian coordinates

$$\mathbf{J}(x, y, p_x, p_y) = \frac{1}{2}(p_x^2 + p_y^2) + yp_x - xp_y - \frac{\mu}{r_1} - \frac{1-\mu}{r_2}, \quad (92)$$

where

$$\begin{aligned} r_1^2 &= (x - (1 - \mu))^2 + y^2, \\ r_2^2 &= (x + \mu)^2 + y^2. \end{aligned}$$

We follow the convention to place the large mass (Sun) to the left of the origin, and the small mass (Jupiter) to the right. The system has a time-reversal symmetry across the $y = 0$ plane:

$$R(x(t), y(t)) = (x(-t), -y(-t)). \quad (93)$$

Recall that the energy \mathbf{J} is a first integral. From now on, let the mass parameter be fixed to $\mu = 0.95387536 \times 10^{-3}$.

In the paper [FGKR16] (Section C.3) we established numerically that, in every energy level $\mathbf{J} \in [\mathbf{J}_-, \mathbf{J}_+] = [-1.731, -1.359]$, there exists a hyperbolic periodic orbit $\lambda_{\mathbf{J}}$ that is close to 3 : 1-resonant and satisfies (19). The periodic orbit and its period depend smoothly on \mathbf{J} . This supports the statements in Item 1 of Ansatz 1.

Figure 4 shows a representative sample of periodic orbits in this family. Consider the surface of section

$$\Sigma := \{y = 0\}$$

and its associated Poincaré map

$$\mathcal{P} : \Sigma \rightarrow \Sigma.$$

Notice that low-energy periodic orbits such as $\mathbf{J} = -1.719$ intersect the section Σ at 4 points. However, if we raise the energy above a certain threshold, periodic orbits such as $\mathbf{J} = -1.535$ have three “loops” at the apohelion, so they intersect Σ at 6 points.

Remark A.1. The appearance of these loops in RPC3BP coordinates further complicates the study of their associated stable/unstable invariant manifolds using a surface of section, due to tangencies of the manifolds with Σ . This fact is illustrated in Figure 5, which shows a resonant periodic orbit and a trajectory in its associated unstable invariant manifold. As the trajectory is integrated forward along the invariant manifold, it precedes clockwise, so that one loop ceases to intersect the surface of section Σ , and later another loop starts to intersect it.

Numerically, it is more convenient to integrate the flow of the RPC3BP in Cartesian than in Delaunay variables. The reason is that, to evaluate the vector field in Delaunay, one needs to find the eccentric anomaly u by solving Kepler’s equation $u - \mathbf{e} \sin u = \ell$, where \mathbf{e} is the eccentricity and ℓ is the mean anomaly. However, Kepler’s equation cannot be solved algebraically for u . Of course, one can still solve Kepler’s equation numerically, but for extreme eccentricities, Newton’s method may take long to converge and can lead to numerical errors. Evaluating the variational equations in Delaunay is even more problematic. Thus, from now on we will always integrate the flow of the RPC3BP in Cartesian coordinates (92). Eventually in Appendix B, we will need to map some phase space points to Delaunay, but this poses no difficulty numerically.

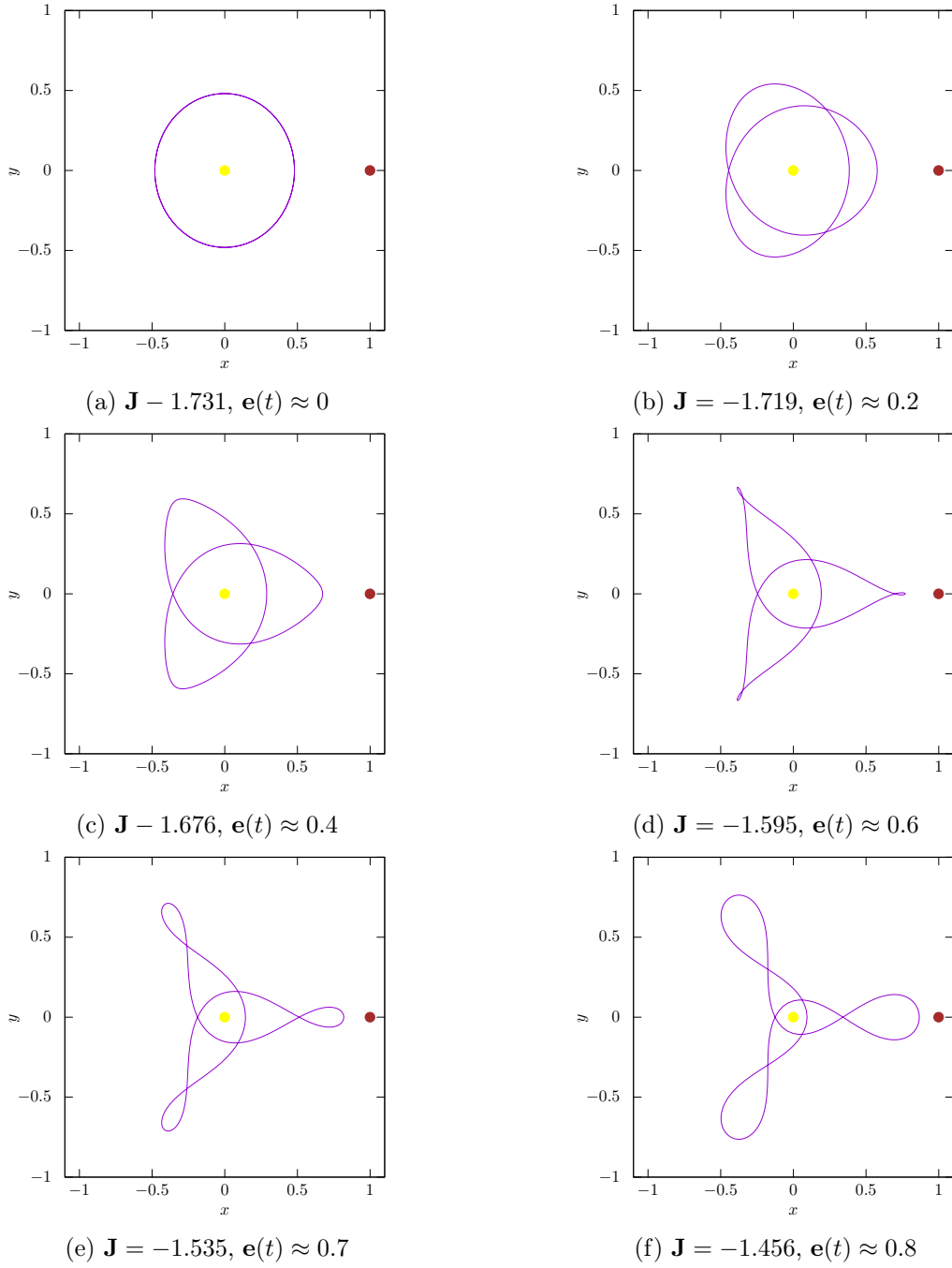


Figure 4: Some (near-)resonant periodic orbits $\lambda_{\mathbf{J}}$ for different energy values \mathbf{J} , or instantaneous eccentricity values $\mathbf{e}(t)$ (xy projection). The location of the Sun and Jupiter are marked with a yellow and brown dot, respectively.

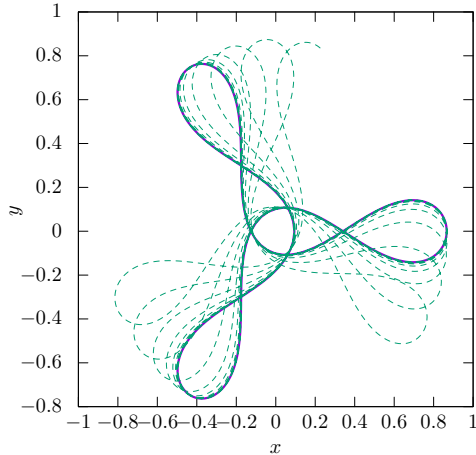


Figure 5: Solid line: resonant periodic orbit $\lambda_{\mathbf{J}}$ with energy $\mathbf{J} = -1.456$. Dashed line: trajectory in its associated unstable invariant manifold. As the unstable trajectory precedes clockwise, the horizontal loop of the trajectory ceases to intersect with the section $\{y = 0\}$. The loop at an angle $-2\pi/3$ will eventually start intersecting the section.

Remark A.2. For all numerical integrations, we use a variable-order Taylor method with local error tolerance 10^{-16} .

Next we explain how the resonance structure and homoclinic points are computed in more detail.

A.2 Periodic points and hyperbolic splittings

We compute the resonant periodic orbits $\lambda_{\mathbf{J}}$ as periodic points of the Poincaré map \mathcal{P} using a Newton-like method. A first guess for the periodic point is obtained from the two-body problem equations. Due to the time-reversal symmetry (93), in this case it is enough to use a 1-dimensional Newton method. This is how Figure 4 was produced.

Remark A.3. The computation of periodic points has an accuracy (absolute error) of 10^{-14} .

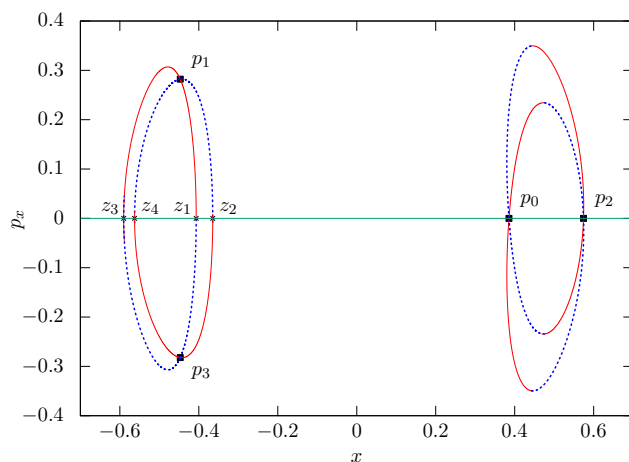
In [FGKR16] we check that the family of periodic orbits $\lambda_{\mathbf{J}}$ is indeed hyperbolic. Each periodic orbit corresponds to a fixed point $p \in \mathbb{R}^2$ for the iterated Poincaré map $\tilde{\mathcal{P}} := \mathcal{P}^4$, whose eigenvalues are not in the unit circle. We also compute the hyperbolic (stable and unstable) directions $E^s(p)$ and $E^u(p)$ associated to the fixed point.

A.3 Invariant manifolds and homoclinic points

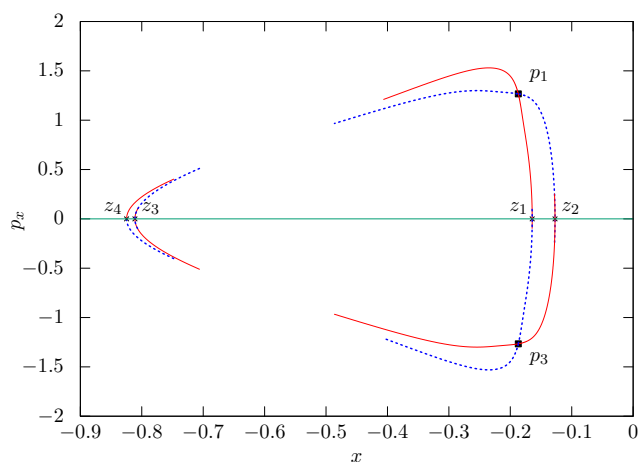
Next step is to extend the 1-dimensional local invariant manifolds in the following way. Let $w^u(\xi)$ be a parametrization of the local unstable manifold W^u (approximated by the linearization at the fixed point). We take a fundamental domain $\xi \in [\xi_-, \xi_+]$ on the local invariant manifold, and iterate it by $\tilde{\mathcal{P}}$ a certain number of times N , until it straddles the symmetry axis $\{p_x = 0\}$. See Figure 6a.

The intersection of the manifolds with the symmetry axis gives four symmetric homoclinic points, that we have denoted $z_1, z_2, z_3, z_4 \in \Sigma$. See Figure 6a.

Remark A.4. In [FGKR16] we already computed z_1 and z_2 on one branch of the manifolds. For this paper we need four homoclinic points, so we have computed the new homoclinic points z_3 and z_4 on the other branch.



(a) Energy level $\mathbf{J} = -1.719$.



(b) Energy level $\mathbf{J} = -1.535$. Only the asymptotic manifolds of p_1 and p_3 are shown, since they are the only relevant ones for this paper.

Figure 6: Hyperbolic structure on the section $\{y = 0\}$ for two different energy levels. The periodic orbit corresponds to p_0, p_1, p_2, p_4 , fixed points for $\tilde{\mathcal{P}}$. The stable manifold is colored in blue, and the unstable in red. Points on the symmetry axis have both $y = 0$ and $p_x = 0 \implies \dot{x} = 0$, so they correspond to symmetric trajectories for the flow. There are four symmetric homoclinic points, denoted z_1, z_2, z_3, z_4 .

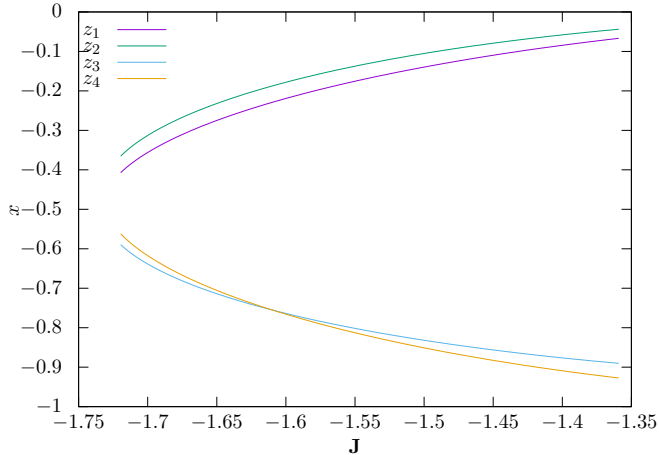


Figure 7: The four families of homoclinic points $z_i(\mathbf{J})$ for $i = 1, 2, 3, 4$. We plot only their x component, since $y = 0$ is given by the surface of section, $p_x = 0$ is given by the symmetry, and p_y can be determined from the energy integral.

Remark A.5. One could also use the homoclinic points between p_0 and p_2 . However these do not lie on the symmetry axis. Numerically, it is more convenient to use symmetric homoclinic points, since they are easier to compute, and we can verify the accuracy of our computations by checking how well the symmetry is preserved.

An intersection corresponds to a root $\xi_* \in [\xi_-, \xi_+]$ of the equation

$$\Pi_{p_x} \tilde{\mathcal{P}}^N(w^u(\xi)) = 0,$$

where Π_{p_x} denotes projection onto the p_x component. To find this root, we use a 1-dimensional root bracketing algorithm (namely Brent’s method).

As the energy is increased, the periodic orbit develops the “loops”, and its asymptotic invariant manifolds become discontinuous, as explained in Remark A.1. See Figure 6b. Despite the discontinuities, the manifolds still intersect the symmetry axis, which allows us to compute the homoclinic points z_i . Figure 7 represents the four families of homoclinic points as a function of \mathbf{J} .

To test the numerical accuracy of the homoclinic points, we repeated the computation using the stable manifold (instead of the unstable one). Then we looked at the difference between the homoclinic point obtained using the unstable manifold and the homoclinic point obtained using the stable manifold. This numerical error is smaller than 10^{-10} for all homoclinic points in Figure 7.

Remark A.6. Of course, the appearance of tangencies between the manifolds and the surface of section depends on the system of coordinates being used. Let us briefly discuss the situation in Delaunay coordinates. The surface $\{g = 0\}$ in *rotating* Delaunay variables is a candidate surface of section for our problem, since in the Kepler problem approximation we have $\dot{g} = -1$. Thus we can assume that in the three-body problem $\dot{g} \leq 0$, but only for *moderate values of the perturbation* by Jupiter (that is both μ small and not too close to collisions with either the Sun or Jupiter). Indeed, when the asteroid’s trajectory becomes very eccentric ($\mathbf{J} \geq -1.485$, or equivalently $\mathbf{e} \geq 0.77$), it passes close to Jupiter and then dg/dt changes sign along the trajectory. See Figure 8. Then $\{g = 0\}$ is not a global Poincaré section anymore. In the companion paper [GKMR23], equation (18), we perform a time reparametrization to have $\frac{d}{ds}g = 1$. This reparametrization is not valid if dg/dt changes sign.

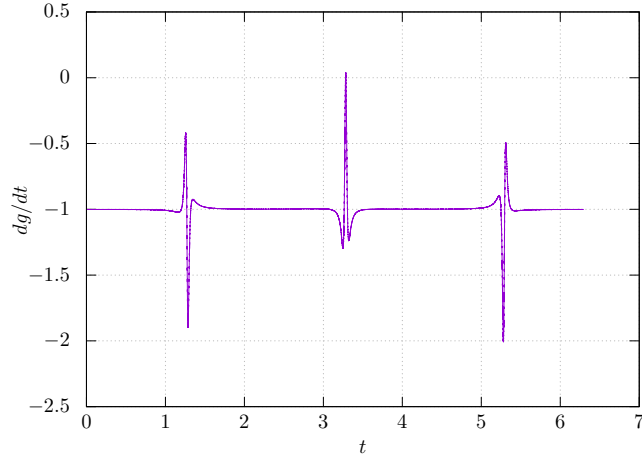


Figure 8: Monitoring dg/dt (rotating Delaunay coordinates) along a homoclinic orbit with energy $\mathbf{J} = -1.485$. Notice that dg/dt changes sign around $t = \pi$.

In order to perform this reparametrization, we must restrict ourselves to moderate eccentricity values $\mathbf{J} < -1.485$ (or equivalently $\mathbf{e} < 0.77$).

A.4 Numerical verification of transversality condition

Let $p \in \Sigma$ be a fixed point for the (iterated) Poincaré map, and let $W^s(p)$ and $W^u(p)$ be the associated stable and unstable 1-dimensional invariant manifolds on Σ . Consider a homoclinic point $z \in W^s(p) \cap W^u(p)$. Let $v^u = (x^u, p_x^u)$ and $v^s = (x^s, p_x^s)$ be the tangent vectors to the unstable and stable manifolds at z . We define the *splitting angle* between $W^s(p)$ and $W^u(p)$ at the homoclinic point z as the directed angle from v_u to v_s :

$$\theta = \arctan(p_x^u/x^u) - \arctan(p_x^s/x^s).$$

We have computed the homoclinic point in Cartesian coordinates. The tangent vectors v_u, v_s are obtained through iteration of the linear stable/unstable directions near the fixed point by the differential of the Poincaré map.

Recall that we are interested in four different homoclinic points. Let θ_i be the splitting angle at the corresponding homoclinic point z_i . Figure 9 shows the splitting angles as a function of the energy value. We see that the splitting angle decreases in magnitude as the energy \mathbf{J} decreases, or equivalently as $\mathbf{e} \rightarrow 0$. The manifolds become tangent (i.e. splitting angle becomes 0) for some values of the energy, but generally they intersect transversally. The particular values of the energy at which the manifolds become tangent are listed in Table 1.

To verify Item 2 of Ansatz 1, we are interested in energy intervals that contain *at least two homoclinic channels without tangencies*. See Table 2 for these intervals. Notice that these are relatively large intervals, where the eccentricity changes by as much as 0.1, or 10%. Due to Remark A.6, we restrict our analysis to energies $\mathbf{J} < -1.485$. Thus, the final diffusion intervals will necessarily be smaller than $\tilde{\mathcal{I}}_1, \tilde{\mathcal{I}}_2, \tilde{\mathcal{I}}_3, \tilde{\mathcal{I}}_4$. In particular, we will work on the smaller diffusion intervals

$$\mathcal{I}_i := \tilde{\mathcal{I}}_i \cap \{\mathbf{J} < -1.485\}.$$

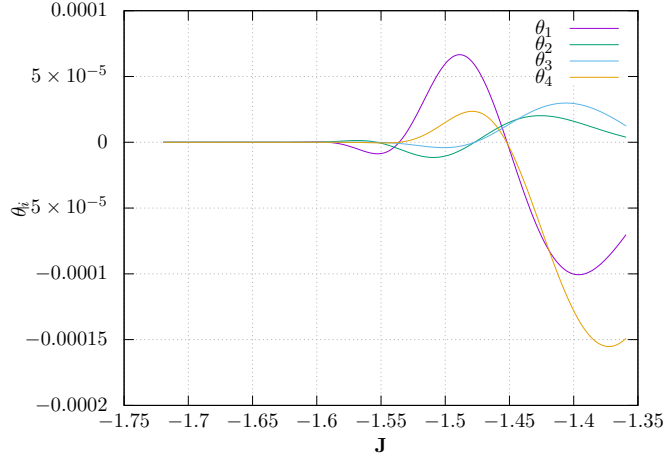


Figure 9: Splitting angles θ_i between the manifolds as a function of energy. Crossings with the horizontal axis correspond to tangencies of the manifolds. Note that two of the splittings (θ_1 and θ_2) were already computed in our previous paper [FGKR16].

splitting angle	energy value of tangencies	
θ_1	-1.535	-1.451
θ_2	-1.551	-1.475
θ_3	-1.551	-1.475
θ_4	-1.535	-1.451

Table 1: Energy levels at which we encounter homoclinic tangencies.

interval	\mathbf{J} -values	e -values
$\tilde{\mathcal{I}}_1$	$[-1.551, -1.475]$	$[0.676, 0.779]$
$\tilde{\mathcal{I}}_2$	$[-1.535, -1.451]$	$[0.700, 0.805]$
$\tilde{\mathcal{I}}_3$	$[-1.475, -1.359]$	$[0.779, 0.888]$
$\tilde{\mathcal{I}}_4$	$[-1.451, -1.359]$	$[0.805, 0.888]$

Table 2: Intervals containing at least two homoclinic channels free of tangencies, given both in terms of the energy \mathbf{J} and the equivalent approximate eccentricity $\mathbf{e}(t)$ of the instantaneous ellipse.

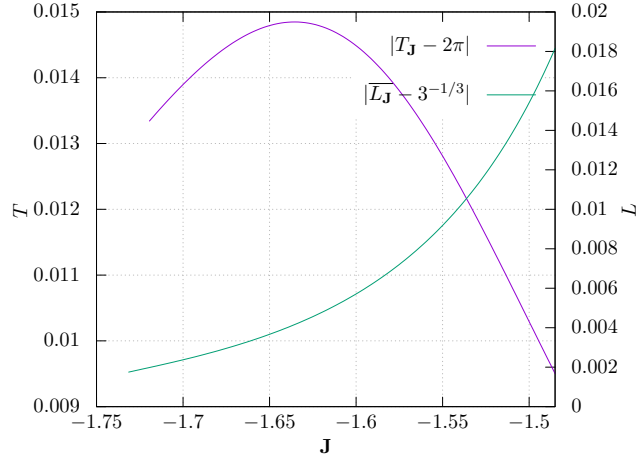


Figure 10: Resonant family of periodic orbits. We show the normalized period $T_{\mathbf{J}} - 2\pi$, and the maximum deviation of the $L_{\mathbf{J}}$ component with respect to the resonant value $3^{-1/3}$.

A.5 Bounds for $T_{\mathbf{J}}$, $L_{\mathbf{J}}$, and $L_i(t, \mathbf{J})$.

Figure 10 shows the normalized period $T_{\mathbf{J}} - 2\pi$ of the resonant periodic orbits as a function of \mathbf{J} . From this Figure, we obtain

$$9\mu < |T_{\mathbf{J}} - 2\pi| < 15\mu,$$

which is the first bound given in Ansatz 1.

Moreover, for each periodic orbit $\lambda_{\mathbf{J}}(t) = (L_{\mathbf{J}}, l_{\mathbf{J}}, G_{\mathbf{J}}, g_{\mathbf{J}})(t)$, we monitor its L component $L_{\mathbf{J}}(t)$ for $t \in [0, T_{\mathbf{J}})$, and compute its deviation with respect to the resonant value $L_0 = 3^{-1/3}$,

$$\overline{L_{\mathbf{J}}} := \sup_{0 \leq t < T_{\mathbf{J}}} |L_{\mathbf{J}} - L_0|.$$

The result is plotted in Figure 10. From this Figure, we obtain

$$\left| L_{\mathbf{J}} - 3^{-1/3} \right| \leq 0.018 \approx 19\mu,$$

which is the second bound given in Ansatz 1.

Ansatz 1 also claims that the homoclinic orbits are confined in the interval $|L - 3^{-1/3}| < 42\mu$. To verify this, fix a homoclinic channel $i \in \{1, 2, 3, 4\}$ and consider the set of homoclinic trajectories $\gamma_i(t, \mathbf{J}) = (L_i, l_i, g_i)(t, \mathbf{J})$ for all $\mathbf{J} \in \tilde{\mathcal{I}}_i$. For each value of \mathbf{J} , i.e. for each homoclinic trajectory, we monitor its L component $L_i(t, \mathbf{J})$ as time t evolves from $-M$ to M with large enough M .

Remark A.7. We use the same value M for the endpoints as in Remark B.2. This guarantees the convergence of the numerical bound.

To monitor the deviation of $L_i(t, \mathbf{J})$ with respect to the resonant value $L_0 = 3^{-1/3}$, we compute the numerical bound

$$\overline{L_i}(\mathbf{J}) := \sup_{-M < t < M} |L_i(t, \mathbf{J}) - L_0|,$$

which is plotted as a function of the energy \mathbf{J} in Figure 11. From this figure we obtain, for any i and for all J , the uniform bound

$$|L_{\mathbf{J}}^i(\sigma) - L_0| \leq 0.04 \approx 42\mu.$$

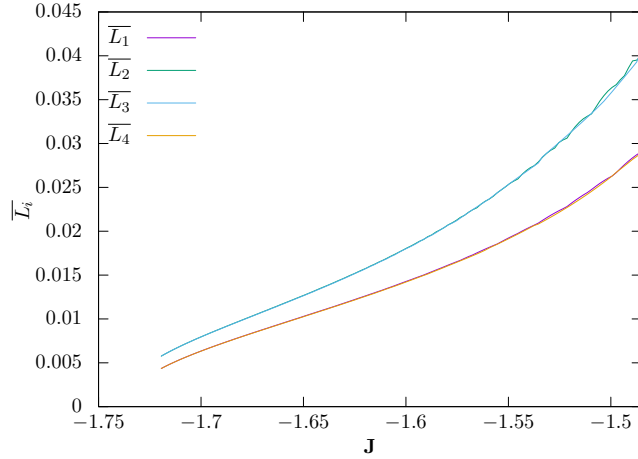


Figure 11: Maximum deviation of $L_i(t, \mathbf{J})$ with respect to the resonant value $L_0 = 3^{-1/3}$. Each curve corresponds to a different homoclinic channel $i \in \{1, 2, 3, 4\}$.

B Numerical verification of Ansatz 2

In this section we verify the non-degeneracy conditions stated in Ansatz 2 numerically. The first step is to compute numerically the functions α_i and B_i , $i = 1, 2, 3, 4$ (one for each homoclinic trajectory), given in Proposition 3.3.

The functions α_i . The functions α_i are computed using numerical integration. In the numerical computation, we approximate the improper integral

$$\alpha_i^\pm(I) = \mu \lim_{N \rightarrow \pm\infty} \left(\int_0^{2\pi N} \frac{(\partial_G \Delta H_{\text{circ}}) \circ \gamma_I^i(\sigma)}{-1 + \mu (\partial_G \Delta H_{\text{circ}}) \circ \gamma_I^i(\sigma)} d\sigma + 2\pi N \nu(I) \right)$$

by a sequence of bounded integrals

$$\alpha_i^\pm(I; N) = \mu \left(\int_0^{2\pi N} \frac{(\partial_G \Delta H_{\text{circ}}) \circ \gamma_I^i(\sigma)}{-1 + \mu (\partial_G \Delta H_{\text{circ}}) \circ \gamma_I^i(\sigma)} d\sigma + 2\pi N \nu(I) \right) \quad \text{for } N = 1, 2, \dots$$

Remark B.1. The function $\partial_G \Delta H_{\text{circ}}$ was given explicitly in [FGKR16], Appendix B.1.

Furthermore, each bounded integral is decomposed into the sum of N integrals of equal size:

$$\alpha_i^\pm(I; N) = \mu \sum_{k=0}^{N-1} \left(\int_{2\pi k}^{2\pi(k+1)} \frac{(\partial_G \Delta H_{\text{circ}}) \circ \gamma_I^i(\sigma)}{-1 + \mu (\partial_G \Delta H_{\text{circ}}) \circ \gamma_I^i(\sigma)} d\sigma + 2\pi \nu(I) \right).$$

We use the QAGS adaptative integrator from the GNU Scientific Library [GG09] to compute each of these N integrals

$$I_{i,k} = \int_{2\pi k}^{2\pi(k+1)} \frac{(\partial_G \Delta H_{\text{circ}}) \circ \gamma_I^i(\sigma)}{-1 + \mu (\partial_G \Delta H_{\text{circ}}) \circ \gamma_I^i(\sigma)} d\sigma, \quad k = 1, 2, \dots, N$$

within a relative error bound $\varepsilon_{\text{rel}} = 10^{-8}$, in such a way that the following inequality holds

$$|\text{RESULT} - I_{i,k}| \leq \varepsilon_{\text{rel}} |I_{i,k}|,$$

where RESULT is the numerical value of the integral obtained by the algorithm.

Remark B.2. We always choose a value of $N = N(I)$ large enough so that $|\alpha_i^\pm(I; N) - \alpha_i^\pm(I; N + 1)| \leq 10^{-6}$. This convergence is illustrated in Figure 12.

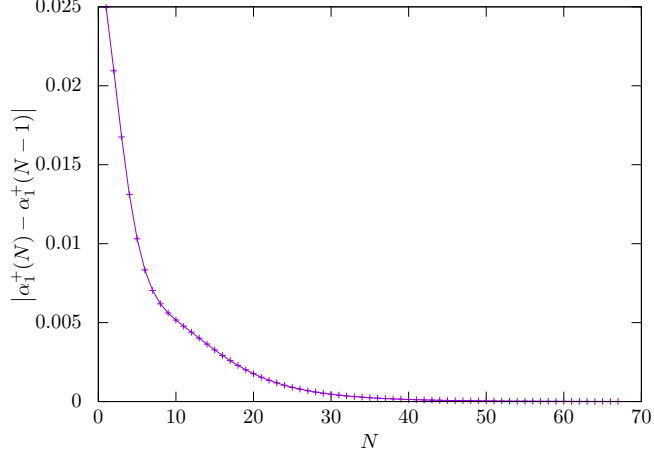


Figure 12: Convergence of the improper integral α_1^+ as a function of N for the energy value $\mathbf{J} = -1.719$. The approximation error is $|\alpha_1^+(67) - \alpha_1^+(68)| < 10^{-6}$, while the value of the integral is of the order of 10^{-1} (see Figure 13).

For numerical stability, on the unstable manifold we always integrate the homoclinic orbit *forward* in time, starting from a homoclinic point on the local unstable manifold. Analogously, on the stable manifold we always integrate the homoclinic orbit *backward* in time, starting from a point on the local stable manifold.

Remark B.3. By the reversibility (93), $\alpha_i^-(I) = -\alpha_i^+(I)$, and thus we have $\alpha_i(I) = 2\alpha_i^+(I)$.

The functions α_i are plotted in Figure 13 for $i = 1, 2, 3, 4$. Two of them coincide at the point $I \approx -1.608$. Note that no more than two phase shifts coincide for a given energy value.

The functions B_i . Next we find the functions B_i^{in} , B_i^{out} , and B_i introduced in Proposition 3.3. Since these functions are complex-valued, we compute their real and imaginary parts separately. They are plotted in Figures 14, 15 and 16 respectively.

Remark B.4. The function $\Delta H_{\text{ell}}^{1,+}$ involved in the numerator of these integrals was given explicitly in [FGKR16], equation (102).

In the numerical computation of the improper integrals B_i^{out} we use the same techniques as for α_i^\pm . Again, these integrals are computed within a relative error bound 10^{-8} .

The first order of the variance $\sigma_0^2(I)$. Finally, we compute σ_0^2 , the first order of the variance, given in Ansatz 2,

$$\sigma_0^2(I) = 2\mathbb{E}_\omega \left| B_i(I) - \mathbb{E}_\omega B_i(I) \frac{1 - e^{i\beta_i^0(I)}}{1 - \mathbb{E}_\omega \left(e^{i\beta_i^0(I)} \right)} \right|^2, \quad (94)$$

where

$$\beta_i^0(I) = \nu(I)\bar{g} + \alpha_i(I). \quad (95)$$

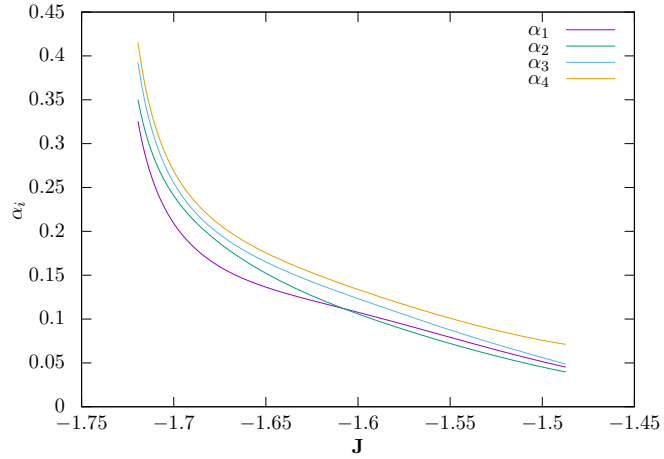


Figure 13: Functions $\alpha_i(\mathbf{J})$. There is a crossing at energy value $\mathbf{J} \approx -1.608$.

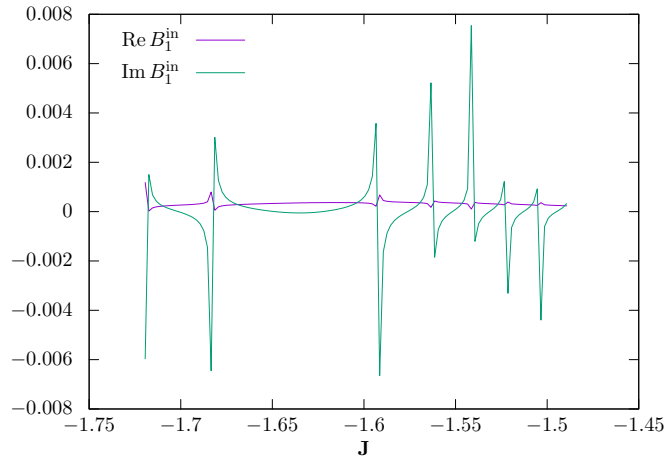


Figure 14: Function $B_1^{\text{in}}(\mathbf{J})$. Functions B_i^{in} for $i = 2, 3, 4$ are very similar; they are not shown for simplicity.

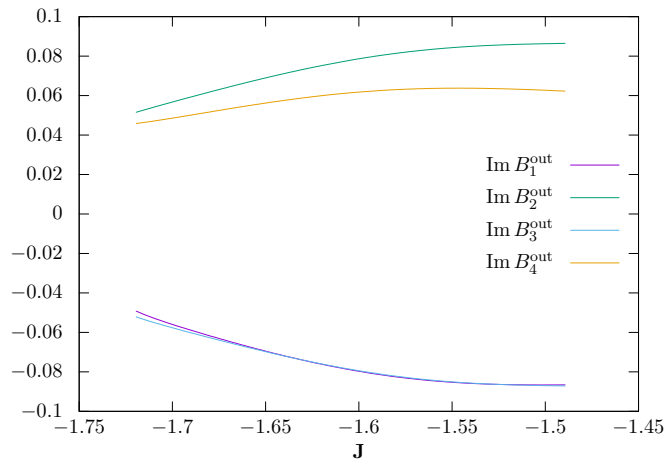


Figure 15: Functions $B_i^{\text{out}}(\mathbf{J})$, $i = 1, 2, 3, 4$. $\text{Re } B_i^{\text{out}}$ are all zero. Only imaginary part is plotted.

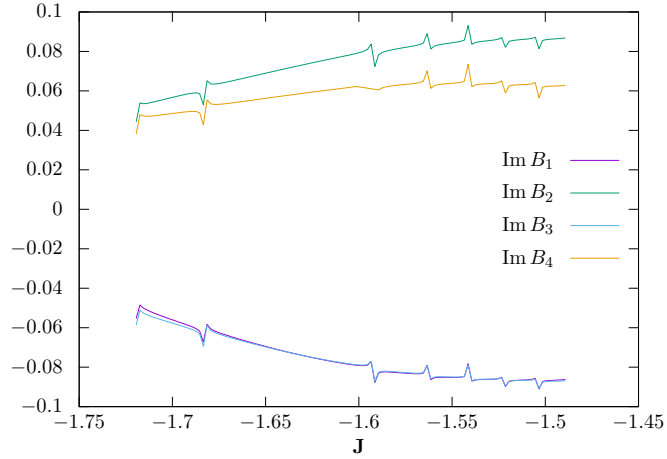


Figure 16: Functions $B_i(\mathbf{J})$, $i = 1, 2, 3, 4$. $\text{Re } B_i$ are all. Only imaginary part is plotted.

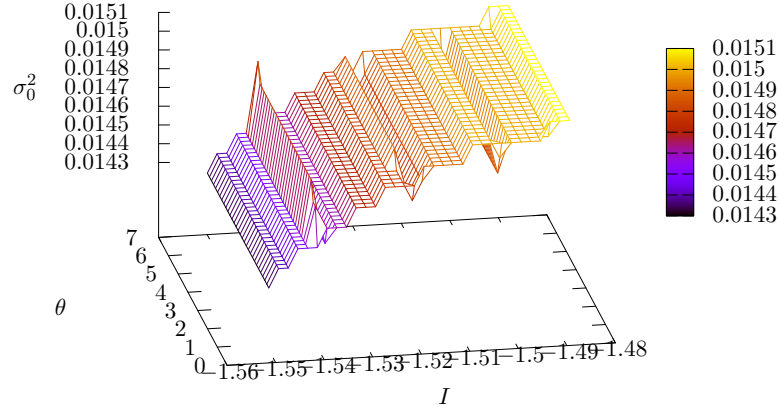


Figure 17: First order of the variance $\sigma_0^2(I, \theta)$.

For definiteness, let us use the pair of homoclinic channels with symbols $i = 2, 3$. These are proper homoclinic channels on the interval $\mathcal{I}_1 = [-1.551, -1.485]$, in the sense that they are free of tangencies in that interval; see Appendix A.4.

Notice that functions α_i and B_i in equations (94) and (95) have already been computed. Further, recall that the operator \mathbb{E}_ω simply denotes the arithmetic mean with respect to $i = 2$ and $i = 3$. For example: $\mathbb{E}_\omega B_i(I) = \frac{1}{2}(B_2(I) + B_3(I))$. Only the term $\theta(I) := \nu(I)\bar{g}$ is unknown. Thus we decide to compute the first order of the variance $\sigma_0^2(I, \theta(I))$ for all possible values of $\theta \in [0, 2\pi)$. See the result in Figure 17. Clearly, σ_0^2 does not vanish on the diffusion interval \mathcal{I}_1 (for any θ value).

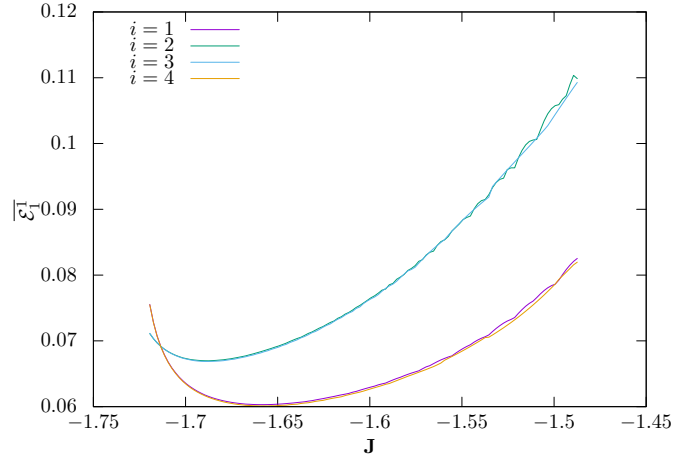


Figure 18: The function $\overline{\mathcal{E}}_1(J)$. Each curve corresponds to a different homoclinic channel $i \in \{1, 2, 3, 4\}$.

C Numerical bounds for $\mathbf{e}(t)$ along the homoclinic channels

For the proof of Theorem 1.2 (see Section 5.4 of the companion paper [GKMR23]), we want to show that $\mathcal{E}_1^1(X, t) = E(\mathbf{J}, L_i(t, \mathbf{J})) - E(\mathbf{J}, L_0)$ is $\mathcal{O}(\mu)$, where the function E is defined as

$$E(\mathbf{J}, L) = \sqrt{1 - \frac{(\mathbf{J} + \frac{1}{2L^2})^2}{L^2}}.$$

For each value \mathbf{J} , we monitor the L component $L_i(t, \mathbf{J})$ along the homoclinic, and compute the numerical bound

$$\overline{\mathcal{E}}_1(\mathbf{J}) := \sup_{-M < t < M} |E(\mathbf{J}, L_i(t, \mathbf{J})) - E(\mathbf{J}, L_0)|.$$

The function $\overline{\mathcal{E}}_1(\mathbf{J})$ is plotted in Figure 18. From this figure we obtain the uniform bound

$$|E(\mathbf{J}, L_i(t, \mathbf{J})) - E(\mathbf{J}, L_0)| \leq 0.12 \approx 126\mu$$

for any i and for all \mathbf{J} in any of the intervals in Table 2.

We also need to show that $E_2(X) = \sqrt{1 - \frac{G^2}{L^2}} - E(\mathbf{J}, L)$ is $\mathcal{O}(\mu)$. For each value \mathbf{J} , we monitor the L and G components $L_i(t, \mathbf{J}), G_i(t, \mathbf{J})$ along the homoclinic, and compute the numerical bound

$$\overline{E}_2(\mathbf{J}) := \sup_{-M < t < M} \left| \sqrt{1 - \frac{G^2}{L^2}} - E(\mathbf{J}, L) \right|.$$

The function $\overline{E}_2(\mathbf{J})$ is plotted in Figure 19. From this figure we obtain the uniform bound

$$\left| \sqrt{1 - \frac{G^2}{L^2}} - E(\mathbf{J}, L) \right| \leq 0.12 \approx 126\mu$$

for any i and for all \mathbf{J} in any of the intervals in Table 2.

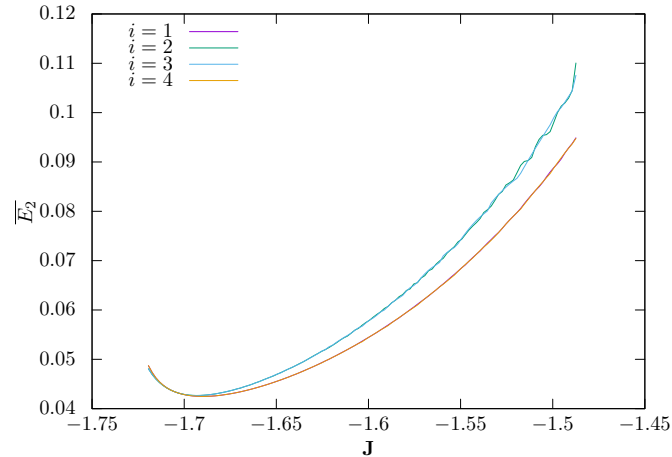


Figure 19: The function $\overline{E}_2(\mathbf{J})$. Each curve corresponds to a different homoclinic channel $i \in \{1, 2, 3, 4\}$.

References

- [Arn63] V. I. Arnold. Small denominators and problems of stability of motion in classical and celestial mechanics. *Uspehi Mat. Nauk*, 18(6 (114)):91–192, 1963.
- [BKZ16] P. Bernard, V. Kaloshin, and K. Zhang. Arnold diffusion in arbitrary degrees of freedom and normally hyperbolic invariant cylinders. *Acta Math.*, 217(1):1–79, 2016.
- [BP12] A. Bounemoura and E. Pennamen. Instability for *a priori* unstable Hamiltonian systems: a dynamical approach. *Discrete Contin. Dyn. Syst.*, 32(3):753–793, 2012.
- [CFG24a] A. Clarke, J. Fejoz, and M. Guardia. A counterexample to the theorem of Laplace-Lagrange on the stability of semimajor axes. *Arch. Ration. Mech. Anal.*, 248(2):Paper No. 19, 73, 2024.
- [CFG24b] A. Clarke, J. Fejoz, and M. Guardia. Why are inner planets not inclined? *Publications Mathematiques de l’Institut des Hautes Etudes Scientifiques*, 2024.
- [FGKR16] J. Féjoz, Marcel Guàrdia, V. Kaloshin, and P. Roldán. Kirkwood gaps and diffusion along mean motion resonances in the restricted planar three-body problem. *J. Eur. Math. Soc. (JEMS)*, 18(10):2315–2403, 2016.
- [FMT03] M. Field, I. Melbourne, and A. Török. Decay of correlations, central limit theorems and approximation by Brownian motion for compact Lie group extensions. *Ergodic Theory Dynam. Systems*, 23(1):87–110, 2003.
- [GG09] M. Galassi and B. Gough. *GNU Scientific Library: Reference Manual*. A GNU manual. Network Theory Limited, 2009.
- [GKMR23] M. Guardia, V. Kaloshin, P. Martín, and P. Roldan. Stochastic behavior along mean motion resonances in the restricted planar three body problem. Preprint, 2023.
- [GKZ16] M. Guardia, V. Kaloshin, and J. Zhang. A second order expansion of the separatrix map for trigonometric perturbations of a priori unstable systems. *Comm. Math. Phys.*, 348(1):321–361, 2016.

- [GT08] V. Gelfreich and D. Turaev. Unbounded energy growth in Hamiltonian systems with a slowly varying parameter. *Comm. Math. Phys.*, 283(3):769–794, 2008.
- [HPS77] M.W. Hirsch, C.C. Pugh, and M. Shub. *Invariant manifolds*, volume 583 of *Lecture Notes in Math*. Springer-Verlag, Berlin, 1977.
- [KZ15] V. Kaloshin and K. Zhang. Normally hyperbolic invariant laminations and diffusive behaviour for the generalized arnold example away from resonances. Preprint available at <http://arxiv.org/abs/1511.04835>, 2015.
- [Mos56] J. Moser. The analytic invariants of an area-preserving mapping near a hyperbolic fixed point. *Comm. Pure Appl. Math.*, 9:673–692, 1956.
- [Nei87] A. I. Neishtadt. Jumps of the adiabatic invariant on crossing the separatrix, and the origin of the Kirkwood gap 3 : 1. *Dokl. Akad. Nauk SSSR*, 295(1):47–50, 1987.
- [NS04] A. I. Neishtadt and V. V. Sidorenko. Wisdom system: dynamics in the adiabatic approximation. *Celestial Mech. Dynam. Astronom.*, 90(3-4):307–330, 2004.
- [Pif06] G. N. Piftankin. Diffusion speed in the Mather problem. *Nonlinearity*, 19(11):2617–2644, 2006.
- [PT07] G. N. Piftankin and D. V. Treshchëv. Separatrix maps in Hamiltonian systems. *Uspekhi Mat. Nauk*, 62(2(374)):3–108, 2007.
- [Shi65] L.P. Shilnikov. A case of the existence of a denumerable set of periodic motions. *Sov. Math. Dokl.*, 6:163–166, 1965.
- [SM95] C. L. Siegel and J. K. Moser. *Lectures on celestial mechanics*. Classics in Mathematics. Springer-Verlag, Berlin, 1995.
- [Tre02] D. Treschev. Multidimensional symplectic separatrix maps. *J. Nonlinear Sci.*, 12(1):27–58, 2002.
- [Wis82] J. Wisdom. The origin of the Kirkwood gaps: a mapping for asteroidal motion near the 3/1 commensurability. *Astronom. J.*, 87(3):577–593, 1982.
- [ZF68] G. M. Zaslavsky and N.N. Filonenko. Stochastic instability of trapped particles and the conditions of applicability of the quasilinear approximation. *Zh. Eksp. Teor. Fiz.*, 54(5):1590–1602, 1968. (in Russian), English translation in *Zh. Eksp. Teor. Fiz.* 25 (1968) 851–863.